UNIVERSITA' DEGLI STUDI DI PERUGIA

A. A. 2023/24

DOTTORATO DI RICERCA IN SANITÀ E SCIENZE SPERIMENTALI VETERINARIE
XXXVII CICLO

settore scientifico disciplinare MVET-01/A

Gonadal development and dynamics in ectotherm models:

insights from *Danio rerio* and *Xenopus tropicalis*

Daniele Marini

(*FIRMA*)

RELATORE

Cecilia Dall'Aglio

(*FIRMA*)

COORDINATORE

Beniamino Terzo Cenci Goga

(*FIRMA*)

"Omnia mirari etiam tritissima."

Carl Nilsson Linnaeus

"Even insects express anger, terror, jealousy, and love."

Charles Robert Darwin

"In all chaos there is a cosmos, in all disorder a secret order."

Carl Gustav Jung

List of Papers

This thesis is based on the following papers, which are referred to in the text by their Roman numerals.

I.   Brouard, V., **Marini, D.***, Roza, M., Svanholm, S., & Berg, C. (2024). Sex differences in gene expression associated with gonadal development during peri-pubertal period in juvenile *Xenopus tropicalis*. *Manuscript*.

II.   Svanholm, S., Roza, M., **Marini, D.,** Brouard, V., Karlsson, O., & Berg, C. (2023). Pubertal sexual development and endpoints for disrupted spermatogenesis in the model Xenopus tropicalis. *Reproductive Toxicology*, 120, 108435.

III. **Marini, D.,** Scattini, G., Mercati, F., Ruegg, J., Schmitz, M., & Dall'Aglio, C. (2024). Transcript trends of leptin system and selected fertility markers in post-spawning zebrafish ovary. *Manuscript Draft ongoing*.

IV.   **Marini, D.,** Schmitz, M., & Dall'Aglio, C. (2024). Follicular population of post spawning zebrafish ovary, *Danio rerio*. *Manuscript Draft ongoing*.

Additional Publications

The following papers were also published during the course of my doctoral studies, but are not included in the thesis.

Adipokines:

- ❖ Martínez-Barbitta, M., Maranesi, M., Mercati, F., **Marini, D.**, Anipchenko, P., Grispoldi, L., Cenci Goga, B.T., Zerani, M. & Dall'Aglio, C. (2023). Presence, Tissue Localization, and Gene Expression of the Adiponectin Receptor 1 in Testis and Accessory Glands of Male Rams during the Non-Breeding Season. *Animals*. 2023; 13(4):601.
- ❖ Maranesi, M., Palmioli, E., Dall'Aglio, C., **Marini, D.**, Anipchenko, P., De Felice, E., Scocco, P. & Mercati F. (2024). Resistin in endocrine pancreas of sheep: Presence and expression related to different diets. *General and Comparative Endocrinology*, 348: 114452.
- ❖ Simoncelli, F., Mercati, F., Di Rosa, I., Palmioli, E., Dall'Aglio, C., **Marini, D.**, & Fagotti, A. (2024). The immunolocalization of adiponectin and its receptors in the testis of the frog *Pelophylax bergeri*. *Zoomorphology*, 143: 459–466.
- ❖ **Marini, D.***, Cappai, M. G., Palmioli, E., Battacone, G., Maranesi, M.*, Dobrzyń, K., Mercati, F. §, & Dall'Aglio, C. § (submitted to *Annals of Anatomy*). Morphological digital assessment and transcripts of gastric and duodenal visfatin in growing piglets fed with increasing amounts of polyphenols from olive mill waste extract.

Ophidiomyces ophidiicola and Ophidiomycosis (Snake Fungal Disease – SFD):

- ❖ Di Nicola, M. R., Coppari, L., Notomista, T., & **Marini, D.** (2022). *Ophidiomyces ophidiicola* detection and infection: a global review on a potential threat to the world's snake populations. *European Journal of Wildlife Research*, 68(5), 1-29.
- ❖ **Marini, D.*** §, Di Nicola, M.R. §, Crocchianti, V., Notomista, T., Iversen, D., Coppari, L., Di Criscio, M., Brouard, V., Dorne, J.L.C.M., Rüegg, J. & Marenzoni, M.L. (2023). Pilot survey reveals ophidiomycosis in dice snakes *Natrix tessellata* from Lake Garda, Italy. *Veterinary Research Communications*, 47, 1707–1719.
- ❖ **Marini, D.**, Filippi, E., Montinaro, G., & Origgi, F.C. (2023). Screening of *Ophidiomyces ophidiicola* in the free-ranging snake community annually harvested for the popular ritual of *San Domenico e dei Serpari* (Cocullo, AQ, Italy). *Acta Herpetologica*, 18(1), 45–52.
- ❖ **Marini, D.**, Szczygieł, P., Kurek, K., Di Nicola, M. R., Dorne, J.L.C., Marenzoni, M. L., Rüegg, J., Bury, S., & Kiraga, Ł. (2024). Retrospective Detection of *Ophidiomyces ophidiicola* from Snake Moults Collected in Bieszczady Mountains, Poland. *Microorganisms*, 12(7), 1467.

Toxicology/Toxinology:

- ❖ Svanholm, S., Brouard, V., Roza, M., **Marini, D.,** Karlsson, O., & Berg, C. (2024). Impaired spermatogenesis and endocrine effects of azole fungicides in peripubertal *Xenopus tropicalis*. *Ecotoxicology and Environmental Safety*, 270: 115876.
- ❖ Paolino, G., Di Nicola, M.R., Ballouard, J.M., Bonnet, X., Damm, M., Le Roux, G., Lüddecke, T., **Marini, D.,** Weinstein, S.A., & Avella, I (2024). A review of bites by non-front-fanged snakes (NFFS) of Europe. *Toxicon*, 108116.

Natural history science and/or Embryology:

- ❖ Cervoni, F., Giardini, M., D'Urbano, S., **Marini, D.**[§], & Grispigni Manetti, C.[§] (2024). A Eurasian otter *Lutra lutra* (Linnaeus 1758) (Carnivora: Mustelidae) in the Tiber basin near Rome: relict or range expansion? Natural History Sciences, 11 (2): 32-36.
- ❖ Brustenga, L., **Marini, D.*,** Guarino, F., Lucentini, L. (in press). Davian behaviour and functional egg fertilization in the Italian stream frog (*Rana italica* Dubois, 1987). *SALAMANDRA - German Journal of Herpetology*, 60(4): xx–xx

§: shared first/last authorship

*: corresponding author

Contents

1. Introduction

Ongoing

2. Aims

Ongoing

3. Background

3.1. Vertebrate ectotherm animals

Ectothermic vertebrates, encompassing fishes, amphibians, and reptiles, represent a vast and diverse group within the animal kingdom. These organisms rely predominantly on external environmental temperatures to regulate their body heat, distinguishing them from endotherms, which internally generate metabolic heat to maintain a constant body temperature (Willmer et al., 2005). The ectothermic mode of thermoregulation has profound implications for their physiology, ecology, and evolutionary history. These flexible physiological characteristics, combined with the diverse range of habitats they occupy, make ectothermic vertebrates valuable and versatile animal models. Understanding these unique characteristics provides perspectives on how wild species respond to global environmental change and contributes to advancements in developmental biology, ecotoxicology, biomedical research and biotechnologies.

Vertebrates (Vertebrata Cuvier 1812 – Fig. <mark>X and X</mark>) are animals characterized by having a skull (cranium) and a backbone composed of vertebrae that protect the spinal cord – ancestrally, the nerve cord (Hedges, 2009). Within them, ectotherms represent a highly diverse and evolutionarily successful group, spanning multiple classes that have adapted to a range of ecological niches.

Fish, as the most basal and diverse ectothermic vertebrates, comprise roughly half of all known vertebrate species and are organized into three major lineages (Hedges, 2009). The paraphyletic group "Cyclostomata", or jawless fishes, includes living vertebrates as lampreys (Petromyzontiformes Berg 1940). These early vertebrates are primitive, with simple body structures that lack jaws and paired fins; they are adapted to various ecological roles, including scavenging and parasitism, which sustain them in both marine and freshwater environments (Osório & Rétaux, 2008). Chondrichthyans (Chondrichthyes Huxley 1880), or cartilaginous fishes, such as sharks, rays, and chimaeras, represent another lineage distinguished by the development of jaws and paired fins. Their cartilaginous skeletons, which contribute to flexibility and buoyancy, have enabled chondrichthyans to become dominant marine predators (Cailliet et al., 2005). Finally,

Osteichthyans (Osteichthyes Huxley 1880), or bony fishes, are the most diverse fish group, including nearly all modern fish species. This lineage is further divided into two clades: Actinopterygii Woodward 1891, or ray-finned fishes, which are highly varied in form and habitat, and Sarcopterygii Romer 1955, or lobe-finned fishes. Actinopterygians are the most species-rich group of vertebrates; their unique fin structure is supported by bony rays that allows for precise and agile movement, enabling them to adapt to a vast range of aquatic environments, from deep oceans to freshwater rivers and lakes (Nelson et al., 2016). Lobe-finned fishes include the lungfishes (Dipnoi Müller 1844) and coelacanths (Coelacanthiformes Jarvik 1942), which possess limb-like fins and a well-developed axial skeleton. These features – along with lungs in Dipnoi – indicate their adaptation to shallow water environments and highlight their role as an evolutionary bridge between aquatic and terrestrial ecosystems. This transition, which began approximately 385 million years ago, marked the early stages of tetrapod evolution (Hedges, 2009).

Amphibians (Amphibia Gray 1825) represent the earliest lineage and class of vertebrates to adapt partially to terrestrial life, while retaining a strong connection to aquatic environments for reproduction. Modern amphibians (Lissamphibia Haeckel 1866) are categorized into three orders: Anura Fischer von Waldheim 1813 (frogs and toads), Caudata Scopoli 1777 (salamanders and newts), and Gymnophiona Rafinesque 1814 (caecilians).
Anurans are the most diverse, making up about 88% of all amphibians with >7000 species, and are widely distributed across tropical and temperate regions. They have maximum 9 vertebrae in front the sacrourostylum, a large pelvic girdle, long hind limbs and all adults lack tail. Salamanders dominate northern temperate zones and exhibit remarkable diversity in reproductive modes, including paedomorphosis, where some species retain larval features into adulthood. Their trunk usually has 12-22 presacral vertebrae, they have well-proportioned head and similar limbs giving the typical aspect of a prototypical land vertebrate. Caecilians live mainly in tropical environments and are usually limbless and burrow underground, with the cloaca located at the very caudal end of the body (Wake & Koo, 2018). Amphibians share several defining characteristics, notably a permeable, moist skin that serves as a respiratory organ and produces various secretions, including toxins for defence. This reliance on moist environments links them to aquatic habitats or high-humidity zones, despite some groups having evolved direct-developing life cycles that allow independence from water for reproduction (Wake & Koo, 2018). In addition to their unique adaptations, amphibians are anamniotes, a classification they share with fish. In these species fertilization is typically external, with eggs and sperm released into water. This strategy, though vulnerable, is balanced by the high number of eggs produced, offsetting the low survival rate. Anamniote eggs lack an amnion, chorion, or allantois and depend on aquatic or moist environments to protect the developing embryo (Duellman & Trueb, 1994; Barresi & Gilbert, 2023). A jelly coat surrounds many of these eggs and allows gases and water to diffuse toward the embryos, but provide scarce defence to physical threats and make them sensitive to environmental factors like pollutants. A yolk, whose size varies by species, sustains the embryos until can autonomously feed in the aquatic environment. These features reflect the adaptations of anamniotes to life in water or damp habitats, where survival depends on both environment and quantity over individual protection (Laurin, 2010).

Reptiles represent a more recent evolutionary advancement among ectothermic vertebrates. Unlike amphibians, reptiles exhibit adaptations that allow them to thrive in terrestrial habitats with minimal dependence on water for reproduction. Key features distinguishing reptiles from other ectotherms include water-resistant, scaly skin and the development of amniotic eggs, which enable them to reproduce successfully outside aquatic environments (Laurin & Reisz, 1995).

The class Reptilia Linnaeus 1758 is a paraphyletic clade. Living reptilian lineages/orders include Squamata Oppel 1811 (lizards, snakes, and amphisbaenians), Rhynchocephalia Günther 1867 (tuataras), Testudines Wagler 1830 (turtles and tortoises), and Crocodylia Wagler 1830 (crocodiles, alligators, and gharials). The latters are included in the clade Archosauria Cope 1869, which include dinosaurs, as the living birds and the more iconic extinct ones. On the other hand, squamates and tuatara belong together to the clade Lepidosauria Duméril & Bibron 1839, whereas the chelonians (Testudines) are the solely living anapsid reptiles (see Marini, 2017).

Squamates are the largest reptilian group and occupy diverse habitats, from arid deserts to dense tropical forests. Testudines are known for their protective shells and adapt to terrestrial, freshwater, and marine ecosystems. Crocodilians, as large semi-aquatic predators, are highly adapted for hunting in both water and land settings. Reptiles' physiological traits, including their efficient water conservation and unique reproductive strategies, have allowed them to occupy a wide array of ecological niches, making them resilient to environmental fluctuations (Anderson et al., 2008; Hedges, 2009, pp. 310–311).
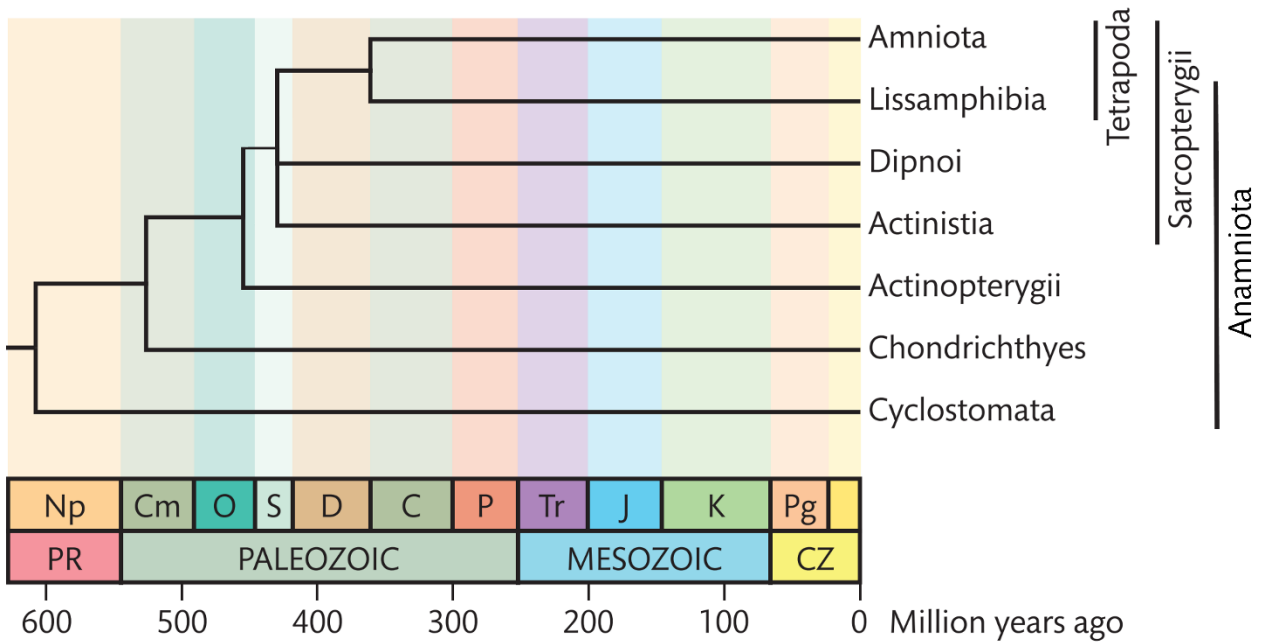
Figure 1: An example of timetree of vertebrates showing major divergence events from 600 million years ago. C (Carboniferous), Cm (Cambrian), CZ (Cenozoic), D (Devonian), J (Jurassic), K (Cretaceous), Np (Neoproterozoic), O (Ordovician), P (Permian), Pg (Paleogene), PR (Proterozoic), S (Silurian), and Tr (Triassic). Modified from Hedges, 2009.
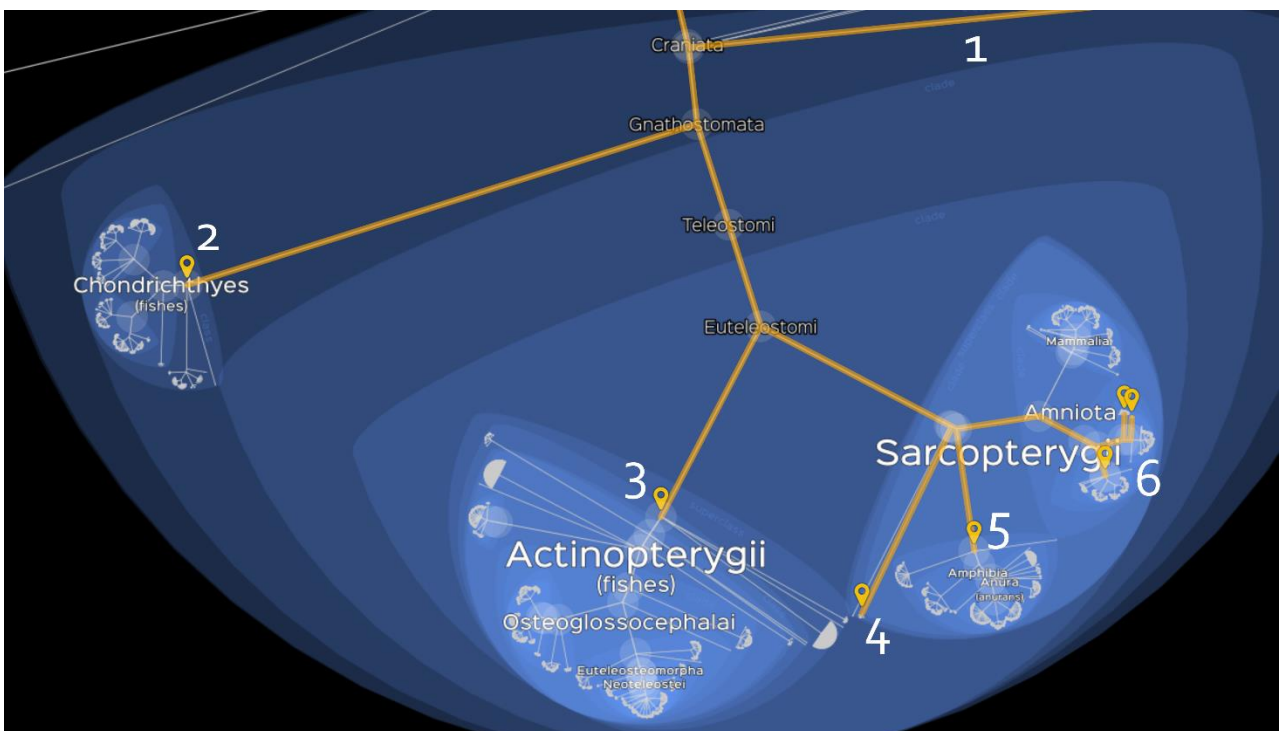

Figure 2: Screenshot from the NCBI Lifemap (https://lifemap-ncbi.univ-lyon1.fr/) showing phylogenetic relationships among major vertebrate groups. The image provide a visual overview of lineage clustering and an approximate quantification of taxa belonging to each clade. Key ectothermic groups are highlighted, including Petromyzontiformes (1), Chondrichthyes (2), Actinopterygii (3), Dipnoi (4), Amphibia (5), and Reptiles (6 – note that the clade Sauropsida include non-ectothermic living reptiles, i.e. the avian species).

ONGOING:

References:

1. Barresi, M., & Gilbert, S. (2023). Developmental Biology. Oxford University Press.
2. Cailliet, G. M., Musick, J. A., Simpfendorfer, C. A., & Stevens, J. D. (2005). Ecology and life history characteristics of chondrichthyan fish. Sharks, rays and chimaeras: the status of the chondrichthyan fishes. IUCN SSC Shark Specialist Group. IUCN, Gland, Switzerland and Cambridge, UK, 12-18.
3. Duellman, W. E., & Trueb, L. (1994). Biology of Amphibians. Johns Hopkins University Press
4. Hedges, S. B. (2009). Vertebrates (Vertebrata). In S. B. Hedges & S. Kumar (Eds.), The Timetree of Life (pp. 309–314). Oxford University Press.
5. Laurin, M. (2010). How Vertebrates Left the Water. University of California Press.
6. Marini, D. (2017). Invasiveness of allochthonous freshwater turtles: monitoring of paths/positions and sanitary status in Lublin region, Poland. Master Thesis in Veterinary Medicine, Università degli Studi di Teramo (p. 0-176). Teramo, 02.11.2017
7. Nelson, J. S., Grande, T. C., & Wilson, M. V. (2016). Fishes of the World. John Wiley & Sons.
8. Osório, J., & Rétaux, S. (2008). The lamprey in evolutionary studies. Development genes and evolution, 218, 221-235.
9. Wake, DB and Koo, MS. 2018. Primer: Amphibians. Current Biology 28(21)
10. Willmer, P., Stone, G., & Johnston, I. (2005). Environmental physiology of animals. John Wiley & Sons.

Paper I

Sex differences in gene expression associated with gonadal development during peri-pubertal period in juvenile *Xenopus tropicalis*

Vanessa Brouard[1], Daniele Marini[1,2,*], Mauricio Roza[3], Sofie Svanholm[1]and Cecilia Berg[1]

[1]Department of Environmental Toxicology, Uppsala University, 754 36 Uppsala, Sweden;

[2] Department of Veterinary Medicine, University of Perugia, 06126 Perugia, Italy;

[3] Science for Life Laboratory, Department of Environmental Science, Stockholm University, 114 18 Stockholm, Sweden;

* Corresponding author: daniele.marini@ebc.uu.se

Abstract

Understanding the prepubertal development of anuran animal models is crucial for studying amphibian reproductive biology and potential environmental impacts on gonad development. This study aims to evaluate gonads histology and gene expression in *X. tropicalis* from metamorphosis to 8 weeks post-metamorphosis (PM) to elucidate key sex-specific developmental timelines. *X. tropicalis* tadpoles obtained from in-lab mating of adult animals were raised until metamorphosis. Weekly samples were collected up to 8 weeks PM and grouped into four clusters: Met 1-2 weeks, Met 3-4 weeks, Met 5-6 weeks, and Met 7-8 weeks. Morphological data and gonad-kidney complexes (GKCs) were collected. The left GKC was used for histology and image analysis, and the right one for gene expression analysis via qPCR. Key genes analyzed included *dmrt1*, *cyp17*, *cyp19*, *amh*, *sox9*, *id4*, *ddx4*, *3βhsd*, *esr1*, *amhr2*, *rsbn1*, *aldh1a2*, and *cyp26b1*. In males, liver and fat body somatic indices peaked at Met 3-4 weeks, decreasing significantly by Met 7-8 weeks. Females showed similar patterns but with delayed peaks at Met 5-6 weeks. Histologically, testis area and maturity scores peaked at Met 7-8 weeks, while ovarian area and follicular oocyte numbers increased significantly with age, peaking at Met 7-8 weeks. Gene expression analysis showed significant age-related changes: *id4* expression decreased in females but was stable in males, and *ddx4* expression increased significantly in both sexes by Met 7-8 weeks. Genes involved in gonad differentiation and steroidogenesis displayed sex-specific patterns consistent with their developmental roles. These findings enhance our understanding of amphibian reproductive biology and lay a baseline for future research on gonadal impairment in environmental toxicology.

Introduction

Gonad differentiation is a complex process that take place during a specific period of development in all vertebrate and allow the individuals to reproduce and perpetuate the species. This process could be separate in two steps: the sex determination, that take place in the undifferentiated and bipotential gonad, and the sexual differentiation when the gonad develops sex-specific structures, genes and hormonals expression. Several mechanisms can be involved in sexual determination; genetic sex determination and environmental sex determination (mainly temperature relative mechanism) are the most common and can be associated to hormonal sex determination; depending on the species. In ectotherms as amphibians, sex determination is defined by genetic and hormonal mechanisms (Capel, 2017; Nagahama et al., 2021).

 To study sexual determination and differentiation in vertebrate and particularly in amphibians, *Xenopus laevis* and *Xenopus tropicalis* have been used for decades in research. Indeed, both are easy to maintain in captivity and to breed, which contribute to major finding in developmental biology (Hirsch et al., 2002; Tadjuidje and Heasman, 2010). More recently, *X. tropicalis* model has shown some advantages in comparison to *X. laevis* in regard of development, reproduction and toxicology investigations. *X. tropicalis* possesses a shorter life cycle, a diploid genome and a comparable hypothalamus-pituitary-gonadal axis and Müllerian duct development to mammals and a well-defined developmental larval stages (Nieuwkoop and Faber (NF) stages (Nieuwkoop and Faber, 1956)) (Berg, 2019; Berg et al., 2009).

In *Xenopus* species, histological sex determination of the gonad is widely used to sex individuals before the puberty and the development of secondary sex characteristics specific to male or female. In *X. laevis* the sex determination period occurs between NF49 and NF53; after NF53 stage, male and female gonads can be discriminate from each other by histology. At NF53 the female gonad present the cortex in its centre preceding the ovarian cavity which is formed at NF56 (Piprek et al., 2018). Similarly, in *X. tropicalis*, the histological differences between male and female gonads are visible between NF48 and NF51; and the clear ovarian cavity structure is observed at NF56 in the females (El Jamil et al., 2008; Haselman et al., 2015).

Further on, sex determination in tadpoles has been improved with genetic and gene expression technics. In *X. laevis*, the females are the heterogametic sex with ZW/ ZZ sex chromosome system. Moreover, the *Dm-w* (DM domain gene on W chromosome) gene, localised on the W chromosome, has been described as a female marker in *X. laevis*. In *X. tropicalis*, *Dm-w* is absent and the genetic sex determination still not fully understood as both male and female can be heterogametic: YZ, YW or ZZ males and ZW and WW females (Roco et al., 2021a, 2015; Yoshimoto et al., 2008).

More recently, other genes have been identified with sex-specific expression pattern in *X. laevis* as earlier as NF53. Indeed, several genes presented an expression level higher in male, such as, *Sox9* (SRY-Box Transcription Factor 9), *Dmrt1* (Double sex and mab-3 related transcription factor 1) and *Cyp17* (Cytochrome P450 family 17 sub family A member 1). Whereas, *Dm-w*, *Foxl2* (forkhead box L2), and *Cyp19* (Cytochrome P450 family 19 sub family A member 1 or Aromatase) expression levels were higher in female (Piprek et al., 2018). In detail, *Sox9* is a transcription factor implicated in male gonad differentiation in several vertebrate specie including mammals. *Sox9* and *Dmrt1* expression are under each other influence and both promote testicular differentiation (Vining et al., 2021). In zebrafish, *Sox9* promotes expression of *Amh* (Anti-Müllerian Hormone) to prevent Müllerian duct development in male individuals and inhibit *Foxl2* and *Cyp19* expression implicated in the female gonad development (Pradhan et al., 2016). *Cyp17* is coding for a steroidogenic enzyme necessary for estrogens and androgens production. In frog, *Cyp17* is described as a male differentiation marker as its expression level is higher in male gonad and increase with age (Iwade et al., 2008; Piprek et al., 2018). In female tadpole, *Dm-w* is a transcription factor that inhibits male sexual differentiation by inhibition of *Dmrt1* expression (Yoshimoto et al., 2010). *Foxl2* is implicated in female gonad differentiation (Navarro-Martín et al., 2012), as well as *Cyp19*, gene coding for the steroidogenic enzyme necessary for estrogens production (Piprek et al., 2018). Those detailed gene expression data are still missing in the *X. tropicalis* model but quantification of *Cyp19* and *Cyp17* gene expression by Real-Time PCR has been validated as a method to defined sex in tadpoles at early developmental stages (Navarro-Martín et al., 2012).

The sex determination period is currently well described in tadpole, with histological observations and gene expression data, in comparison with the sex differentiation period. The sexual differentiation take place from the end of the sex determination period until the first complete spermatogenesis or oogenesis. In amphibians, it has been described that ovaries adopt the same developmental pattern observed in mammals. At each breeding season, the mature follicular oocytes are recruited from a defined and limited pool of immature oogonia formed during the early oogenesis in the tadpoles (Ogielska et al., 2013). At metamorphosis, the ovary is composed with primary oogonia and oocytes at early meiosis stage (preleptoten stage) (Kvarnryd et al., 2011). Immature oocyte goes under meiosis until diploten stage I, at this stage the oocyte develop into follicular oocytes stage I and stage II before vitelogenic stages (stage III to stage VI) which will allow the oocyte to collect enough resources for the future embryo (Rasar and Hammes, 2006). In *X. tropicalis* females, it has been shown that the oocytes development starts at 16 weeks PM associated with the increase of estradiol and vitellogenin concentration in the blood and then, followed by increasing in pre-vitellogenic and vitellogenic oocytes in correlation with a significant gain in the ovary and the oviduct mass.

Yet, based on cells composition of the gonad, the females are only sexually mature around 26 weeks PM or ~7 months old (Olmstead et al., 2009). Shorter time has been observed in laboratory condition where females were able to reproduce at 6 months old (Hirsch et al., 2002). Moreover, studies from our laboratory shown that females ovary cell composition did not significantly differ between 4 and 8 weeks PM, however, the more mature germ cells observed were the pre-vitellogenic oocytes stages II (Svanholm et al., 2021, Svanholm et al. submitted).

In males, the sexual differentiation is described in two phases; distinction between tadpole stages: the prespermatogenesis and during juvenile / adult age: the spermatogenesis. The prespermatogenesis is characteristic of gonocytes and establishment of the stem cell pool whereas the spermatogenesis is characteristic of pale and dark spermatogonial stem cells (SSC). The spermatogenesis is active when differentiated SSC; the dark SSC, are observed. The dark SSC are going under differentiation toward secondary spermatogonia and then spermatocyte, which is the stage of the meiosis before morphological differentiation of the germ cell at spermatid and spermatozoa stages. The active

spermatogenesis is initiated at metamorphosis stage (Haczkiewicz et al., 2017). After metamorphosis, testosterone concentration increase at 8 weeks PM and its followed with the sperm count increase at 10 weeks PM. In *X. tropicalis*, the males are sexually mature around 20 weeks PM or ~5,5 months old (Olmstead et al., 2009), however in laboratory condition males were sexually mature at 4 months old (Hirsch et al., 2002). Recently, precise description of the testis composition at 4 and 8 weeks PM revealed that spermatozoa are produce as early as 8 weeks (Säfholm et al., 2016; Svanholm et al., 2021; Svanholm et al. manuscript). Those results suggest that major developmental event occurs between metamorphosis and 8 weeks PM although, the precise timeline of juvenile germ cell differentiation in *X. tropicalis* is not fully understood and no data are available on gene expressions during this developmental period.

Thereby, we aim to analyze the mRNA level of genes implicated into gonad development at several time point during prepubertal period in *X. tropicalis*. Based on previous data from amphibians and mammals models, we selected genes implicated in gonadal differentiation and development (Kelley, 1996; Nagahama et al., 2021; Piprek et al., 2018; Roco et al., 2021b).

Lead by Piprek et al. study in *X. leavis* (Piprek et al., 2018), we investigated gene expression specific to male and female development in *X. tropicalis* : *Dmrt1*, *Cyp17*, *Cyp19*, *Amh* and *Sox9* gene expression were analysed. Moreover, we also complement our investigation with genes specific to germ cells ; *Id4* (Inhibitor of DNA binding 4 gene) specific to undifferentiated germ cells and *Ddx4* (DEAD-box helicase 4) express in early stage germ cells (Sun et al., 2015; Xu et al., 2014). Then, we evaluated the expression of genes involved in steroidogenesis and hormone signalisation : *3βhsd* (3-beta-hydroxysteroid dehydrogenase) encoding for the enzyme involved in the transformation of pregnelonone to progesterone and *Esr1* (Estrogen receptor 1) implicated in estrogen signalling pathway (Carreau and Hess, 2010; Maruo et al., 2008). Genes implicated in the male's gonad differentiation were analysed; Amh receptor *Amhr2* (Amh receptor 2) and the gene *Rsbn1* (Round spermatid basic protein 1) specific to spermatid cells in the testis (Moritz and Hammoud, 2022; Ohyama et al., 2015; Tlapakova et al., 2016). Finally, we also investigated genes of the retinoic acid pathway, critical for the germ cells meiosis; *Aldh1a2* (Aldehyde dehydrogenase 1 family member A2)

implicated in retinoic acid production and *Cyp26b1* (Cytochrome P450 family 26 subfamily B member 1) necessary for the retinoic acid degradation (Piprek et al., 2013).

Thus, we proposed to evaluate 1) the all body and gonadal tissue growth and 2) the expression of gene implicated in the development of the testis and the ovary of *X. tropicalis* juveniles. We focused our study on the prepubertal period; from metamorphosis up to two months post-metamorphosis as previous data suggest it as a critical developmental window. Our results help to understand the sex specific gene expression chronology in male and female gonads correlated to general and gonad tissue growth during the puberty establishment.

Material and Methods

Animal Handling

X. tropicalis tadpoles were generated from 2 different mating pairs of adults. Adult frogs from Carolina Biological Supply Company (Burlington, North Carolina, USA) were prepared for mating by injection of human chorionic gonadotropin (in 0.9% saline solution) into the dorsal lymph sac (Pettersson et al., 2006). 72 hours after fertilization, tadpoles were arranged in five 15 L aquaria, each containing 60 tadpoles. During the weeks before metamorphosis, tadpoles were moved to new aquarium depending on the developmental stage to obtain a more homogenous population in each tank. During the tadpole period, each aquarium was cleaned and fresh water added 3 times per week. Then, the frogs with a similar metamorphosis date were place together and kept until the desire age (weeks post-metamorphosis (PM)) in a flow-through aquaria. Water temperature, pH, conductivity, were monitored every day. Moreover, the nitrite and ammonia/ammonium levels were measured once a week, using standard kits from Sera (Gibbon, Sweden). During the early stages, tadpoles were fed three times per day with Sera Micron (Sera, Heinsberg, Germany). From metamorphosis, the frogs were introducing progressively to Sera Vipan Baby food (Sera, Heinsberg, Germany) and Tropical Energy food (Aquatic Nature, Roeselare, Belgium) and Sera Micron was eliminated. This study was approved by Uppsala Ethics Committee for Animal Care and Use.

Dissection and Samplings

Between 5 and 10 animals were sampled every week after metamorphosis up to 8 weeks PM. We obtain 8 groups; from frogs at Met + 1 week of age up to Met + 8 weeks of age. To obtain enough males and females for each age group, we decided to pooled together the individuals by group of 2 weeks of age. Thereby, frogs from Met+1week and Met+2weeks are pooled together as the Met + 1-2 weeks group. So, for further analysis, we used the pooled groups Met + 1-2 weeks, Met + 3-4 weeks, Met + 5-6 weeks and Met + 7-8 weeks. When the desired age was reach, the animal was anesthetized in 0.3% buffered MS-222 solution (Sigma Aldrich, Saint-Louis, USA) before being euthanized by decapitation. For each animal, the morphological data have been evaluated: body weight, body length, fore limb length, hind limb length, liver weight and the fat body weight have been measured. The liver and fat body somatic index have been calculated as: the organ weight divided by the body weight x100. Finally, the presence of nuptial pad was recorded. Then, with the help of the dissection microscope, the right half of the GKC was excised from the complex and snap-frozen in liquid nitrogen for gene expression analysis, whereas the left half was fixed in 4% formalin for histological evaluation.

Histological processing and analysis

After sampling, half of the GKC was fixed in formalin 4% for at least 48h then the tissue was stored in 70% ethanol before embedding in paraffin. The dehydration of the tissue started with 150 min bath in 96% ethanol, then 50 min in 100% ethanol. The clarification of the tissue was made in Xylene for 45 min then the infiltration in paraffin for 50 min before the final step of embedding. The tissue was sectioned at 10 µm sections and stained with toluidine blue to assess the position in the tissue, when the gonads were first visible the sections were decrease to 5 µm and used for haematoxylin-eosin staining. For each animal, at least two sections, separate with 20 µm of tissue length, were stained with haematoxylin-eosin for determination of the sex and evaluation of gonadal maturation.

The area of the gonad and the germ cell maturity were evaluated with NDP. View 2 program (Hamamatsu, Shizuoka, Japan). The testis maturity was defined with a scoring system using precise

histology description of the male germ cell establish by our laboratory (Svanholm et al, manuscript). The maturity score was assigned to the testis, depending of the most mature germ cells observed: 1: Pale spermatogonial stem cell, 2: Dark spermatogonial stem cell, 3: Secondary spermatogonia, 4: Primary spermatocyte, 5: Secondary spermatocyte, 6: Spermatid, 7: Spermatozoa. For the ovary, the maturation was assessed as number of follicular oocytes (oocytes surrounded by a layer of follicle cells) in one ovary section.

Gene expression analysis

Half of the GKC for each individual was processed for gene expression analysis. Before RNA was extracted, the samples were homogenized with two steps. The GKC were disrupted by using a plastic potter in 1.5 ml tube, first by itself, and then with addition of 100 µl PureZOL (Biorad, Hercules, USA). For the second step, the homogenate was then transferred to a 2 ml SafeSeal tube and an additional 100 µl PureZOL and titanium beads were added to the samples before using the bullet blender (Bullet blender Storm 24, NextAdvance, Troy, USA) two times for 1 min at speed 8. After homogenization, RNA was extracted using the Aurum Total RNA Mini kit (BioRad, Hercules, USA), following the manufacturer's protocol. Thus, 800 µl of PureZOL was added to each sample before the 5 min incubation at room temperature (RT), then 200 µl chloroform were added to the lysate and the tube was agitated vigorously for 30 seconds. The sample was incubated 5 min at RT while mixing regularly by inversion before centrifugation at 12 000 g for 15 min at 4°C. After centrifugation, the top aqueous phase was transfer into a new tube and an equal volume of ethanol 70% were added to the lysate and mixed thoroughly by pipetting, then the lysate was transfer into the RNA column. After centrifugation at 12 000 g for 1 min, the RNA column was wash with buffer solution before DNAse I treatment. The DNase I solution mix was freshly prepared as described by the manufacturer (Biorad, Hercules, USA), placed on the RNA column membrane and incubated for 15 min. After DNAse I treatment, the RNA column was washed two times before elution of the RNA sample with 30 µl of elution solution by centrifugation. Finally, the RNA concentration as well as the quality (ratio

230/280 nm and 260/280 nm) were determined spectrophotometrically with Spark micro-plate reader (Tecan, Männedorf, Switzerland).

Reverse transcription of RNA samples was performed with the iScript cDNA synthesis kit (BioRad, Hercules, USA). 500 ng of RNA were used for the reverse transcription into complementary DNA (cDNA). For each sample, 4 µl of iScript reaction mix and 1µl of iScript reverse transcriptase were mixed with the RNA sample. To obtain the final volume of 20 µl, water was added if necessary. BioRad Thermocycler T100 (Biorad, Hercules, USA) was used for the reverse transcription run with a protocol of 5 min at 25°C, 20 min at 46°C and 1 min at 95°C.

The cDNA sample concentration was adjusted to obtain 20 ng cDNA/µl for the quantitative polymerase chain reaction (qPCR). iQ Sybr Green Supermix (Biorad, Hercules, USA) was used in a final volume of 10 µl containing: 5 µl of Sybr Green Supermix, 0.3 µl of primers mix (forward and reserve primers together), 0.7 µl of water and 4 µl of cDNA sample. The Biorad CFX384 instrument (Biorad, Hercules, USA) was used for the qPCR run: 3 min at 95°C followed by 45 cycles of 10 s at 95°C and 30 s at 60°C (62°C were used for *Cyp19* primers), and ended by the melting curve from 55°C up to 95°C with increment of 0.5°C every 5 s. Each sample was analysed in triplicate. The relative gene expressions were calculated by the 2ΔCT method using the average of two housekeeping genes: elongation factor 1-alpha (Ef1) and ribosomal protein L8 (Rpl8) (Orton et al., 2018; Verbrugghe et al., 2019) (Table1).

For each set of primers, efficiency was determined with a standard curve using adult male and female GKC tissues with 6 different concentrations from 0.93 to 30 ng/ul of cDNA and a negative control with only water. The percentage of efficiency was calculated using: Efficiency = $(10^{(-1/a)}-1)$ x100 where a= slope of the graphical representation of (average CT value compare to the Log of the concentration). The efficiency of the primer sets used for this study was 103.9 ±12 % for the male and 99.3 ±13 % for the female samples.

Statistical analysis

The testis maturity score, the testis area, the follicular oocytes number and the ovary area data were compare between age groups using Kruskal-Wallis test with Dunns's multiple comparisons test. The correlation between the gonad parameters and the age, as well as with the body measurement and the gene expression were determined using the Pearson correlation test. To analyse the genes expression associated to the sex and the age we used the Generalized Linear Models form the gamma family of distribution with log link function. We did a pairwise comparisons using Z-tests, corrected with Holm's sequential Bonferroni procedure for each gene.

Relationships between mRNA levels of genes involved in sex-specific gonadal development and results from quantitative and qualitative morphological and histological analysis were determined with a principle component analysis (PCA) using the FactoMineR and factoextra R packages. The PCA analysis was based on the individuals for which both mRNA and histological data were available and any missing values were imputed using the missMDA R package.

Bayesian network analysis was conducted using JASP (v.0.18.1) with the Gaussian copula graphical model (GCGM) estimator. The analysis was stratified by the variable "Sex" and "Met" to explore differences in network structure across groups. For the variable "Met" the indivuduals were clustered in younger (from the first to the fourth week post-metamorphosis: Met1-4) and older (from the fifth to the eight week post metamorphis: Met5-8). A Markov Chain Monte Carlo (MCMC) approach was used with 10,000 iterations and a burn-in period of 5,000 iterations to ensure convergence. To allow for reproducibility, a fixed random seed was set to 1. The prior probability of edge inclusion (g prior) was set to 0.5, with the initial configuration for prior edge inclusion set to "empty" and 3 degrees of freedom for the G-Wishart prior. The threshold for edge inclusion was set to a Bayes Factor (BF_{10}) greater than 10. Plots generated included the network plot, edge evidence plot (including evidence for inclusion, exclusion, and absence of evidence), and centrality plot. Tables created included the weights matrix and edge evidence probability table, reporting edge inclusion probability and Bayes Factors.

Results

Morphological data

In males, the body weight and length show an increase with age but not significantly (Fig.1A and B). The liver and fat body somatic index show an increase from Met + 1-2 weeks to Met + 3-4 weeks, followed by a significant decrease from Met + 3-4 weeks to Met + 7-8 weeks ($p<0.05$, Fig.1C and D). Then, correlation analysis shows that body weight, body length, fore limb length and hind limb length are significantly correlated with each other ($p<0.0001$, Pearson correlation) but not with the liver weight and the fat body weight. Moreover, the liver weight and fat body weight are significantly correlated with each other ($r=0.75$ with $p<0.001$, Pearson correlation) (supplementary table 1A).

In female, the morphological data for different age groups shows the similar pattern as observed for the males but slightly later in time and reach their higher at Met + 5-6 weeks of age. Indeed, the body weight, the body length and the fat body somatic index are significantly increasing from Met + 1-2 weeks to Met + 5-6 weeks ($p<0.05$, Fig.1E, F and H). No significant difference was found for the liver somatic index in different age groups in the females (Fig.1G). Moreover, the morphological data are significantly correlated with each other ($p<0.01$, Pearson correlation) except, the fore limb length which is not correlated with the liver weight and the fat body weight (supplementary table 1B).

Histological evaluation of the gonads

The testis area and the testis maturity score increased with age in juvenile *X. tropicalis* with a significantly larger and more mature testis at Met + 7-8 weeks compare to Met + 1-2 weeks ($p<0,05$, Fig.2A, B). The testis area and the testis maturity score are significantly positively correlated to the age of the frogs ($r=0,49$ and $r=0,54$ respectively, $p<0,001$, Fig.2C, D). Finally, the testis area and the testis maturity score are also significantly and positively correlated together ($r=0,71$, $p<0,001$, Fig.2E).

Ovary area and the number of follicular oocytes increase with age in juvenile *X. tropicalis* with a significantly larger ovary area and more follicular oocytes at Met + 7-8 weeks compare to Met + 1-2 weeks ($p<0,05$; Fig.3A). Also, the ovary area and the number of follicular oocytes are significantly positively correlated to age ($r=0,39$ with $p<0,01$ and $r=0,37$ with $p<0,05$ respectively, Fig.3C, D).

Finally, the ovary area and the follicular oocytes number are significantly and positively correlated to each other (r=0,90; p<0,001; Fig.3E).

Finally, the gonadal development is positively correlated with the body development in males but not in female frogs. Testis area and testis maturity score are positively correlated with body weight, body length, hind limb length and fore limb length (p≤0,05, Pearson correlation). The testis area and the testis maturity score are not significantly correlated to the liver weight and the fat body weight (supplementary table 2).

Gene expression ontogeny

Relative gene expression has been analysed from gonad-kidney complex samples from males and females in post-metamorphic immature frogs. We focused our research on genes implicated in germ cell development, steroidogenic pathway and retinoic synthesis.

Relative expression for germ cells specific gene *Id4* present a significant decrease between Met + 1-2 weeks to Met + 7-8 weeks in females, whereas no significant variation is found overtime in males. At Met + 7-8 weeks, *Id4* relative expression is significantly higher in males compare to females (Fig.4A). *Ddx4* relative expression increase significantly between Met + 5-6 weeks and Met + 7-8 weeks in males and between Met + 3-4 weeks and Met + 7-8 weeks in females. Moreover, *Ddx4* relative expression is higher in female compare to male at all ages (Fig.4B). Finally, we analysed *Dmrt1* relative gene expression and no significant difference has been found between sexes and overtime (Fig.4C).

Then, we analysed the expression of genes involved in steroidogenesis; *Cyp17* is increasing with time in males' frogs at Met + 1-2 weeks compare to Met + 7-8 weeks whereas no change is observed overtime for the females. Moreover, *Cyp17* expression is significantly higher in males compare to females at all age (Fig.4D). Finally, relative expression of the gene *3βhsd* (Fig.4E) and gene expression of *Cyp19* (Fig.4F) do not present significant differences between sexes or ages.

For the genes implicated in male's gonad differentiation, *Amh* relative expression do not significantly change overtime in males neither in females but, it is significantly higher in males compare to females

at Met + 7-8 weeks (Fig.4G). The gene expression of its receptor, *Amhr2*, is significantly decreasing in female individuals from Met + 3-4 weeks to Met + 7-8 weeks and no significant difference is found in males overtime. At Met + 7-8 weeks, *Amhr2* level is significantly lower in females compare to males (Fig.4H). Then, *Sox9* relative expression in post-metamorphic frogs do not show significant differences between sexes or age's groups (Fig.4I). Finally, we analysed *Rbsn1* gene expression and a significant increase is observed in females between Met + 1-2 weeks and Met + 7-8 weeks whereas no significant difference is found overtime in males. Also, *Rbsn1* gene expression is significantly higher in females compare to males at Met + 5-6 weeks and Met + 7-8 weeks (Fig.4J).

Finally, for the genes implicated in the retinoic acid pathway, *Aldh1a2* expression was analysed and shows a significant increase in females from Met + 1-2 weeks to Met + 5-6 weeks and Met + 7-8 weeks whereas no significant variation is observed in male's individuals with time. Moreover, *Aldh1a2* expression is significantly higher in females compare to males at Met + 5-6 weeks and Met + 7-8 weeks (Fig.4K). Lastly, the *Cyp26b1* gene expression do not significantly differ overtime for males or females and no sexes difference is found (Fig.4L).

Principal Component Analysis

The Principal Component Analysis (PCA) representation including sex-specific gene expression in male and female frogs shows a different repartition of female and male individuals suggesting a strong association between the sex and the relative gene expression (Fig.5A). The genes associated with female individuals are *Ddx4*, *Aldh1a2* and *Rbsn1*; and the genes strongly associated with male individuals are *Cyp17*, *Dmrt1*, *Amh*, *Esr1*, *Amhr2*, *Id4* and *Cyp26b1* (Fig.5A). When looking at PCA for male individuals only, the representation including the gene expression, the gonad parameters and the age, no strong association were observed. Also, the PCA representation present a strong association between body measurements and gonad maturity data and a negative association between *3βhsd* gene expression and *Dmrt1*, *Amh*, *Amhr2*, *Cyp17* and *Cyp26b1* genes as the arrows are pointed in opposite direction (Fig.5B). For the females, the PCA representation shows a strong association between gonad maturity data and *Ddx4*, *Aldh1a2* and *Rsbn1* relative expression (Fig.5C).

Correlation between gene expression and gonadal development

More in details, the correlation between the relative gene expression of sex-specific genes and gonad maturity data has been analysed in male and female post-metamorphosis frogs (Table 2). The data obtained shows R coefficient after Pearson correlation analysis and the statistical significance. In male, testis area and the testis maturity are positively correlated with relative expression of *Ddx4*, *Dmrt1*, *Cyp17*, *Amhr2* and *Cyp26b1*. In female, ovary area is positively correlated with relative expression of *Ddx4*, *Aldh1a2* and *Rsbn1* and negatively correlated with *Amhr2* and *3βhsd*. Finally, the number of follicular oocytes is positively correlated with *Ddx4*, *Aldh1a2* and *Rsbn1* (Table 2).

Bayesian network analysis

The network structure is illustrated in the network plot in Fig. 6. Only connections with strong evidence for inclusion ($BF_{10} > 10$), highlighted in Fig. S1, are discussed here.

Within the Met1-4 group, seven nodes exhibited significant and strong associations (Fig. S1A). Among these, three connections were negative (ddx4-dmrt1, dmrt1-esr1, and esr1-amh), and two were positive (id4-ddx4 and 3βhsd-cyp19) (Fig. 1A). In the Met5-8 group, nine nodes demonstrated significant associations (Fig. S1B), including three strong connections: two negative (dmrt1-amhr2 and aldh1a2-cyp19) and one positive (ddx4-3βhsd) (Fig. 1B). The only significant connection retained across both Met1-4 and Met5-8 groups was esr1-amh. Notably, this connection appeared to lose its negative correlation as age increased.

Regarding the grouping by sex, in the male group, only four nodes exhibited significant associations (Fig. S1C). Among these, the connection aldh1a2-cyp19 was strongly negative, while amhr2-sox9 showed a moderate negative association (Fig. 1C). In the female group, seven nodes demonstrated significant associations (Fig. S1D). Three connections were strongly negative (amhr2-3βhsd, id4-sox9, and ddx4-aldh1a2), one was moderately negative (id4-cyp26b1), and one was positive (id4-ddx4). No significant connections were retained across both male and female groups

Discussion

In this study, we investigated the post-metamorphic development of *Xenopus tropicalis* by analyzing morphological parameters, gonadal maturation at histological level, gene expression profiles, and network associations among key genes involved in sex differentiation and gonadal development. Our findings reveal sex-specific patterns in growth and development, distinct gene expression trajectories and dynamics, and interactions among genes that correlate with gonadal maturation and histological features.

Both male and female frogs exhibited increases in body weight and length with age, although these changes were not statistically significant in males. Females showed significant growth in body weight and body length from Metamorphosis (Met) +1–2 weeks to Met +5–6 weeks (Fig 1E, F). The liver and fat body somatic indices in males increased from Met +1–2 weeks to Met +3–4 weeks but decreased significantly by Met +7–8 weeks (Fig 1C, D). This pattern may reflect shifts in energy storage and utilization during development. In contrast, the fat body somatic index of females increases for longer time compared to male, significantly peaking at Met5–6 (Fig. 1H). Females did not exhibit significant changes in liver somatic index across age groups, but it follows a trend similar to the fat body somatic index, reaching a peak at Met5–6 (Fig. 1G). Altogether, the data indicating possible differences in metabolic demands or storage strategies between sexes, as well as a sex-specific growth rates post-metamorphosis, potentially linked to differing energy allocations between somatic growth and reproductive development.

Gonadal maturation correlated with age in both sexes but manifested differently. Males showed significant increases in testis area and maturity score by Met7–8, which were positively correlated with body measurements such as body weight, body length, and limb lengths. This suggests that somatic growth and testicular development are closely linked in males. In females, ovary area and follicular oocyte numbers increased significantly, particularly at Met +7–8 weeks. However, female gonadal development did not correlate with body measurements, implying that ovarian maturation may be regulated independently of overall body growth after metamorphosis. This is in line with what

is observed in female *Xenopus* tadpoles, which show heterochrony of ovarian differentiation, independent of the somatic development (Ogielska & Kotusz, 2004).

Our gene expression analysis revealed sex-specific patterns over time. In males, genes associated with steroidogenesis and male differentiation, such as *Cyp17* and *Amh*, showed increased expression with age. The consistently increasing expression of *Cyp17* in males aligns with its role in androgen synthesis, essential for testicular development and spermatogenesis (Payne & Hales, 2004). Similarly, *Amh* plays a critical role in male sex differentiation by inhibiting the development of female reproductive structures (Josso & Clemente, 2003). Our results corroborate findings by Jansson et al. (2016), who reported sex-dependent expression of *amh* during sex organ differentiation in *Xenopus tropicalis*, from NF 53 to 6 days post-metamorphosis. Females exhibited increased expression of *Ddx4*, *Aldh1a2*, and *Rbsn1* with age. *Ddx4* is a germ cell marker, and its elevated expression corresponds with the increase in follicular oocytes, consistent with its role in oogenesis (Raz, 2000). The upregulation of *Aldh1a2*, involved in retinoic acid synthesis, suggests a role in ovarian development, as retinoic acid is critical for meiosis initiation in germ cells. Correlation analyses showed that in males, testis area and maturity score were positively correlated with the expression of genes like *Ddx4*, *Dmrt1*, *Cyp17*, *Amhr2*, and *Cyp26b1*, highlighting the coordinated regulation of genes involved in germ cell development, steroidogenesis, and retinoic acid metabolism during testicular maturation. *Dmrt1* is a well-established regulator of male sex determination and testis development in vertebrates (Matson & Zarkower, 2012), but its role on *X. tropicalis* is understudied. While in *X. laevis dmrt1* seems to act with its duplicated variant (*dwm*) to inhibits or promote masculinization (Yashimoto et al., 2008, 2010), in *X. tropicalis* this paralogue is missing because the gene duplication (~10 million years ago) was subsequent to speciation from *X. leavis* (~58 million years ago – Matson & Zarkower, 2012; Kumar et al., 2022). Our results did not show significant differences of *Dmrt1* transcripts among ages and sexes of post-metamorphic *X. tropicalis*, likely due to its differential action on sex determination during the late premetamorphosis. It would be interesting to further investigate the role of this transcript on influencing sex determination previously the climax. In females, ovary area and follicular oocyte numbers were positively correlated with

Ddx4, *Aldh1a2*, and *Rbsn1* expression, reinforcing the importance of these genes in ovarian development and oocyte formation.

The Principal Component Analysis (PCA) provided a clear distinction between male and female gene expression profiles. Males clustered with genes like *Cyp17* and *Amh*, critical for testicular function and male differentiation. Females associated with *Ddx4*, *Aldh1a2*, and *Rbsn1*, reflecting their roles in oogenesis and ovarian development. To further understand the interactions among genes, we performed a Bayesian network analysis. Within the younger age group (Met +1–4 weeks), significant associations included negative connections between *ddx4* and *dmrt1*, *dmrt1* and *esr1*, and *esr1* and *amh*, as well as positive connections between *id4* and *ddx4*, and *3βhsd* and *cyp19*. These findings suggest that in early post-metamorphic stages, *Dmrt1* may negatively regulate *Ddx4*, a germ cell marker, and *Esr1* – or viceversa – , the estrogen receptor, which in turn negatively regulates *Amh* – or viceversa –, a key male differentiation gene. In the older age group (Met +5–8 weeks), significant associations included negative connections between *dmrt1* and *amhr2*, and *aldh1a2* and *cyp19*, and a positive connection between *ddx4* and *3βhsd*. The persistent negative association between *dmrt1* and *amhr2* suggests a regulatory mechanism where *Dmrt1* suppresses *Amhr2* expression – or viceversa – as gonadal maturation progresses. The negative association between *aldh1a2* (involved in retinoic acid synthesis) and *cyp19* (aromatase) may indicate a shift in retinoic acid metabolism affecting estrogen synthesis pathways during development. Analyzing data by sex, in males, significant associations included a strong negative connection between *aldh1a2* and *cyp19*, and a moderate negative association between *amhr2* and *sox9*. The negative association between *aldh1a2* and *cyp19* aligns with the suppression of estrogen synthesis pathways in males. The negative association between *amhr2* and *sox9*, both important for male differentiation, may reflect complex feedback mechanisms during testis development. In females, significant associations included strong negative connections between *amhr2* and *3βhsd*, *id4* and *sox9*, and *ddx4* and *aldh1a2*, as well as a positive connection between *id4* and *ddx4*. The negative association between *amhr2* and *3βhsd* suggests that as *Amhr2* expression decreases, possibly indicating reduced anti-Müllerian hormone signaling, *3βhsd* expression also decreases, affecting steroidogenesis. The positive association between *id4* and *ddx4*

supports their roles in germ cell development, with *Id4* potentially promoting *Ddx4* expression during oogenesis.

Integrating the outcomes from different methods, we observe that morphological development, gonadal maturation, gene expression patterns, and gene network interactions are interconnected. In males, the increase in testis size and maturity correlates with elevated expression of genes essential for testis development and function (*Dmrt1*, *Amh*, *Cyp17*), and these genes are interconnected through regulatory networks identified in the Bayesian analysis. The negative associations among *dmrt1*, *esr1*, and *amh* suggest that male differentiation involves the suppression of estrogen pathways, consistent with the low expression of *Cyp19* (aromatase) in males. In females, the increase in ovary size and follicular oocyte numbers correlates with higher expression of genes involved in oocyte development (*Ddx4*, *Aldh1a2*, *Rbsn1*), and these genes are positively associated in the Bayesian network. The negative associations between *amhr2* and *3βhsd*, and between *id4* and *sox9*, indicate that as ovarian maturation progresses, there is a downregulation of male differentiation pathways and certain aspects of steroidogenesis. The PCA further supports these findings by clustering individuals based on gene expression profiles corresponding to their sex and developmental stage. This integration of morphological data, gene expression, PCA, and Bayesian network analysis provides a comprehensive view of the developmental processes in *X. tropicalis*, highlighting the complex interplay between growth, gonadal maturation, and molecular regulation.

The differential gene expression patterns and network associations suggest sex-specific regulatory mechanisms guiding gonadal development post-metamorphosis. In males, the upregulation of genes involved in androgen synthesis (*Cyp17*), male differentiation (*Amh*), and retinoic acid metabolism (*Cyp26b1*) likely drives testicular maturation. The negative associations between *dmrt1* and genes like *esr1* and *amhr2* indicate that *Dmrt1* may suppress estrogen signaling pathways and modulate anti-Müllerian hormone signaling during testis development. In females, the increased expression of genes associated with retinoic acid synthesis (*Aldh1a2*) and germ cell markers (*Ddx4* along with their positive associations, indicates a focus on oocyte development and maturation. The negative

associations between *amhr2* and *3βhsd*, and between *id4* and *sox9*, suggest a downregulation of male differentiation pathways and certain steroidogenic enzymes as the ovary matures.

One limitation of our study is the use of gonad-kidney complex samples for gene expression analysis, which may include signals from non-gonadal tissues. Isolating pure gonadal tissue could provide more precise insights into gene expression changes. Additionally, the sample sizes for some age groups were relatively small, potentially affecting the statistical power of the analyses. While the Bayesian network analysis provides insights into potential regulatory relationships, it does not establish causality, and experimental validation is necessary to confirm these interactions.

Conclusions

Our study demonstrates that post-metamorphic development in *X. tropicalis* is characterized by sex-specific growth patterns, gonadal maturation, distinct gene expression profiles, and complex gene interactions. The coordinated regulation of genes involved in germ cell development, steroidogenesis, and retinoic acid synthesis underscores the intricate molecular mechanisms driving sexual maturation. Integrating outcomes from different methods allowed us to construct a comprehensive picture of the developmental processes, highlighting the importance of multifaceted approaches in understanding biological systems.

Investigating the regulatory networks and hormonal cues that govern the observed gene expression patterns will further elucidate the mechanisms of gonadal development in is animal model. Experimental studies to validate the predicted gene interactions from the Bayesian network analysis are necessary. Understanding these processes in *X. tropicalis* can provide valuable insights into vertebrate reproductive biology and inform studies on environmental factors affecting sexual development.

References

1. Berg, C., 2019. The Xenopus tropicalis Model for Studies of Developmental and Reproductive Toxicity, in: Hansen, J.M., Winn, L.M. (Eds.), Developmental Toxicology, Methods in Molecular Biology. Springer New York, New York, NY, pp. 173–186. https://doi.org/10.1007/978-1-4939-9182-2_12

2. Berg, C., Gyllenhammar, I., Kvarnryd, M., 2009. *Xenopus tropicalis* as a Test System for Developmental and Reproductive Toxicity. J. Toxicol. Environ. Health A 72, 219–225. https://doi.org/10.1080/15287390802539079

3. Capel, B., 2017. Vertebrate sex determination: evolutionary plasticity of a fundamental switch. Nat. Rev. Genet. 18, 675–689. https://doi.org/10.1038/nrg.2017.60

4. Carreau, S., Hess, R.A., 2010. Oestrogens and spermatogenesis. Philos. Trans. R. Soc. Lond. B. Biol. Sci. 365, 1517–1535. https://doi.org/10.1098/rstb.2009.0235

5. El Jamil, A., Magre, S., Mazabraud, A., Penrad-Mobayed, M., 2008. Early aspects of gonadal sex differentiation in Xenopus tropicalis with reference to an antero-posterior gradient. J. Exp. Zool. Part Ecol. Genet. Physiol. 309A, 127–137. https://doi.org/10.1002/jez.439

6. Haczkiewicz, K., Rozenblut-Kościsty, B., Ogielska, M., 2017. Prespermatogenesis and early spermatogenesis in frogs. Zoology 122, 63–79. https://doi.org/10.1016/j.zool.2017.01.003

7. Haselman, J.T., Olmstead, A.W., Degitz, S.J., 2015. Global gene expression during early differentiation of Xenopus (Silurana) tropicalis gonad tissues. Gen. Comp. Endocrinol. 214, 103–113. https://doi.org/10.1016/j.ygcen.2014.06.009

8. Hirsch, N., Zimmerman, L.B., Grainger, R.M., 2002. Xenopus, the next generation: X. tropicalis genetics and genomics. Dev. Dyn. Off. Publ. Am. Assoc. Anat. 225, 422–433. https://doi.org/10.1002/dvdy.10178

9. Iwade, R., Maruo, K., Okada, G., Nakamura, M., 2008. Elevated expression of P450c17 (CYP17) during testicular formation in the frog. Gen. Comp. Endocrinol. 155, 79–87. https://doi.org/10.1016/j.ygcen.2007.02.032

10. Jansson, E., Mattsson, A., Goldstone, J., & Berg, C. (2016). Sex-dependent expression of anti-Müllerian hormone (amh) and amh receptor 2 during sex organ differentiation and characterization of the Müllerian duct development in Xenopus tropicalis. General and Comparative Endocrinology, 229, 132-144.

11. Josso, N., & di Clemente, N. (2003). Transduction pathway of anti-Müllerian hormone, a sex-specific member of the TGF-β family. Trends in Endocrinology & Metabolism, 14(2), 91-97.

12. Kelley, D., 1996. Sexual differentiation in Xenopus laevis. Biol. Xenopus.

13. Kumar, S., Suleski, M., Craig, J. M., Kasprowicz, A. E., Sanderford, M., Li, M., ... & Hedges, S. B. (2022). TimeTree 5: an expanded resource for species divergence times. *Molecular biology and evolution*, *39*(8), msac174.

14. Kvarnryd, M., Grabic, R., Brandt, I., Berg, C., 2011. Early life progestin exposure causes arrested oocyte development, oviductal agenesis and sterility in adult Xenopus tropicalis frogs. Aquat. Toxicol. Amst. Neth. 103, 18–24. https://doi.org/10.1016/j.aquatox.2011.02.003

15. Maruo, K., Suda, M., Yokoyama, S., Oshima, Y., Nakamura, M., 2008. Steroidogenic gene expression during sex determination in the frog Rana rugosa. Gen. Comp. Endocrinol. 158, 87–94. https://doi.org/10.1016/j.ygcen.2008.04.019

16. Matson, C. K., & Zarkower, D. (2012). Sex and the singular DM domain: insights into sexual regulation, evolution and plasticity. *Nature Reviews Genetics*, *13*(3), 163-174.

17. Moritz, L., Hammoud, S.S., 2022. The Art of Packaging the Sperm Genome: Molecular and Structural Basis of the Histone-To-Protamine Exchange. Front. Endocrinol. 13, 895502. https://doi.org/10.3389/fendo.2022.895502

18. Nagahama, Y., Chakraborty, T., Paul-Prasanth, B., Ohta, K., Nakamura, M., 2021. Sex determination, gonadal sex differentiation, and plasticity in vertebrate species. Physiol. Rev. 101, 1237–1308. https://doi.org/10.1152/physrev.00044.2019

19. Nakamura, M., 2010. The mechanism of sex determination in vertebrates-are sex steroids the key-factor? J. Exp. Zool. Part Ecol. Genet. Physiol. 313, 381–398. https://doi.org/10.1002/jez.616

20. Navarro-Martín, L., Velasco-Santamaría, Y.M., Duarte-Guterman, P., Robertson, C., Lanctôt, C., Pauli, B., Trudeau, V.L., 2012. Sexing Frogs by Real-Time PCR: Using Aromatase *(cyp19)* as an Early Ovarian Differentiation Marker. Sex. Dev. 6, 303–315. https://doi.org/10.1159/000343783

21. Nieuwkoop, P.D., Faber, J. (Eds.), 1956. Normal table of Xenopus laevis (Daudin): a systematical and chronological survey of the development from the fertilized egg till the end of metamorphosis. Garland Pub, New York.

22. Ogielska, M., & Kotusz, A. (2004). Pattern and rate of ovary differentiation with reference to somatic development in anuran amphibians. Journal of morphology, 259(1), 41-54.

23. Ogielska, M., Kotusz, A., Augustyńska, R., Ihnatowicz, J., Paśko, Ł., 2013. A stockpile of ova in the grass frog Rana temporaria is established once for the life span. Do ovaries in amphibians and in mammals follow the same evolutionary strategy? Anat. Rec. Hoboken NJ 2007 296, 638–653. https://doi.org/10.1002/ar.22674

24. Ohyama, K., Ohta, M., Hosaka, Y.Z., Tanabe, Y., Ohyama, T., Yamano, Y., 2015. Expression of anti-Mumlerian hormone and its type II receptor in germ cells of maturing rat testis. Endocr. J. 62, 997–1006. https://doi.org/10.1507/endocrj.EJ15-0370

25. Olmstead, A.W., Korte, J.J., Woodis, K.K., Bennett, B.A., Ostazeski, S., Degitz, S.J., 2009. Reproductive maturation of the tropical clawed frog: Xenopus tropicalis. Gen. Comp. Endocrinol. 160, 117–123. https://doi.org/10.1016/j.ygcen.2008.10.025

26. Orton, F., Säfholm, M., Jansson, E., Carlsson, Y., Eriksson, A., Fick, J., Uren Webster, T., McMillan, T., Leishman, M., Verbruggen, B., Economou, T., Tyler, C.R., Berg, C., 2018. Exposure to an anti-androgenic herbicide negatively impacts reproductive physiology and fertility in Xenopus tropicalis. Sci. Rep. 8, 9124. https://doi.org/10.1038/s41598-018-27161-2

27. Orton, F., Tyler, C.R., 2015. Do hormone-modulating chemicals impact on reproduction and development of wild amphibians?: Endocrine disruption in amphibians. Biol. Rev. 90, 1100–1117. https://doi.org/10.1111/brv.12147

28. Payne, A. H., & Hales, D. B. (2004). Overview of steroidogenic enzymes in the pathway from cholesterol to active steroid hormones. Endocrine Reviews, 25(6), 947–970.

29. Pettersson, I., Arukwe, A., Lundstedt-Enkel, K., Mortensen, A.S., Berg, C., 2006. Persistent sex-reversal and oviducal agenesis in adult Xenopus (Silurana) tropicalis frogs following larval exposure to the environmental pollutant ethynylestradiol. Aquat. Toxicol. 79, 356–365. https://doi.org/10.1016/j.aquatox.2006.07.004

30. Piprek, R.P., Damulewicz, M., Kloc, M., Kubiak, J.Z., 2018. Transcriptome analysis identifies genes involved in sex determination and development of Xenopus laevis gonads. Differentiation 100, 46–56. https://doi.org/10.1016/j.diff.2018.02.004

31. Piprek, R.P., Pecio, A., Laskowska-Kaszub, K., Kloc, M., Kubiak, J.Z., Szymura, J.M., 2013. Retinoic acid homeostasis regulates meiotic entry in developing anuran gonads and in Bidder's organ through Raldh2 and Cyp26b1 proteins. Mech. Dev. 130, 613–627. https://doi.org/10.1016/j.mod.2013.09.001

32. Pradhan, A., Olsson, P.-E., Pradhan, A., Olsson, P.-E., 2016. Regulation of zebrafish gonadal sex differentiation. AIMS Mol. Sci. 3, 567–584. https://doi.org/10.3934/molsci.2016.4.567

33. Rasar, M.A., Hammes, S.R., 2006. The physiology of the Xenopus laevis ovary. Methods Mol. Biol. Clifton NJ 322, 17–30. https://doi.org/10.1007/978-1-59745-000-3_2

34. Roco, Á.S., Olmstead, A.W., Degitz, S.J., Amano, T., Zimmerman, L.B., Bullejos, M., 2015. Coexistence of Y, W, and Z sex chromosomes in Xenopus tropicalis. Proc. Natl. Acad. Sci. U. S. A. 112, E4752-4761. https://doi.org/10.1073/pnas.1505291112

35. Roco, Á.S., Ruiz-García, A., Bullejos, M., 2021a. Interaction between sex-determining genes from two species: clues from Xenopus hybrids. Philos. Trans. R. Soc. Lond. B. Biol. Sci. 376, 20200104. https://doi.org/10.1098/rstb.2020.0104

36. Roco, Á.S., Ruiz-García, A., Bullejos, M., 2021b. Testis Development and Differentiation in Amphibians. Genes 12, 578. https://doi.org/10.3390/genes12040578

37. Säfholm, M., Jansson, E., Fick, J., Berg, C., 2016. Molecular and histological endpoints for developmental reproductive toxicity in Xenopus tropicalis: Levonorgestrel perturbs anti-Müllerian hormone and progesterone receptor expression. Comp. Biochem. Physiol. 10.

38. Sun, F., Xu, Q., Zhao, D., Degui Chen, C., 2015. Id4 Marks Spermatogonial Stem Cells in the Mouse Testis. Sci. Rep. 5, 17594. https://doi.org/10.1038/srep17594

39. Svanholm, S., Säfholm, M., Brande-Lavridsen, N., Larsson, E., Berg, C., 2021. Developmental reproductive toxicity and endocrine activity of propiconazole in the Xenopus tropicalis model. Sci. Total Environ. 753, 141940. https://doi.org/10.1016/j.scitotenv.2020.141940

40. Tadjuidje, E., Heasman, J., 2010. Xenopus as an Experimental Organism, in: ELS. John Wiley & Sons, Ltd. https://doi.org/10.1002/9780470015902.a0002030.pub2

41. Tlapakova, T., Nguyen, T.M.X., Vegrichtova, M., Sidova, M., Strnadova, K., Blahova, M., Krylov, V., 2016. Identification and characterization of *Xenopus tropicalis* common progenitors of Sertoli and peritubular myoid cell lineages. Biol. Open 5, 1275–1282. https://doi.org/10.1242/bio.019265

42. Verbrugghe, E., Martel, A., Pasmans, F., 2019. Reference Gene Validation for Quantitative Real-time PCR Studies in Amphibian Kidney-derived A6 Epithelial Cells. Altern. Lab. Anim. 47, 63–70. https://doi.org/10.1177/0261192919862936

43. Vining, B., Ming, Z., Bagheri-Fam, S., Harley, V., 2021. Diverse Regulation but Conserved Function: SOX9 in Vertebrate Sex Determination. Genes 12, 486. https://doi.org/10.3390/genes12040486

44. Xu, H., Lim, M., Dwarakanath, M., Hong, Y., 2014. Vasa Identifies Germ Cells and Critical Stages of Oogenesis in the Asian Seabass. Int J Biol Sci 10, 11.

45. Yoshimoto S, Ikeda N, Izutsu Y, Shiba T, Takamatsu N, Ito M (2010) Opposite roles of DMRT1 and its W-linked paralogue, DM-W, in sexual dimorphism of Xenopus laevis: implications of a ZZ/ZWtype sex-determining system. Development 137:2519–2526

46. Yoshimoto, S., Ikeda, N., Izutsu, Y., Shiba, T., Takamatsu, N., Ito, M., 2010. Opposite roles of DMRT1 and its W-linked paralogue, DM-W, in sexual dimorphism of Xenopus laevis: implications of a ZZ/ZW-type sex-determining system. Development 137, 2519–2526. https://doi.org/10.1242/dev.048751

47. Yoshimoto, S., Okada, E., Umemoto, H., Tamura, K., Uno, Y., Nishida-Umehara, C., Matsuda, Y., Takamatsu, N., Shiba, T., Ito, M., 2008. A W-linked DM-domain gene, DM-W, participates in primary ovary development in Xenopus laevis. Proc. Natl. Acad. Sci. 105, 2469–2474. https://doi.org/10.1073/pnas.0712244105

48. Yoshimoto, S., Okada, E., Umemoto, H., Tamura, K., Uno, Y., Nishida-Umehara, C., ... & Ito, M. (2008). A W-linked DM-domain gene, DM-W, participates in primary ovary development in Xenopus laevis. *Proceedings of the National Academy of Sciences*, *105*(7), 2469-2474.

Tables, Figures and Supplementary files

Sex differences in gene expression associated with gonadal development during peri-pubertal period in juvenile *Xenopus tropicalis*

Vanessa Brouard[1], Daniele Marini[1,2,*], Mauricio Roza[3], Sofie Svanholm[1]and Cecilia Berg[1]

[1]Department of Environmental Toxicology, Uppsala University, 754 36 Uppsala, Sweden;

[2] Department of Veterinary Medicine, University of Perugia, 06126 Perugia, Italy;

[3] Science for Life Laboratory, Department of Environmental Science, Stockholm University, 114 18 Stockholm, Sweden;

* Corresponding author: daniele.marini@ebc.uu.se

| Gene name	Accession #	Forward Sequence	Reverse Sequence
Eukaryotic translation elongation Factor 1 alpha (Ef1)	NM_001016692.2	CTCTCAGGCTGACTGTGCTG	ATGCTCACGAGTTTGTCCGT
Ribosomal protein L8 (Rpl8) [a]	BC059744	CCCTCAACCATCAGGAGAGA	TCTTTGTACCACGCAGACGA
SRY-Box Transcription Factor 9 (Sox9)	NM_001016853.2	ACATTCAGGTCAGTCCCAAGG	TCCCTCTTCAGGTCTGGCTT
Cytochrome P450 family 17 subfamily A member 1 (Cyp17)	NM_001127045.1	ATAAAGAGGCGTTTTGCGGC	AGTCCGACCTCCTGGGAAAT
3 Beta-hydroxysteroid dehydrogenase (3β-hsd)	XM_031896427.1	CCAATCCCTGGTTACTAAGGCA	GTTTAGTGACTCCCCAATGGCA
Doublesex and Mab-3 Related Transcription Factor 1 (Dmrt1)	XM_031890717.1	GGACAGAGTGTACCCAACCC	GAGAAAGCACTGCACTTGCC
Inhibitor of DNA binding 4 (Id4)	NM_001004839.1	CGCCGAACAAGAAAGTCAGC	CGGGTCAGTATTGAGGTCCG
Round spermatid basic protein 1 (Rbsn1)	NM_001112954.2	CCATACGCAGGTAAGCAGGA	CTCTTCGTCAACAGCACCCA
DEAD-box helicase 4 (ddx4)	NM_001016823.3	TGAAAGGGGTGGGCCTACTA	ATTCCAATCACCTCTTCCTCGAA
Cytochrome P450 Family 19 Subfamily A Member 1 (Cyp19)[b]	NM_001097161.1	GAATCCCGTGCAGTATAACAGC	ACAGGTCTCCTCTTGATTCCATAG
Aldehyde dehydrogenase 1 family member A2 (Aldh1a2)	NM_001045731.1	ATTGGCGTGTGTGGTCAGAT	ACAGGGCAGGAGCAATCTTC
Cytochrome P450 family 26 subfamily B member 1 (Cyp26b1)	NM_001079187.2	TCCCCTGTACAAAGCATAGACAA	GGTGTTACAATGCACTGCCC
Estrogen receptor 1 (Esr1)	NM_203535.1	AATGTGCCTCCAAGTCCTGT	TCTGTTGTCTGAACTTGACCTGT
Anti-Mullerian Hormone (Amh)	XM_004911423.4	GTCAGTCCAAGCTTTAGTACCCA	ATCGCCAACACTGTGATCGT
Anti-Mullerian Hormone Receptor 2 (Amhr2) [b]	ENSXETT00000063675	AAAGACGGCCACAGCTTCC	CAGGATCCCAGCAATCTTCC

Table1. qPCR primers sequence for *Xenopus tropicalis* used in this study.
[a] Orton *et al*. 2018; [b] Jansson *et al*. 2016
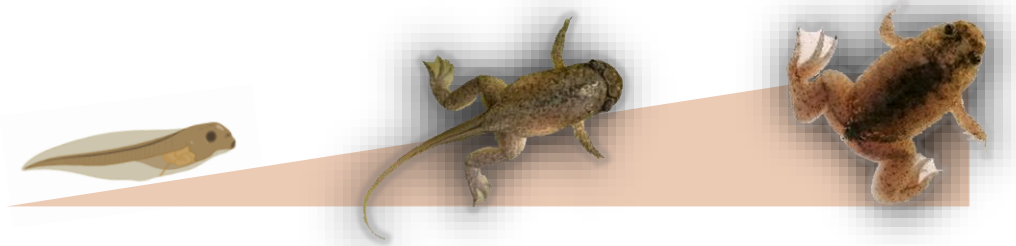
Wild type *X. tropicalis*
>80 individuals raised UNTIL METHAMORPHOSIS →
i.e. weeks post methamorphosis (WPM)
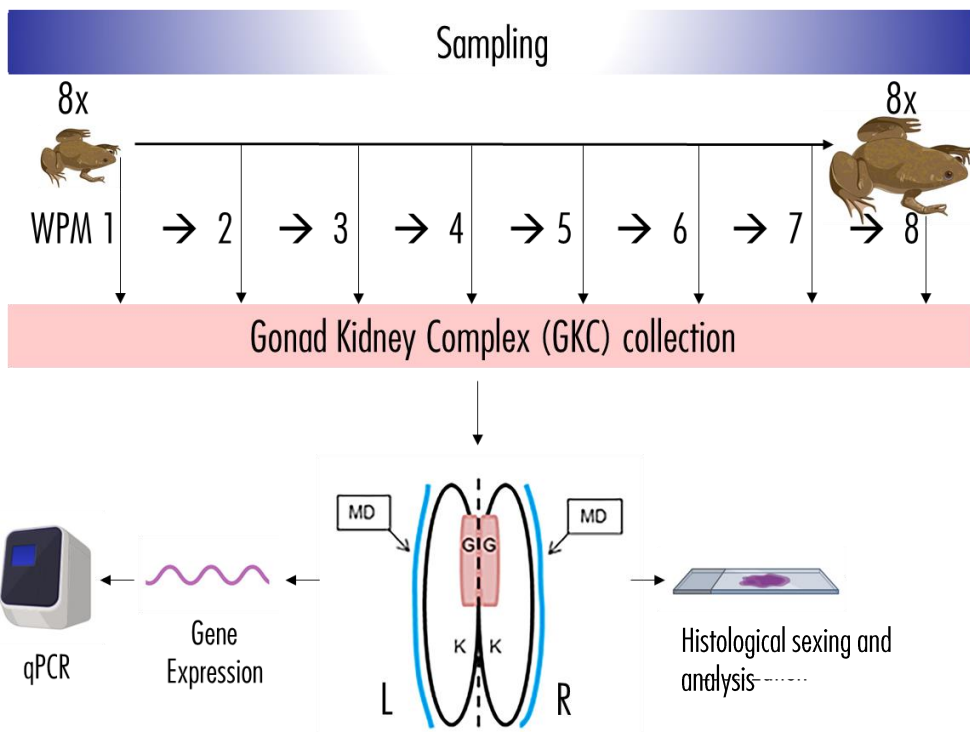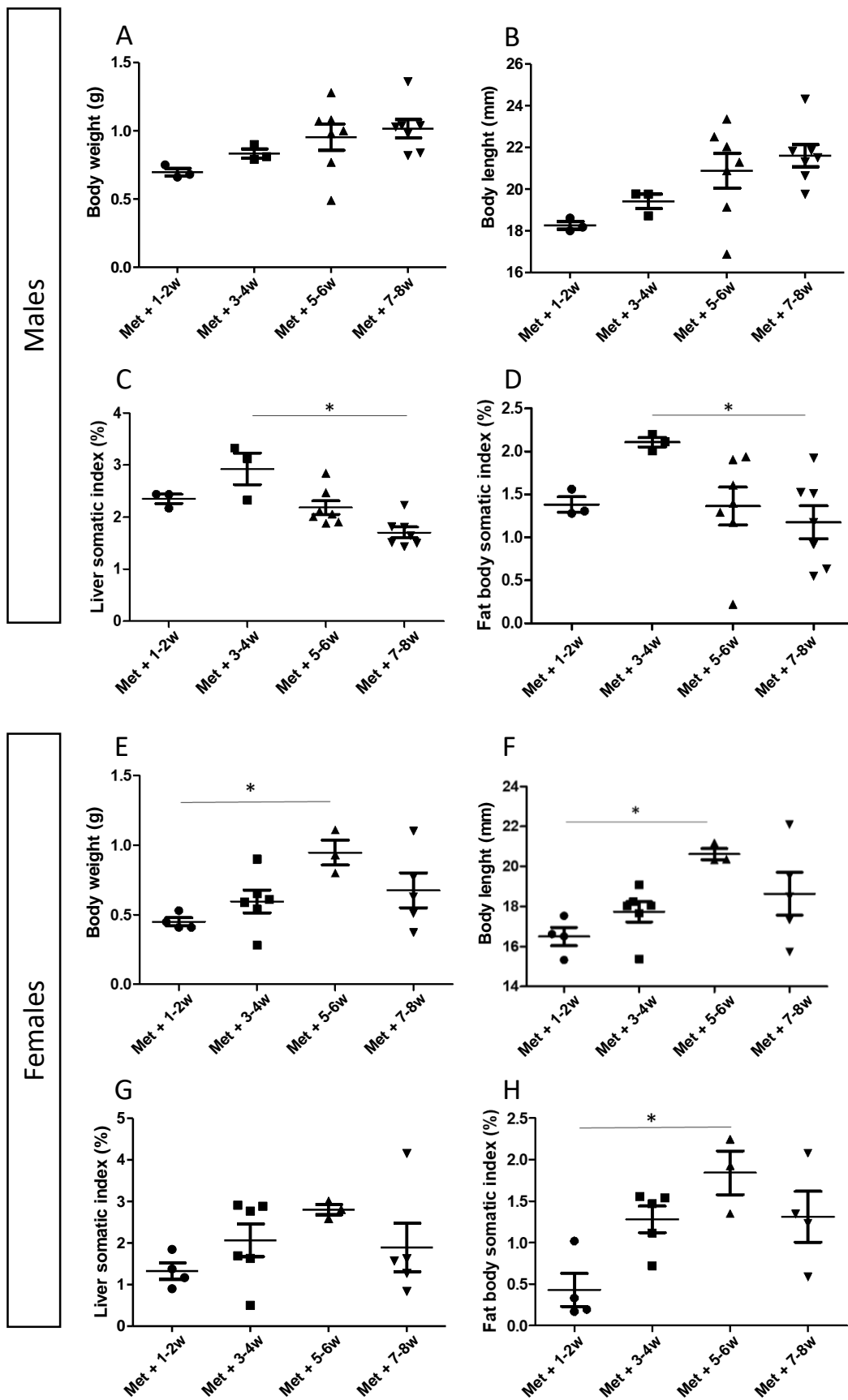

Graphical abstract of experimental design

Fig. 1 : Body, liver and fat body measurement in post metamorphosis male and female frogs.
(A) Male and (E) female body weight at different age after metamorphosis. (B) Male and (F) female body length at different age after metamorphosis. (C) Male and (G) female liver somatic index at different age after metamorphosis. (D) Male and (H) female fat body somatic index at different age after metamorphosis. Statistical significance were analysed using Kruskall-Wallis test followed by Dunn's comparison with * p< 0,05.
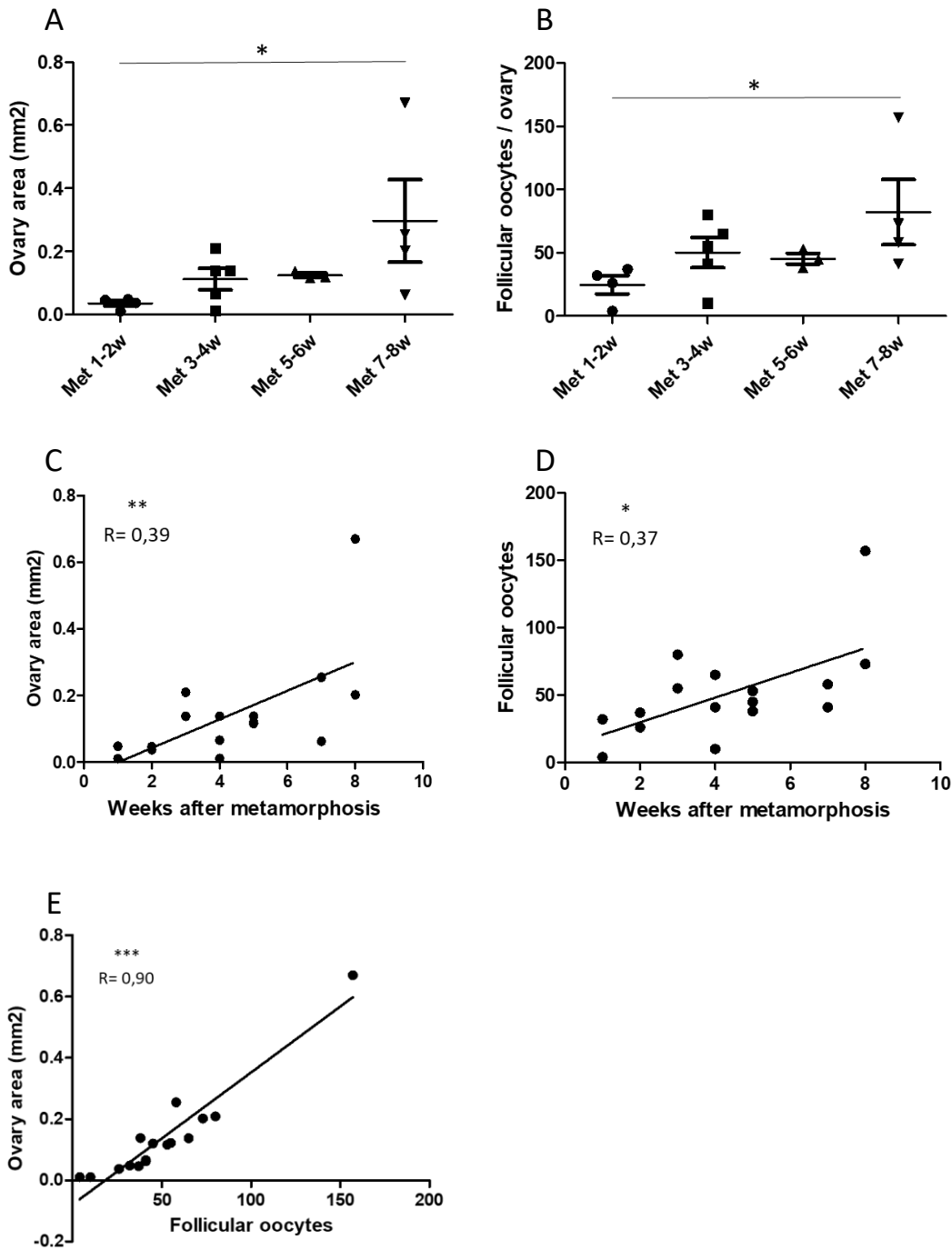
Males
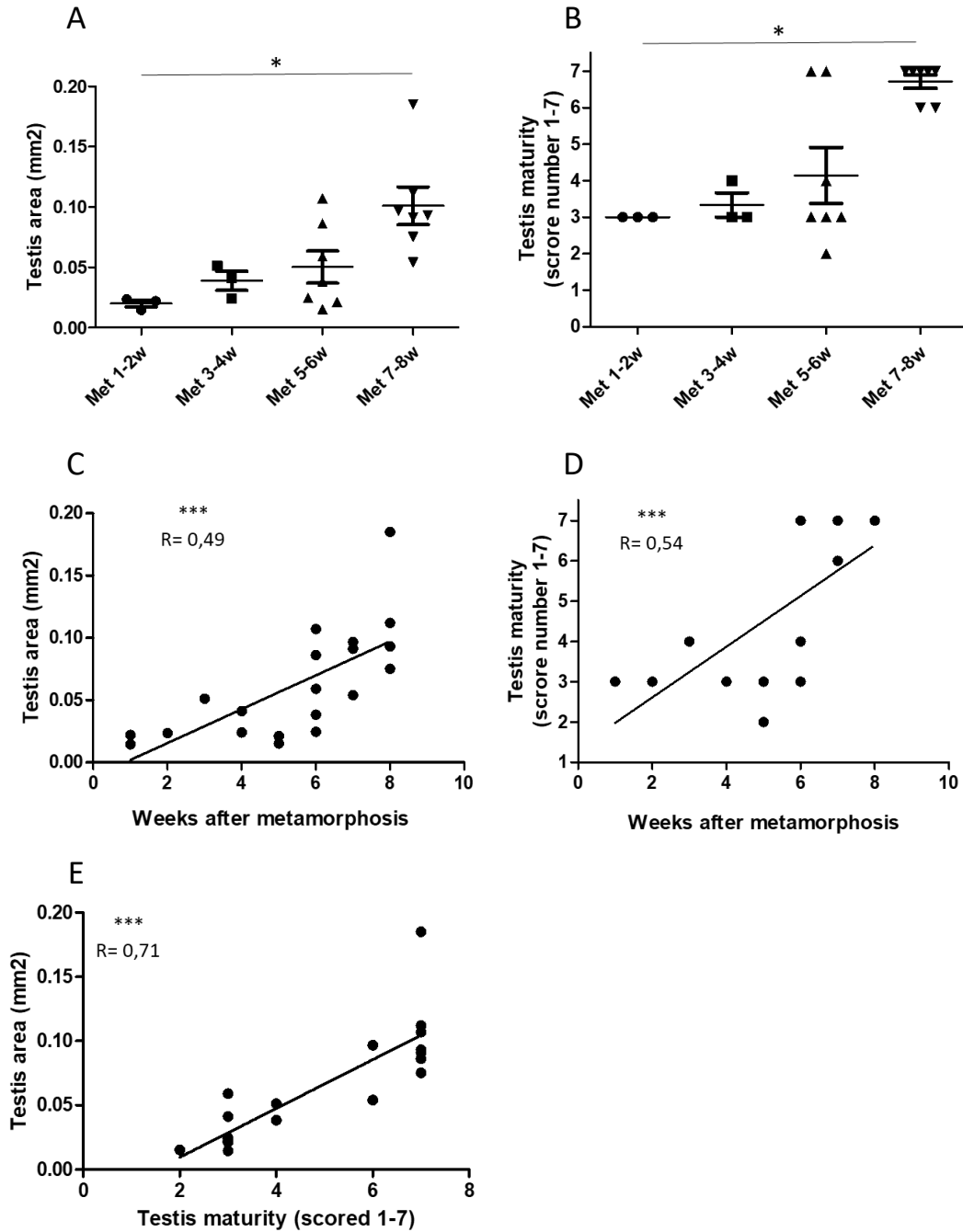
Fig. 2 : Histological analysis of male gonads in post metamorphosis frogs.
(A) Quantification of the testis area at different age after metamorphosis. (B) Evaluation of testis maturity at different age after metamorphosis. Testis maturity was defined with a scoring system assigned depending on the most mature germ cells observed; 1: Pale primary spermatogonia, 2: Dark primary spermatogonia, 3: Secondary spermatogonia, 4: Primary spermatocyte, 5: Secondary spermatocyte, 6: Spermatid, 7: Spermatozoa. (C) Correlation between the testis area and the frog age, (D) between the testis maturity and the age; and between (E) the testis maturity and the testis area. Statistical significance were analysed using Kruskall-Wallis test followed by Dunn's comparison or linear regression correlation test with * p< 0,05 and *** p< 0,001.
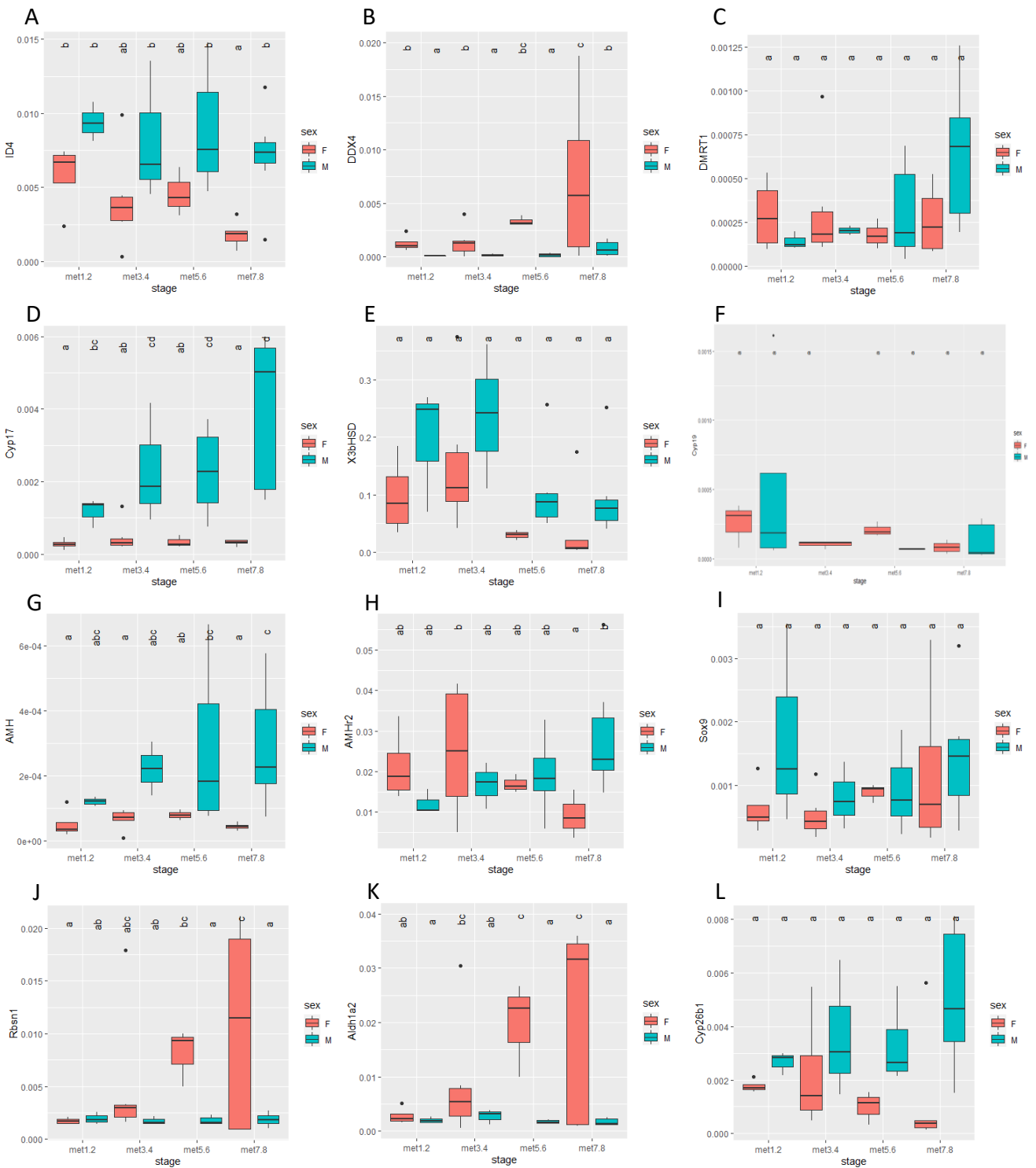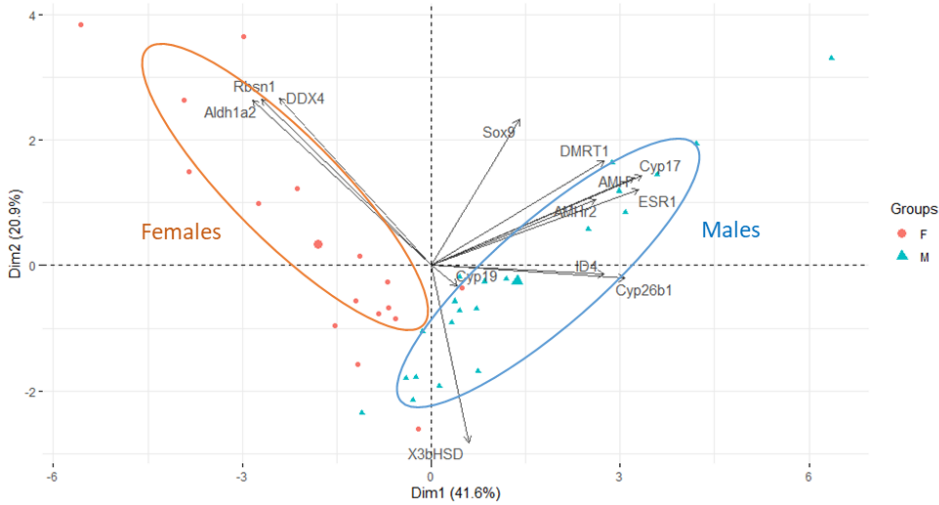
Females

Fig. 3 : Histological analysis of female gonads in post metamorphosis frogs.
(A) Quantification of the ovary area at different age after metamorphosis. (B) Number of follicular oocytes for the corresponding area at different age after metamorphosis. (C) Correlation between the ovary area and the frog age, (D) between the number of follicular oocytes and the age; and between (E) the follicular oocytes number and the ovary area. Statistical significance were analysed using Kruskall-Wallis test followed by Dunn's comparison or linear regression correlation test with * p< 0,05 and *** p< 0,001.

Fig. 4 : Gene expression ontogeny gonad/kidney complex in post metamorphosis frogs.
Relative genes expression in gonad kidney complex in males (blues box) and females (red boxes) from met. 1.2 weeks to met. 7.8 weeks. Relative expression for germ cells specific genes : (A) ID4, (B) DDX4 and (C) DMRT1; steroidogenic specific genes : (D) Cyp17, (E) 3bHSD and (F) Cyp19; male differentiation specific genes: (G) AMH, (H) AMHr2, (I) Sox9 and (J) Rsbn1 gene; retinoic pathway specific genes: (K) Aldh1a2 and (L) Cyp26b1.
Statistical significance p<0,05 is achieve if the letter are different between two groups.

A PCA Males and Females

B PCA Males
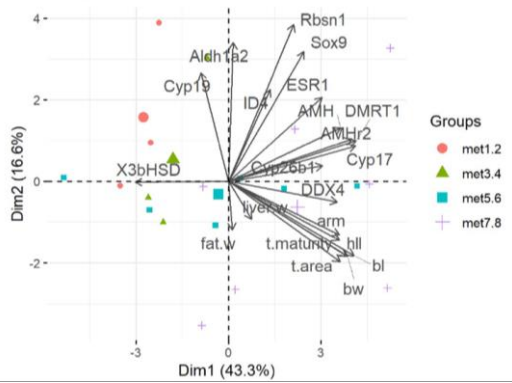
C PCA Females
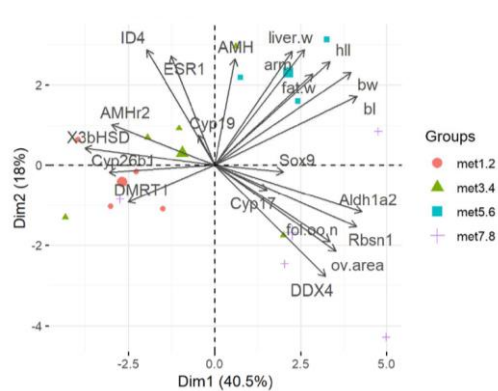
Fig. 5 : Principal component analysis (PCA) for sex-specific genes expression in gonad/kidney complex, body measurements and gonad maturity in post metamorphosis frogs.
(A) Principal component analysis representation for sex-specific genes expression in gonad/kidney complex in males (M, blue symbol) and females (F, red symbol) post-metamorphosis frogs. (B) PCA for post-metamorphosis males frogs with body measurements, gonad maturity and relative gene. (C) PCA for post-metamorphosis females frogs with body measurements, gonad maturity and relative gene expression. Relative gene expression for germ cells specific genes : ID4, DDX4 and DMRT1; steroidogenic specific genes : Cyp17, 3bHSD and Cyp19; male differentiation specific genes: AMH, AMHr2, Sox9 and Rsbn1 gene; retinoic pathway specific genes: Aldh1a2 and Cyp26b1.
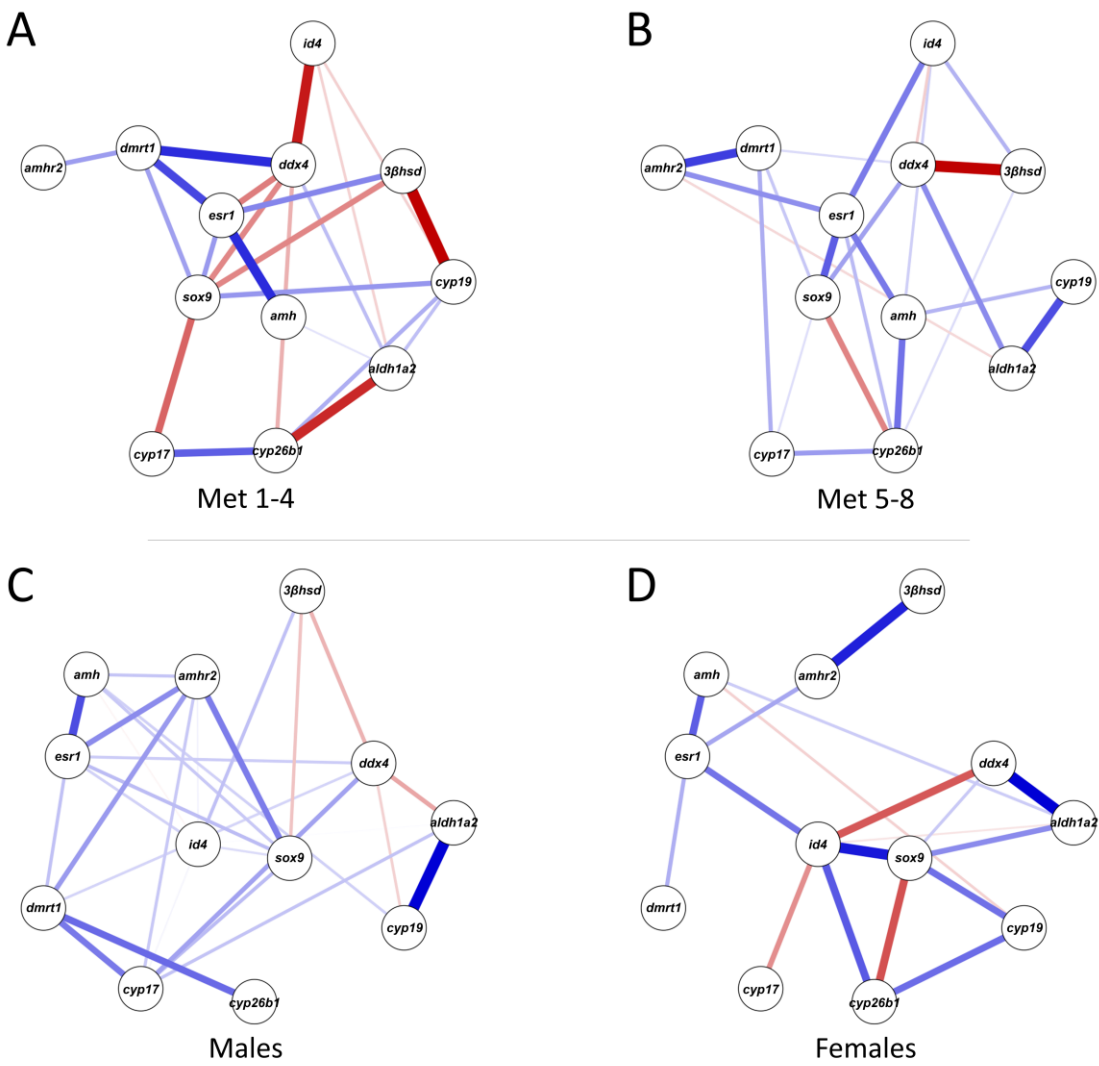
Fig. 6 : Bayesian Network Plots illustrating associations between transcripts from the gonad/kidney complex in post-metamorphosis frogs, stratified by age (A, B) and sex (C, D).
(A) Plot of relative gene expression data from younger froglets, spanning the first to fourth weeks post-metamorphosis (Met1-4). (B) Plot of mRNA data from older frogs, spanning the fifth to eighth weeks post-metamorphosis (Met5-8). (C) Plot based on relative gene expression data from male frogs. (D) Plot based on mRNA data from female frogs. The thickness and color of edges represent the strength and direction of associations, with red edges indicating positive correlations and blue edges indicating negative associations. Germ cells specific genes : ID4, DDX4 and DMRT1; steroidogenic specific genes : Cyp17, 3bHSD and Cyp19; male differentiation specific genes: AMH, AMHr2, Sox9 and Rsbn1 gene; retinoic pathway specific genes: Aldh1a2 and Cyp26b1.

	ID4	DDX4	DMRT1	Sox9	Cyp17	AMH	AMHr2	3bHSD	ESR1	Cyp19	Cyp26b1	Aldh1a2	Rsbn1
Testis area	-0.08	0.71***	0.61**	0.23	0.62**	0.45	0.49*	-0.39	0.16	-0.29	0.47*	-0.23	0.01
Testis maturity	-0.01	0.60**	0.66**	0.28	0.57*	0.44	0.58**	-0.43	0.15	-0.29	0.59**	-0.24	0.19
Ovary area	-0.47	0.92****	-0.36	0.19	0.12	-0.02	-0.52*	-0.54*	-0.34	-0.36	-0.46	0.75***	0.83****
Follicular oocytes number	-0.42	0.86****	-0.36	0.21	0.14	0.08	-0.47	-0.49	-0.31	-0.32	-0.43	0.69**	0.76***

Table 2 : Correlation between sex-specific genes expression and gonad maturity in post metamorphosis frogs.
Correlation between relative genes expression in gonad kidney complex and gonad histology in post metamorphic frogs. Relative expression for germ cells specific genes : ID4, DDX4 and DMRT1; steroidogenic specific genes : Cyp17, 3bHSD and Cyp19; male differentiation specific genes: AMH, AMHr2, Sox9 and Rsbn1 gene; retinoic pathway specific genes: Aldh1a2 and Cyp26b1. Numbers represent the R coefficient of Pearson correlation and statistical significance *p≤0,05; **p<0,01; *** p<0,001 and **** p<0,0001.

Supplementary table 1

MALES	BW	BL	HLL	FLL	LW
BL	0.97****				
HLL	0.92****	0.93****			
FLL	0.86****	0.81****	0.83****		
LW	0.45	0.36	0.26	0.13	
FBW	0.37	0.28	0.23	0.08	0.75***

Supplementary table 1A : Correlation between body measurment in male post metamorphic frogs.

Morphological data evaluated at dissection : the body weight (BW), body length (BL), fore limb length (FLL), hind limb length (HLL), liver weight (LW), fat body weight (FBW). Numbers represent the R coefficient of Pearson correlation and statistical significance *** p<0,001 and **** p<0,0001.

FEMALES	BW	BL	HLL	FLL	LW
BL	0.96****				
HLL	0.89****	0.86****			
FLL	0.68**	0.67**	0.72**		
LW	0.81***	0.75***	0.64**	0.42	
FBW	0.89****	0.83***	0.72**	0.42	0.94****

Supplementary table 1B : Correlation between body measurements in female post metamorphic frogs.

Morphological data evaluated at dissection : the body weight (BW), body length (BL), fore limb length (FLL), hind limb length (HLL), liver weight (LW), fat body weight (FBW). Numbers represent the R coefficient of Pearson correlation and statistical significance : **p<0,01; *** p<0,001 and **** p<0,0001.

Supplementary table 2

MALES	Testis area	Testis maturity
Testis maturity	0.84****	
BW	0.78****	0.67**
BL	0.80****	0.71***
HLL	0.72***	0.70***
FLL	0.60**	0.54*
LW	0.15	0.02
FBW	0.04	0.09

FEMALES	Ovary area	Follicular oocytes
Follicular oocytes	0.95****	
BW	0.42	0.40
BL	0.47	0.44
HLL	0.31	0.30
FLL	0.05	0.04
LW	0.11	0.19
FBW	0.23	0.20

Supplementary table 2: Correlation between body measurement data and gonad maturity in male and female post metamorphic frogs.
Gonad maturity evaluated has testis area and testis maturity score in males and ovary area and follicular oocytes number in females. Morphological data evaluated at dissection : the body weight (BW), body length (BL), fore limb length (FLL), hind limb length (HLL), liver weight (LW), fat body weight (FBW). Numbers represent the R coefficient of Pearson correlation and statistical significance : *p<0,05; **p<0,01; *** p<0,001 and **** p<0,0001.
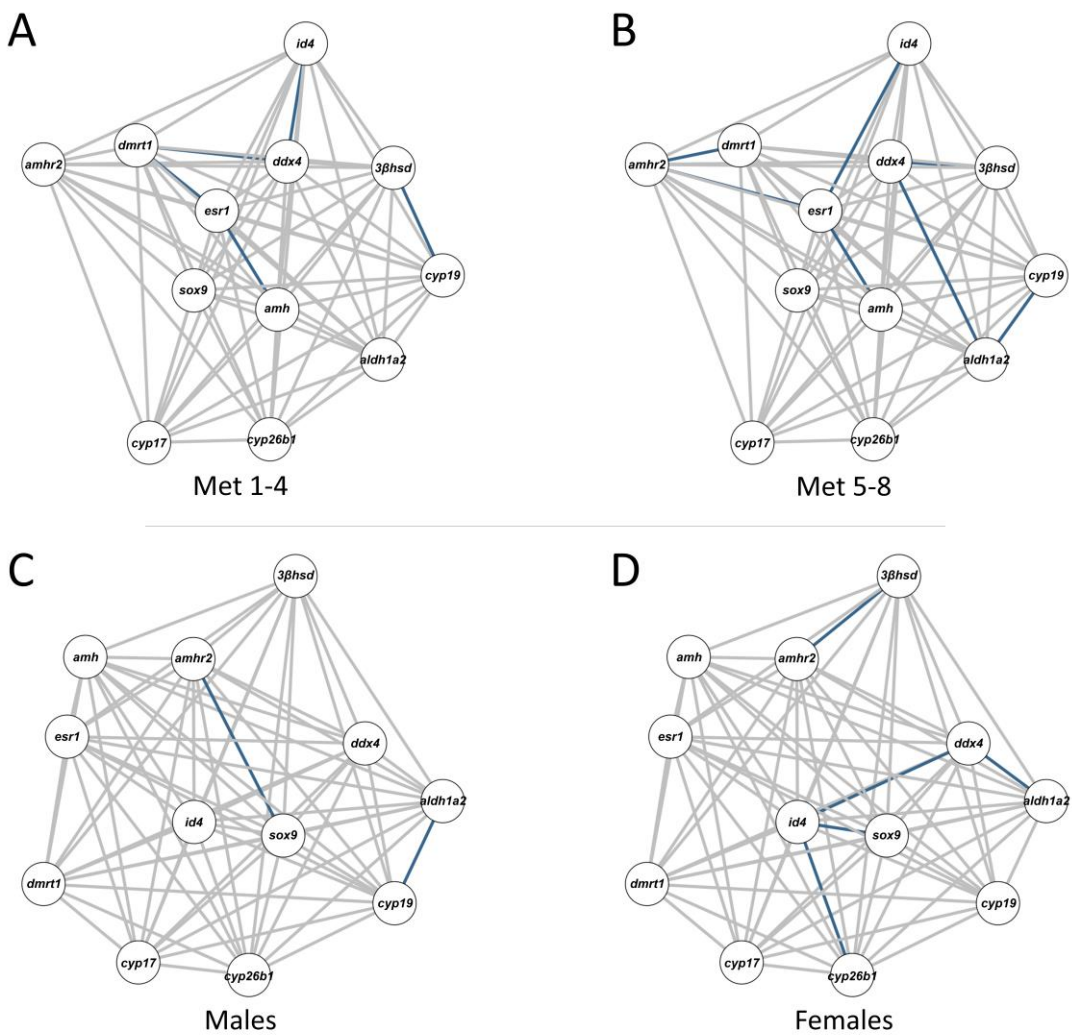
Supplementary Fig. 1 : Edge Evidence Plot showing the strength of connections between transcripts from the gonad/kidney complex in post-metamorphosis frogs, stratified by age (A, B) and sex (C, D). The plots indicate included edges ($BF_{10} > 10$; blue lines) and excluded edges ($BF_{10} < 10$; grey lines) among nodes.

(A) Plot based on relative gene expression data from younger froglets, covering the first to fourth weeks post-metamorphosis (Met1-4). (B) Plot from mRNA data for older frogs, covering the fifth to eighth weeks post-metamorphosis (Met5-8). (C) Plot from gene expression data for male frogs. (D) Plot from gene expression data for female frogs. Germ cells specific genes : ID4, DDX4 and DMRT1; steroidogenic specific genes : Cyp17, 3bHSD and Cyp19; male differentiation specific genes: AMH, AMHr2, Sox9 and Rsbn1 gene; retinoic pathway specific genes: Aldh1a2 and Cyp26b1.
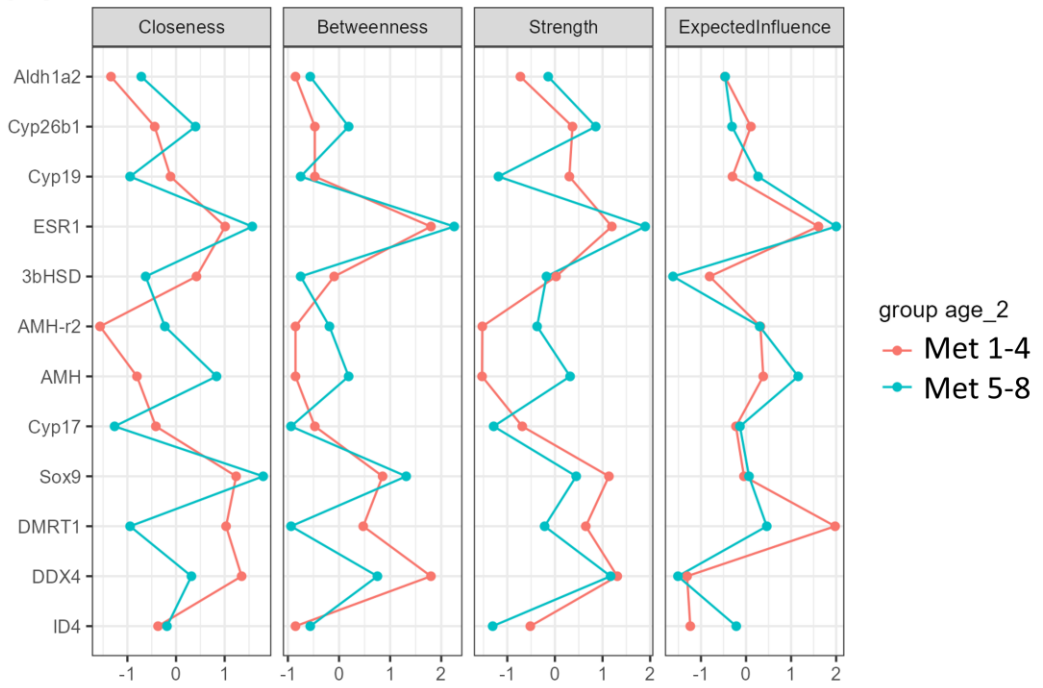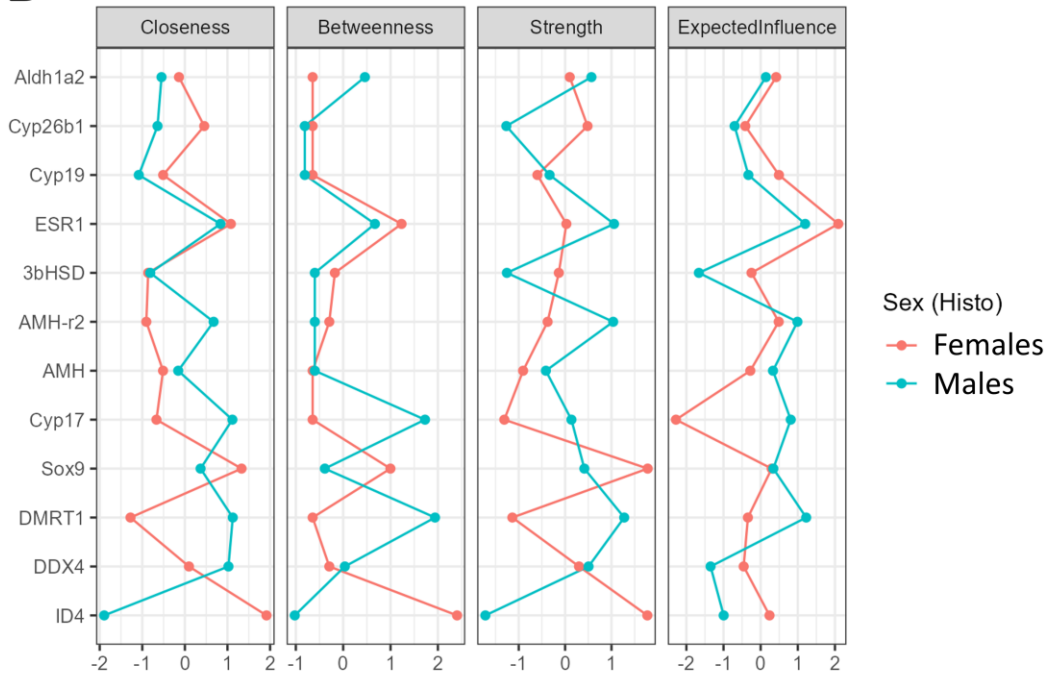
Supplementary Fig. 2 : Centrality plots for transcripts from the gonad/kidney complex in post-metamorphosis frogs stratified by age (A) and sex (B). The plots display four centrality metrics—Closeness, Betweenness, Strength, and Expected Influence—across each transcript. Data are separated by groups within age and sex. Higher centrality values suggest greater importance of nodes within the network.

Paper II
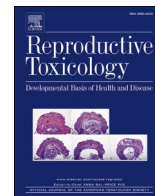
Pubertal sexual development and endpoints for disrupted spermatogenesis in the model *Xenopus tropicalis*

Sofie Svanholm [a,*], Mauricio Roza [b], Daniele Marini [a,c], Vanessa Brouard [a], Oskar Karlsson [b], Cecilia Berg [a]

[a] *Department of Environmental Toxicology, Uppsala University, Uppsala 754 36, Sweden*
[b] *Science for Life Laboratory, Department of Environmental Science, Stockholm University, Stockholm 114 18, Sweden*
[c] *Department of Veterinary Medicine, University of Perugia, Perugia 06126, Italy*

ARTICLE INFO

ABSTRACT

Peripubertal models to determine effects of anti-androgenic endocrine disrupting chemicals are needed. Using the toxicological model species *Xenopus tropicalis*, the aims of the study were to 1) provide data on sexual maturation and 2) characterise effects of short-term exposure to an anti-androgenic model substance. Juvenile (2.5 weeks post metamorphosis old) *X. tropicalis* were exposed to 0, 250, 500 or 1000 μg flutamide/L (nominal) for 2.5 weeks. Upon exposure termination, histology of gonads and Müllerian ducts was characterised in detail. New sperm stages were identified: pale and dark spermatogonial stem cells (SSCs). The testes of control males contained spermatozoa, indicating pubertal onset. The ovaries were immature, and composed of non-follicular and pre-vitellogenic follicular oocytes. The Müllerian ducts were more mature in females than males indicating development/regression in the females and males, respectively. In the 500 μg/L group, the number of dark SSCs per testis area was decreased and the number of secondary spermatogonia was increased. No treatment effects on ovaries or Müllerian ducts were detected. To conclude, our present data provide new knowledge on spermatogenesis, and pubertal onset in *X. tropicalis*. New endpoints for evaluating spermatogenesis are suggested to be added to existing assays used in endocrine and reproductive toxicology.

1. Introduction

The development of the reproductive system is tightly regulated by hormones and is consequently sensitive to exposure to endocrine disrupting chemicals (EDCs). A large number of substances in the environment has been shown to inhibit the action of androgens in the organism by antagonizing the androgen receptor [1]. Exposure to such anti-androgenic EDCs are suspected to contribute the observed adverse reproduction outcomes including reduced sperm quality in humans and wildlife [2]. Animal models for toxicological studies are needed in order to provide evidence for cause-effect relationships with regard to adverse effects of exposure to EDCs during critical phases of development such as puberty.

Testosterone is the main androgen involved in spermatogenesis in higher vertebrates [3]. Androgens are produced and secreted by the interstitial Leydig cells and act on Sertoli cells via binding to the androgen receptor or other transcription factors [4]. In mice, the absence of androgen receptors resulted in inhibited meiosis [5] and in

frogs, the absence of androgens resulted in arrested germ cell maturation, and a lack of spermatids and spermatozoa [6]. Many chemicals have demonstrated anti-androgenic properties *in vitro* indicating a potential to interfere with sperm development *in vivo* [7–10]. Exposure during the pubertal period to the androgen receptor antagonist flutamide resulted in decreased sperm motility which caused infertility in adult rats [11]. Research findings in amphibians and mammals indicate that, in addition to androgens, thyroid hormones are involved in testis development and function [12–14].

Histological evaluation of sperm stages is challenging as certain stages are morphologically similar and are only distinguished using methods such as scanning electron microscopy [15]. In the amphibian model species *X. laevis,* the histologically characterized sperm stages are: spermatogonial stem cells (SSCs, in some studies referred to as primary spermatogonia), secondary spermatogonia, primary and secondary spermatocytes, spermatids, and spermatozoa [16–19]. These stages have been reported also in *X. tropicalis* [18–21] using the criteria by Kalt [16] though detailed morphological criteria to identify them histologically

have not been characterized. The most detailed histological characterisation of sperm stages in amphibians includes the additional stages; gonocytes, and pale and dark SSCs in *Rana esculenta, Pelophylax lessonae* and *P. ridibundus* [15,22]. To our knowledge, there are no previous reports identifying pale and dark SSCs histologically in the most commonly used amphibian model organisms *X. laevis* and *X. tropicalis*. Previous research has identified the early stage of sperm development as a target for developmental exposure to anti-androgens [19,23]. It is therefore important to characterise dark and pale SSCs in *X. laevis* and *X. tropicalis* to enable detailed investigation into spermatogenesis and the effects of anti-androgens and other substances.

Xenopus frogs (*tropicalis* and *laevis*) have proven useful as toxicological models to investigate endocrine and reproductive toxicity following early life exposure to EDCs [24–27]. In *X. tropicalis*, reproductive development includes the sex determination which occurs at the larval stage, and the sex differentiation (gonadal and brain maturation), and secondary sex characteristics development that starts during the larval stage and continues up to 3 months post metamorphosis (PM) for males and 4.5 months for females, when the animals have reached sexual maturation [28–30]. Mature germ cells (spermatozoa or mature oocytes) in the gonads, oviducts (developed from Müllerian ducts) in females and vas deferens in males are present only after sexual maturation. In addition, secondary sex characteristics, such as a pear-shaped body in female and nuptial pads (breeding "glands") on the forearms of males are also regulated by sex hormones and develop during sexual maturation in *Xenopus* [31]. There is however little information on the onset of specific processes of the sexual development, such as spermatogenesis in *Xenopus*. These questions need to be addressed to further develop *Xenopus* as a toxicological model.

The overall aims of the present study were to increase the understanding of peripubertal sexual development including pubertal onset and to explore potential endpoints for anti-androgenic effects in juvenile *X. tropicalis*. Specifically, the objectives were to: 1) characterize gonadal maturity, spermatogenesis, oogenesis, and Müllerian duct maturity, and 2) characterize apical and detailed histological effects of the anti-androgenic model substance flutamide on sexual maturity in juvenile *X. tropicalis*.

2. Material and method

2.1. Experimental design

To address the first aim, a detailed histological characterisation of gonadal and Müllerian duct maturity was conducted, and pubertal onset was assessed in the control animals. Pubertal onset was assessed by determining the presence of mature germ cells and secondary sex characteristics (nuptial pads or pear-shaped body). If one of these criteria was fulfilled, the animal was classified as having entered puberty. Gonadal maturity was assessed by determining the most mature germ cell present and Müllerian duct maturity was assessed using a scoring system based on histology. The spermatogenesis and oogenesis (distribution germ cell stages in the gonad) were characterized, and gonadal size (cross-section area) was measured and related to the number of germ cells.

To address the second aim, control and anti-androgen treated groups were compared with regard to detailed histological characterisation of gonadal and Müllerian duct maturity as well as spermatogenesis, oogenesis, gonadal size and apical endpoints. The apical endpoints included presence of secondary sex characteristics, hind limb length (as an endpoint for thyroid disruption) and growth (body weight and length).

The age of analysis was based on previous observations regarding sexual maturation in *X. tropicalis*. At four weeks PM, males have not entered puberty, but have an active spermatogenesis and at eight weeks PM they have entered puberty as shown by the presence of mature spermatozoa in the testis [20,21]. However, there is scanty information on gametogenesis, gonadal maturity or effects of EDCs in the period in-between these time points for *X. tropicalis*. The duration of the exposure was based on the OECD test: Fish Short Term Reproduction Assay [32] using juvenile Japanese medaka (*Oryzias latipes*) [33], but with minor changes due to practical reasons.

2.2. Animal husbandry and exposure

Juvenile *X. tropicalis* frogs (obtained from in-lab mating of adult animals originating from Xenopus1, Dexter, MI, USA) at the age of 17.5 ± 4 days PM were exposed for 17 ± 2 days to flutamide (reference standard, CAS: 13311–84–7, Sigma Aldrich) at three nominal concentrations: 0 (Control), 250 (Low), 500 (Mid) and 1000 (High) µg/L under semi-static conditions. Acetone (0.0008 %) was used as a solvent in all tanks including controls. Half of the water and flutamide/acetone solution or acetone alone was exchanged three times per week. To saturate the aquaria with the test compound, the water changing routine was started one week prior the start of the exposure. Two replicate tanks (15 L, Ferplast, Vicenza, Italy) were used for all flutamide treatments, and three for the control group. There were 12–25 animals in each tank (Supplementary table S1). The variation in numbers of juveniles per tank was due to a difference in time to reach metamorphosis which resulted in a variable number of age-matched individuals that could be assigned to an exposure tank at any given time point.

The animals were kept in a 12:12 light:dark cycle (with one hour dawn and one hour dusk). Once a week, before water change, nitrite (standard kit from Sera, Gibbon, Sweden), ammonia/ammonium (standard kit from Sera, Gibbon, Sweden), oxygen saturation, and pH, were recorded in all the tanks, and temperature was monitored daily. The animals were fed Sera vipan baby (Sera, Heinsberg, Germany), and Energy food (Sera, Heinsberg, Germany) three times per day in weekdays and once a day with double amount on weekends. This study was approved by Uppsala Ethics Committee for Animal Care and Use (5.8.18–09239/2018) and Uppsala University and carried out in accordance with relevant guidelines and regulations including the ARRIVE guidelines.

2.3. Sampling and apical endpoints

Upon discontinuation of the exposure, at five weeks PM, the frogs were sacrificed by decapitation after first being anaesthetised in 0.3 % buffered Tricaine (Sigma-Aldrich, Saint-Louis, USA). The hind limb length, snout-vent length (SVL) and body weight were measured. Any presence of nuptial pads and a pear-like body shape was noted. The gonad-kidney complex (including kidneys, gonads and Müllerian ducts) was fixed in 4 % buffered formaldehyde for histological processing and analysis of gonadal and Müllerian duct histology. Brain, thyroid and the rest of the body (without intestines) were also sampled during dissection, but for purposes beyond the present study. During the dissection, the evaluator was aware of which exposure the animals had been subjected to.

2.4. Histological processing

The gonad-kidney complexes were dehydrated in increasing concentrations of ethanol and embedded in hydroxyethyl methacrylate after being infiltrated overnight (Technovit 7100, KULZER GmbH, Germany). Transversal sections were taken at three levels with a distance of 300 µm in-between, starting from the anterior part of the gonads from 26 Controls, 10 Low, 11 Mid and 26 High animals. One Section (2 µm thick) per individual, from the centre of the gonad, was stained with haematoxylin-eosin, the other sections were stained with toluidine blue. The sample size was based on previous studies on histological effects on gonads [23].

2.5. Histological analysis

The histological slides were scanned with a histological scanner (NanoZoomer 2.0-H, Hamamatsu) and evaluated using NDP.view (Hamamatsu Photonics K.K, version 2.7.52, 2019). Gonadal distribution of germ cell stages and gonadal size (cross-section area) were assessed in one haematoxylin-eosin stained section from the center of the gonads for each individual. Determination of the most mature germ cell present was assessed using all three sections per individual. For each individual, both the left and right hand side gonad were evaluated and a mean value of the data from the two was used for statistical analysis. All histological analyses were performed by one person using coded slides.

2.5.1. Testis histology and spermatogenesis

The sperm stages that were analysed included gonocytes, pale SSCs, dark SSCs, secondary spermatogonia, primary spermatocytes, secondary spermatocytes, spermatids and spermatozoa using a combination of morphological criteria presented in Table 1 [15–17,22]. The number of cells per sperm stage was determined in 15 Controls, 7 Low, 6 Mid and 6

High, and the most mature germ cell stage was noted for each individual. The testis cross-section area was measured with ImageJ (National Institute of Health, Bethesda, MD, USA) and related to number of germ cells.

2.5.2. Ovary histology and oogenesis

In 12 Control, 3 Low, 4 Mid and 20 High females, the number of oocytes was determined, and the most mature germ cell present noted. The following non-follicular oocyte types were counted: premeiotic oogonia and oocytes in very early meiotic prophase i.e. primary oogonia, secondary oogonia, preleptotene oocytes, leptotene oocytes, pachytene oocytes and early diplotene oocytes. The follicular oocyte types counted were: stage I, II, III, IV, V and VI oocytes [34]. The oocytes were then combined into the two categories and a ratio of follicular: non-follicular oocytes was calculated. Ovary cross-section area was measured with ImageJ (National Institute of Health, Bethesda, MD, USA) and related to the number of oocytes.

Table 1

Summary of histological characteristics and functional features for sperm cell stages in amphibians. These morphological criteria were used for the identification of sperm cell stages in juvenile Xenopus tropicalis.

Sperm stage	Histological characteristics	Functional feature	Species[a] (reference)
Gonocytes	Large, single cells. Occupying the major part/space of the sex cords. One or two nucleoli.	Only present during pre-spermatogenesis. Differentiate into pale SSCs.	*Pelophylax Lessonae* ([15]) *P. ridibundus* ([15])
Pale SSCs	Large, single cells. Slightly irregular shape, with light pink cytoplasm and homogenous chromatin.	Form the stem cell reserve. Differentiate into dark SSCs or self-renew.	*P. lessonae* ([15]) *P. ridibundus* ([15]) *Rana esculenta* ([22])
Dark SSCs	Round cells. Similar appearance as pale SSCs but smaller and with a darker cytoplasm and more heterochromatin. Present individually or in clusters of two.	Differentiate into secondary spermatogonia.	*P. lessonae* ([15]) *P. ridibundus* ([15]) *R. esculenta* ([22])
Secondary spermatogonia	Clearly organized into spermatocysts. The nucleus is irregularly shaped either round or slightly elongated, with visible nucleoli and chromatin patches. Undergo mitosis, hence their size is gradually decreased, and the cell shape is altered from elongated to more round.	Proliferate and differentiate into primary spermatocytes	*Xenopus laevis* ([16,17]) *P. lessonae* ([15]) *P. ridibundus* ([15])
Primary spermatocytes	Chromosome appearance typical to the phase of meiosis (prophase, metaphase, anaphase or telophase). Cells in prophase are round with a nucleus that is large in relation to the cytoplasm, containing loosely packed chromatin. Cells in later meiotic phases are classified according to the stage of chromosomal division.	Undergo the first meiosis.	*X. laevis* ([16]) *P. lessonae* ([15]) *P. ridibundus* ([15])
Secondary spermatocytes	Round, smaller than primary spermatocytes, with a small, round, condensed nucleus.	Undergo the second meiosis	*X. laevis* ([16]) *P. lessonae* ([15]) *P. ridibundus* ([15])
Spermatids	Either completely round or slightly elongated. Condensed nucleus and dissolved cytoplasm. Cells connected via a spider net-like structure.	Differentiate into spermatozoa	*X. laevis* ([16]) *X. tropicalis* ([18]) *P. lessonae* ([15]) *P. ridibundus* ([15])
Spermatozoa	Elongated cells, completely lacking cytoplasm. Either in nests, with heads pointing towards the lumen or released and free in the lumen.	Mature sperm	*X. laevis* ([16]) *X. tropicalis* ([18]) *P. lessonae* ([15]) *P. ridibundus* ([15])

SSCs: spermatogonial stem cells.

[a] Species for which histological characteristics are presented for the specific sperm stages.

2.5.3. Müllerian duct maturity

Müllerian duct maturity was evaluated on a toluidine stained slide containing sections from the middle of the gonad in males (15 Control, 7 Low, 6 Mid and 6 High) and females (12 Controls, 3 Low, 4 Mid and 20 High). The Müllerian ducts were assigned maturity scores from 1 to 5 as defined in Jansson et al., (2016). Score 1 was assigned to the earliest stage ducts characterised by a small protrusion of loosely packed connective tissue from the kidney. The criteria for score 5 ducts were: a clear tubular structure with a cavity, directly adjacent to the kidney. The criteria for scores 2–4 include increasing formation of a tubular structure.

2.6. Statistical analysis

The data from all replicate tanks were visually examined, to estimate the variability. If no apparent difference between the replicates, the data were pooled according to level of exposure. Linear regression analyses were conducted to evaluate the relationship between gonadal area and the number of germ cell in each stage in control males and females. Müllerian duct maturity in control males and females were compared using Mann Whitney test.

Mortality in the treatment groups was compared to the control group using Fisher's exact test. Generalized linear models were used to test for treatment effects and different distributions and link functions were selected in order to better fit the data. A Gaussian family of distribution with identity link function was used for normally distributed data (body weight, SVL, hind limb length and germ cell counts/area) and gamma family of distribution with log link function was used for non-normal positive continuous data (gonadal area and Müllerian duct maturity). The quality of the models was assessed by checking the distribution of the residuals. Multiple comparisons of treatments to control were performed and p-values were adjusted using the Holm-Bonferroni method. Gonadal maturity (the most mature germ cell present) was analysed with the Chi-square test.

Generalized linear models were conducted in R version 4.0.2 (R Core Team, Vienna, Austria) and R Studio version 1.3.1093 (RStudio Team, Boston, MA, US) where the package DHARMa was used for model diagnostics and emmeans was used for multiple comparisons. Fisher's exact test, Chi-square test, Mann Whitney test and linear regression, were performed in GraphPad Prism 5.0 (GraphPad Software, San Diego, CA, USA). Data were considered statistically significant if $p \leq 0.05$.

3. Results

3.1. Husbandry conditions, and apical endpoints

There was no significant difference in mortality between controls and treatments (3/56, 4/36, 4/44 and 1/37 individuals for Control, Low, Mid and High respectively) and no other signs of treatment related health impairment. No treatment effects on body weight, SVL or hind limb length were found (Supplementary table S3) with the exception that the High males had increased SVL compared to Control males (p = 0.0213). No secondary sex characteristics were observed in the males nor females. Information on husbandry conditions is found in Supplementary table S2.

3.2. Testicular histology and spermatogenesis

The testes mainly consisted of seminiferous cords and a few seminiferous tubuli characterised by a lumen (Fig. 1A). All animals had established the dark SSCs in the testis, and no gonocytes (precursor cells to SSCs) were therefore identified. The pale and dark SSCs (Fig. 1B), and spermatozoa (Fig. 1G) were the germ cell stages easiest to distinguish as their morphology was completely different compared with the other stages. The SSCs appeared as large single cells inside cysts and the spermatozoa were mainly present as detached from the germinal epithelium, free in the lumen. Primary spermatocytes (Fig. 1D) were morphologically similar to later stages of secondary spermatogonia (Fig. 1C), except with regard to the appearance of the nuclei and the packing of chromatin. In secondary spermatogonia, a nucleolus was not always visible and, therefore, chromatin patches, packing of the chromatin and the shape of the nucleus were more reliable morphological features. Secondary spermatocytes (Fig. 1E) were only observed in one nest in one animal and they did not show the typical features of second
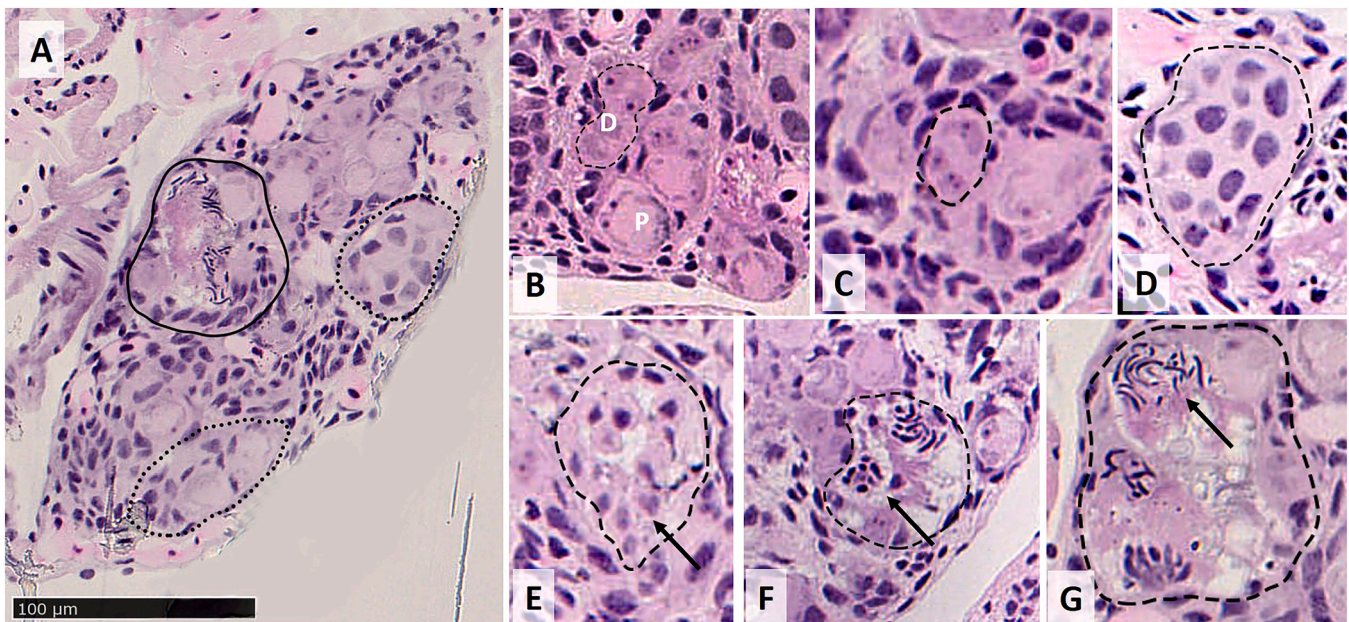

Fig. 1. Histomicrographs of testes from juvenile *Xenopus tropicalis*, five weeks post metamorphosis, showing A) seminiferous chords (dotted line) and seminiferous tubuli containing a lumen (solid line), B) spermatogonial stem cells (SSCs); pale SSCs (P) and dark SSCs (D), C) nests with proliferating secondary spermatogonia, D) nest with primary spermatocytes, E) secondary spermatocytes starting to differentiate into spermatids (arrow), F) spermatids (arrow). G) Fully mature spermatozoa (arrow). Sections are stained with haematoxylin-eosin. Dashed lines encircle germ cell nests.

meiosis. Spermatids (Fig. 1F), were also rarely observed but were easily distinguished from the secondary spermatocytes due to their almost complete lack of cytoplasm, and very round nucleus.

In the Control males, the frequencies of testicular maturity stages, as determined by the most mature germ cell stage observed, were: 6/15 with fully mature spermatozoa in the seminiferous tubule lumen, 4/15 with primary spermatocytes, 4/15 with secondary spermatogonia and 1/15 with dark SSCs.

The total number of SSCs per testis cross-section area was not correlated with the cross-section area in the Controls. However, when the SSCs group was split into the two subtypes, it was found that the number of dark SSCs was positively correlated to the testis cross-section area (p = 0.0443, r^2 =0.28, linear regression), whereas the number of pale SSCs was not (Supplementary Fig. S3). The numbers of secondary spermatogonia and primary spermatocytes did not show any significant correlation to the testis cross-section area either. No correlation analyses were performed on the other germ cells (secondary spermatocytes, spermatids and spermatozoa), as the frequencies of testis showing presence of them were too low.

In the Mid group, there was a significant decrease in the number of dark SSCs per testis area (p = 0.0142) and a significant increase in the number of secondary spermatogonia (p = 0.0040) compared to Control (Table 2). No other significant difference between treatments and Control with regard to number of germ cell stages in relation to area was detected. No differences between the Control and treatment groups with regard to testis area (Table 2) or testis maturity (Fig. 2) were found.

3.3. Ovarian histology and oogenesis

All Control ovaries consisted of non-follicular and follicular previtellogenic stage I or II oocytes (Supplementary Fig. S1). No mature stage VI oocytes were detected. There was a positive correlation between ovary cross-section area and total number of oocytes ($r^2 = 0.93$, p < 0.0001). This was driven by the follicular oocytes as the area positively correlated to number of follicular oocytes (r^2 =0.88, p < 0.0001, linear regression), but not to the number of non-follicular oocytes (Supplementary Fig. S4). In all females but three in the High group, follicular oocytes were observed. No significant difference between Control and treatments was detected with regard to ovary maturity, ovary cross-section area, the number of non-follicular, follicular or total oocytes, or the ratio follicular:non-follicular oocytes (Table 3).

3.4. Müllerian duct maturity

In 6/15 Control males, a Müllerian duct score of 2 for both right and left duct was determined and in 2/15 individuals, both ducts were scored 1 were. In several males, the two ducts were given different maturity scores. In 5/15 males one duct was assigned score 2 and the other score 1, and in 1/15 males the two ducts were assigned score 2 and score 3 (Supplementary Fig. S2). One male could not be evaluated as the
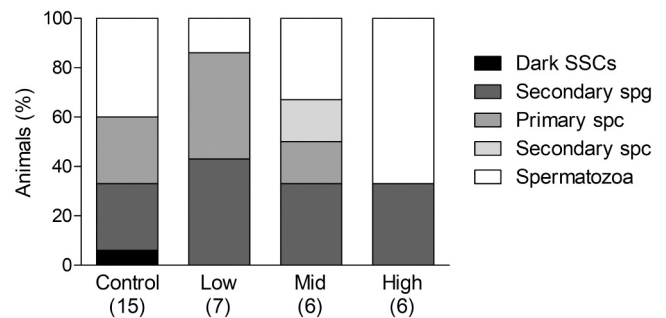

Fig. 2. Testis maturity as determined by the most mature germ cell stage observed per male *Xenopus tropicalis* after short-term peripubertal exposure to 0, (Control), 250 (Low), 500 (Mid) or 1000 (High) μg flutamide/L. SSCs: spermatogonial stem cells, spg: spermatogonia, spc: spermatocytes. Number of individuals (n) is shown within the parenthesis.

lateral parts of the kidneys including the Müllerian ducts were missing from the section.

In 4/12 Control females, a score of 2 was determined for both ducts. In 4/12 females both ducts were given the score 3 and in 1/12 females, the score 5 was assigned to both ducts. In 2/12 females, the right duct was given the score 3 and the left duct was assigned score 2. In 1/12 females, the right duct was given score 2 and the left duct the score 1 (Supplementary Fig. S2). The mean Müllerian duct maturity score in the Control group was significantly higher in females than in males (p = 0.0024, Mann Whitney test) (Table 4). No difference in Müllerian duct maturity between treatments in either of the sexes was found (Table 4).

4. Discussion

In the present study, we aimed to characterise sexual development including gametogenesis in peripubertal *X. tropicalis* and potential effects of anti-androgenic EDCs on these processes. Using detailed histological analysis of the testes we identified dark and pale SSCs, two sperm stages that, to our knowledge, were previously not described in Xenopus. We found that male *X. tropicalis* can reach sexual maturity in 5 weeks PM. The number of dark SSCs and secondary spermatogonia were altered in flutamide exposed males (500 μg/L) suggesting that processes regulating these stages in spermatogenesis may be targeted by exposure to anti-androgens during pubertal development.

By the histological identification of dark and pale SSCs in *X. tropicalis*, we found all sperm stages that were previously described in other amphibian species i.e. *X. laevis*, *P. lessonae* and *P. ridibundus* [15–17]. Haczkiewicz et al. [15] concluded that the sperm stages described in anurans can be translated to the mammalian sperm stages i. e. A spermatogonia, B spermatogonia, primary spermatocytes, secondary spermatocytes, spermatids and spermatozoa. Accordingly, A_{dark} and

Table 2
Detailed histological analysis of testes in juvenile *Xenopus tropicalis* five weeks post metamorphosis after exposure for 17 ± 2 days to 0 (Control), 250 (Low), 500 (Mid) or 1000 (High) μg flutamide/L. Data are presented as mean (SD) and represent both gonads for each individual.

	Control (n = 15)	Low (n = 7)	Mid (n = 6)	High (n = 6)
Testis area (mm^2)	0.03 (0.01)	0.03 (0.01)	0.03 (0.01)	0.03 (0.01)
Total SSCs (no./mm^2)	914.0 (411.6)	1052.4 (437.9)	667.2 (199.0)	928.4 (346.6)
Pale SSCs (no./mm^2)	432.6 (285.5)	707.3 (383.2)	453.2 (169.5)	624.6 (308.1)
Dark SSCs (no./mm^2)	481.4 (222.3)	345.0 (244.8)	214.0 (108.0)*	303.8 (92.4)
Secondary spermatogonia (no./mm^2)	335.1 (311.8)	379.2 (215.4)	870.0 (633.2)**	476.9 (172.8)
Primary spermatocytes (no./mm^2)	124.2 (169.1)	99.6 (137.2)	96.8 (182.0)	283.6 (284.0)
Secondary spermatocytes (no./mm^2)	23.7 (72.6)	0.0 (0.0)	39.6 (97.1)	26.7 (65.5)
Spermatids (no./mm^2)	1.4 (5.2)	0.0 (0.0)	0.0 (0.0)	10.5 (20.3)
Lumen with spermatozoa (no./mm^2)	9.0 (16.9)	6.7 (17.2)	2.6 (6.5)	40.3 (48.5)

SSC: spermatogonial stem cell. *Statistically significant from control (p < 0.05). **Statistically different from control (p < 0.01). Generalized linear model (negative binomial distribution, log link) with Holm-Bonferroni as post hoc test).

Table 3
Detailed histological analysis of ovaries in juvenile *Xenopus tropicalis* five weeks post metamorphosis after exposure for 17 ± 2 days to 0 (Control), 250 (Low), 500 (Mid) or 1000 (High) μg flutamide/L. Data are presented as mean (SD) and represent both gonads for each individual.

	Control (n = 12)	Low (n = 3)	Mid (n = 4)	High (n = 20)
Ovary area (mm²)	0.10 (0.08)	0.05 (0.04)	0.07 (0.02)	0.09 (0.07)
Total oocytes (no./mm²)	983.3 (481.0)	1170.7 (601.9)	989.1 (128.9)	1232.0 (659.2)
Non-follicular oocytes[a] (no./mm²)	495.2 (363.4)	773.1 (519.0)	459.5 (263.1)	741.0 (565.5)
Follicular oocytes[b] (no./mm²)	488.1 (224.9)	397.6 (315.0)	621.2 (516.9)	491.0 (481.0)
Follicular:non-follicular oocytes	1.65 (1.22)	0.92 (0.75)	0.72 (0.27)	1.09 (0.83)

[a] Premeiotic oogonia and oocytes in very early meiotic prophase i.e. primary oogonia, secondary oogonia, preleptotene oocytes, leptotene oocytes, pachytene oocytes and early diplotene oocytes.

[b] Previtellogenic, follicular stage I and II oocytes.

Table 4
Histological analysis of Müllerian duct maturity[a] in juvenile *Xenopus tropicalis* five weeks post metamorphosis after exposure for 17 ± 2 days to 0 (control), 250 (low), 500 (mid) or 1000 (high) μg flutamide/L. Data are presented as mean (SD) and represent both ducts for each individual.

Control		Low		Mid		High	
Male (n = 14)	Female (n = 12)	Male (n = 6)	Female (n = 3)	Male (n = 6)	Female (n = 4)	Male (n = 6)	Female (n = 20)
1.7 (0.4)	2.6 (0.9)**	1.8 (0.6)	2.7 (0.6)	1.9 (0.2)	2.0 (0.3)	2.0 (0.5)	2.6 (0.9)

[a] Maturation score based on criteria by Jansson et al., 2016. "1 - a small rounded bulge of irregularly packed mesenchymal cells at the lateral side of the kidney, 2– a small bud protruding from the kidney, 3 – a distinct structure attached to the lateral side of the kidney, 4 – a distinct tubular structure without a cavity, and 5 – a distinct tubular structure with a cavity lined by elongated epithelial cells". * *Significantly different from Control males (p < 0.01), Mann Whitney test.

A$_{pale}$ spermatogonia (monkeys and humans) or A$_{single}$ (rodents) are equivalent to SSCs in amphibians, and B spermatogonia (monkeys and humans) and A$_{paired}$, A$_{aligned}$ and B spermatogonia (rodents) equivalent to secondary spermatogonia in amphibians. The different types of A spermatogonia are scarcely found and are difficult to distinguish in mammals, hence information about anti-androgenic effects on early spermatogenesis in mammals is very limited [35,36]. The *X. tropicalis* model may therefore be a valuable animal model for studies on the spermatogenesis, in particular the early stages.

The presence of mature sperm suggests that the male frogs had entered puberty. We have previously detected mature spermatozoa at eight weeks PM [21]. The present results further specify the onset of puberty for male *X. tropicalis* to five weeks PM. The presence of mature spermatozoa implies that intratesticular testosterone levels were sufficient to induce spermatogenesis. However, no nuptial pads were noticed, indicating that the concentration of circulating testosterone was likely still too low at this age for induction of their development. The female *X. tropicalis* had not entered puberty which was expected [28]. At five weeks PM the ovaries were similar in composition as at four and eight weeks PM [20,21], with no vitellogenic or mature oocytes observed. The timing of regression and sexual dimorphism of Müllerian ducts in four weeks PM *X. tropicalis* has been unclear [20,29]. In the present study, the ducts in males were less mature compared to those in females. This indicates that the time around four-five weeks PM might be the start of the development of Müllerian duct sexual dimorphism, resulting from Müllerian duct growth in females and/or regression in males. In the present study, gonadal histology was the earliest and most unambiguous indicator of pubertal onset.

The dark SSCs was the only germ cell stage for which the number of cells was positively correlated to testis area, indicating that testis growth was associated with either increased differentiation of pale SSCs into dark SSCs or proliferation of dark SSCs. Regardless of which, the present results imply that testis growth during the start of puberty is driven by activation of spermatogenesis as defined as the formation of dark SSCs which is the germ cell stage entering the spermatogenic cycle in juvenile male *X. tropicalis*.

The increased number of secondary spermatogonia, and decreased number of dark SSCs observed in the testes of the males of the Mid group, suggest that short-term flutamide exposure during the prepubertal period interfered with the pre-meiotic phase of spermatogenesis.

Follicle stimulating hormone (FSH) promotes SSC differentiation via activine A and follistatin, whereas androgens have an inhibitory effect on SSC differentiation and proliferation by exerting negative feedback on the hypothalamic-gonadal-axis in mammals [37,38]. Inhibition of the negative feedback in flutamide exposed frogs, may have stimulated increased FSH secretion, thereby causing increased differentiation of dark SSCs into secondary spermatogonia. Developmental exposure to flutamide has been shown to increase the total number of spermatogonia in amphibians, and to cause effects on spermatogenesis that persist into adulthood [19]. The resolution of the analysis, however, was not enough to establish possible effects on the respective SSCs. Anti-androgenic effects on dark SSC (or the equivalent stage) differentiation have, to our knowledge, not been reported previously in any vertebrate species. The variation in sample size for the histological analyses was a result of some mistakes in the preliminary sexing during dissection and not knowing the definite sex of the frogs until after the histological analysis of the gonads, however, this was not considered to influence the outcome of the analysis. The present study therefore contributes to the general knowledge on potential targets for anti-androgenic EDCs in the spermatogenesis.

In standardized test guidelines for chemical testing, histology based endpoints for adverse effects on spermatogenesis are not adequately specified. The standard tests the Larval Amphibian Growth and Development Assay (LAGDA) and the Peripubertal Male Rats Assay [25,39] include analysis of general testicular histopathology in juveniles, based on severity grading of general pathology. Hence, there is a risk in overlooking small changes in germ cell populations such as SSCs [40]. To increase the sensitivity and resolution of reproductive toxicity assays such as LAGDA to detect potential anti-androgenic/estrogenic effects of chemicals, the number of dark SSCs (or the equivalent) could be included as a fully quantitative and objective endpoint. Such refinement of existing test guidelines would contribute to the principles of the 3Rs (replace, reduce, refine).

The lack of treatment effects on the maturation of the ovaries and Müllerian ducts suggests that these processes were not susceptible to impact of short-term exposure conditions during the early juvenile phase. Androgens are important in oocyte maturation, but mainly at the later follicular stages [41], which might explain the lack of treatment effects on these developmental processes. It cannot however, be ruled out that effects can be seen later in life and five weeks PM may not be an

optimal age to evaluate anti-androgenic effects on the ovary maturation.

The increased SVL in the High males was unexpected and might suggest a stimulatory effect on body growth in juvenile frogs. In juvenile fish, flutamide exposure did not affect the body length [33,42,43]. There is limited information available on the potential mechanism of anti-androgens to affect juvenile body length in male amphibians. This observation is therefore currently not understood.

5. Conclusion

Two new sperm stages, dark and pale SSCs, were identified histologically in *X. tropicalis*. To our knowledge, these sperm stages have previously not been described in *Xenopus*. Additionally, we further specified pubertal onset in males to occur between four and five weeks PM. The number of dark SSCs and secondary spermatogonia were altered in flutamide exposed males suggesting that these stages in spermatogenesis may be targeted by exposure to anti-androgens during pubertal development. In conclusion, the present study contributes with new knowledge on spermatogenesis and sexual development of *X. tropicalis*. We furthermore suggest counts of dark SSCs and secondary spermatogonia as quantitative, objective endpoints for disrupted spermatogenesis to be included in existing test guidelines for EDCs.

CRediT authorship contribution statement

S.S: Conceptualization, Methodology, Investigation, Formal analysis, Data interpretation, Writing – original draft, Writing – review & editing, Visualization. M.R: Formal analysis, Data interpretation, Writing – review & editing. V.B: Data interpretation, Writing – review & editing. D.M: Technical assistance, Data interpretation, Writing – review & editing. O.K: Data interpretation, Writing – review & editing. C.B: Conceptualization, Methodology, Data interpretation, Writing - review & editing, Supervision, Project administration, Funding acquisition.

Declaration of Competing Interest

The authors declare that they have no known competing financial interests or personal relationships that could have appeared to influence the work reported in this paper.

Data Availability

The datasets used and/or analyzed during the current study are available from the corresponding author on reasonable request.

Acknowledgements

Appendix A. Supporting information

Supplementary data associated with this article can be found in the online version at doi:10.1016/j.reprotox.2023.108435.

References

[1] D.C. Luccio-Camelo, G.S. Prins, Disruption of androgen receptor signaling in males by environmental chemicals, J. Steroid Biochem. Mol. Biol. 127 (2011) 74–82, https://doi.org/10.1016/j.jsbmb.2011.04.004.

[2] V.L. Marlatt, S. Bayen, D. Castaneda-Cortès, G. Delbès, P. Grigorova, V.S. Langlois, C.J. Martyniuk, C.D. Metcalfe, L. Parent, A. Rwigemera, P. Thomson, G. Van Der Kraak, Impacts of endocrine disrupting chemicals on reproduction in wildlife and humans, Environ. Res. 208 (2022), https://doi.org/10.1016/j.envres.2021.112584.

[3] J. Singh, D.J. Handelsman, The effects of recombinant FSH on testosterone-induced spermatogenesis in gonadotrophin-deficient (hpg) mice, J. Androl. 17 (1996) 382–393, https://doi.org/10.1002/j.1939-4640.1996.tb01804.x.

[4] W.H. Walker, Molecular mechanisms of testosterone action in spermatogenesis, Steroids 74 (2009) 602–607, https://doi.org/10.1016/J.STEROIDS.2008.11.017.

[5] S. Yeh, M.Y. Tsai, Q. Xu, X.M. Mu, H. Lardy, K.E. Huang, H. Lin, S. Der Yeh, S. Altuwaijri, X. Zhou, L. Xing, B.F. Boyce, M.C. Hung, S. Zhang, L. Gan, C. Chang, Generation and characterization of androgen receptor knockout (ARKO) mice: an in vivo model for the study of androgen functions in selective tissues, Proc. Natl. Acad. Sci. U. S. A. 99 (2002) 13498–13503, https://doi.org/10.1073/pnas.212474399.

[6] M. Ogielska, J. Bartmańska, Spermatogenesis and male reproductive system in Amphibia-Anura, Reprod. Amphib. (2009) 34–99.

[7] S. Aït-Aïssa, S. Laskowski, N. Laville, J.M. Porcher, F. Brion, Anti-androgenic activities of environmental pesticides in the MDA-kb2 reporter cell line, Toxicol. Vitro 24 (2010) 1979–1985, https://doi.org/10.1016/j.tiv.2010.08.014.

[8] H. Fang, W. Tong, W.S. Branham, C.L. Moland, S.L. Dial, H. Hong, Q. Xie, R. Perkins, W. Owens, D.M. Sheehan, Study of 202 natural, synthetic, and environmental chemicals for binding to the androgen receptor, Chem. Res. Toxicol. 16 (2003) 1338–1358, https://doi.org/10.1021/tx030011g.

[9] H. Kojima, E. Katsura, S. Takeuchi, K. Niiyama, K. Kobayashi, Screening for estrogen and androgen receptor activities in 200 pesticides by in vitro reporter gene assays using Chinese hamster ovary cells, Environ. Health Perspect. 112 (2004) 524–531, https://doi.org/10.1289/ehp.6649.

[10] F. Orton, E. Rosivatz, M. Scholze, A. Kortenkamp, Widely used pesticides with previously unknown endocrine activity revealed as in vitro antiandrogens, Environ. Health Perspect. 119 (2011) 794–800, https://doi.org/10.1289/ehp.1002895.

[11] J.E. Perobelli, T.R. Alves, F.C. de Toledo, C.D.B. Fernandez, J.A. Anselmo-Franci, G.R. Klinefelter, W.D.G. Kempinas, Impairment on sperm quality and fertility of adult rats after antiandrogen exposure during prepuberty, Reprod. Toxicol. 33 (2012) 308–315, https://doi.org/10.1016/J.REPROTOX.2011.12.011.

[12] T.B. Hayes, Sex determination and primary sex differentiation in amphibians: genetic and developmental mechanisms, J. Exp. Zool. 281 (1998) 373–399, https://doi.org/10.1002/(SICI)1097-010X(19980801)281:5<373::AID-JEZ4>3.0.CO;2-L.

[13] D.R. Holsberger, S.E. Kiesewetter, P.S. Cooke, Regulation of neonatal sertoli cell development by thyroid hormone receptor α1, Biol. Reprod. 73 (2005) 396–403, https://doi.org/10.1095/biolreprod.105.041426.

[14] S.M.L.C. Mendis-Handagama, H.B.S. Ariyaratne, Leydig cells, thyroid hormones and steroidogenesis, Indian J. Exp. Biol. 43 (2005) 939–962.

[15] K. Haczkiewicz, B. Rozenblut-Kościsty, M. Ogielska, Prespermatogenesis and early spermatogenesis in frogs, Zoology 122 (2017) 63–79, https://doi.org/10.1016/j.zool.2017.01.003.

[16] M.R. Kalt, Morphology and kinetics of spermatogenesis in Xenopus laevis, J. Exp. Zool. 195 (1976) 393–407, https://doi.org/10.1002/jez.1401950306.

[17] K. Takamune, T. Kawasaki, S. Ukon, The first and the second mitotic phases of spermatogonial stage in Xenopus laevis: secondary spermatogonia which have differentiated after completion of the first mitotic phase acquire an ability of mitosis to meiosis conversion, Zool. Sci. 18 (2001) 577–583, https://doi.org/10.2108/zsj.18.577.

[18] I. Gyllenhammar, L. Holm, R. Eklund, C. Berg, Reproductive toxicity in Xenopus tropicalis after developmental exposure to environmental concentrations of ethynylestradiol, Aquat. Toxicol. 91 (2009) 171–178, https://doi.org/10.1016/j.aquatox.2008.06.019.

[19] F. Orton, M. Säfholm, E. Jansson, Y. Carlsson, A. Eriksson, J. Fick, T. Uren Webster, T. McMillan, M. Leishman, B. Verbruggen, T. Economou, C.R. Tyler, C. Berg, Exposure to an anti-androgenic herbicide negatively impacts reproductive physiology and fertility in Xenopus tropicalis, Sci. Rep. 8 (2018) 1–15, https://doi.org/10.1038/s41598-018-27161-2.

[20] M. Säfholm, E. Jansson, J. Fick, C. Berg, Molecular and histological endpoints for developmental reproductive toxicity in Xenopus tropicalis: levonorgestrel perturbs anti-Müllerian hormone and progesterone receptor expression, Comp. Biochem. Physiol. Part - C. Toxicol. Pharm. 181–182 (2016) 9–18, https://doi.org/10.1016/J.CBPC.2015.12.001.

[21] S. Svanholm, M. Säfholm, N. Brande-Lavridsen, E. Larsson, C. Berg, Developmental reproductive toxicity and endocrine activity of propiconazole in the Xenopus tropicalis model, Sci. Total Environ. 753 (2021), 141940, https://doi.org/10.1016/j.scitotenv.2020.141940.

[22] M. Ogielska, J. Bartmańska, Development of testes and differentiation of germ cells in water frogs of the Rana esculenta - complex (Amphibia, Anura), Amphib. Reptil 20 (1999) 251–263, https://doi.org/10.1163/156853899507059.

[23] O. Karlsson, S. Svanholm, A. Eriksson, J. Chidiac, J. Eriksson, F. Jernerén, C. Berg, Pesticide-induced multigenerational effects on amphibian reproduction and metabolism, Sci. Total Environ. 775 (2021), 145771, https://doi.org/10.1016/j.scitotenv.2021.145771.

[24] C. Berg, The Xenopus tropicalis model for studies of developmental and reproductive toxicity, in: Methods Mol. Biol., Humana Press Inc., 2019, pp. 173–186, https://doi.org/10.1007/978-1-4939-9182-2_12.

[25] OECD, OECD Guidline for the testing of chemicals 241: The Larval Amphibian Growth and Development Assay (LAGDA), (2015) 1–38.

[26] OECD, OECD Guidline for the testing of chemicals 231: Amphibian Metamorphosis Assay, OECD Guidel. Test. Chem. (2009). https://doi.org/10.1787/9789264076242-en.

[27] W. Kloas, I. Lutz, R. Einspanier, Amphibians as a model to study endocrine disruptors: II. Estrogenic activity of environmental chemicals in vitro and in vivo, Sci. Total Environ. 225 (1999) 59–68, https://doi.org/10.1016/S0048-9697(99)80017-5.

[28] N. Hirsch, L.B. Zimmerman, R.M. Grainger, Xenopus, the next generation: X. tropicalis genetics and genomics, Dev. Dyn. 225 (2002) 422–433, https://doi.org/10.1002/dvdy.10178.

[29] E. Jansson, A. Mattsson, J. Goldstone, C. Berg, Sex-dependent expression of anti-Müllerian hormone (amh) and amh receptor 2 during sex organ differentiation and characterization of the Müllerian duct development in Xenopus tropicalis, Gen. Comp. Endocrinol. 229 (2016) 132–144, https://doi.org/10.1016/j.ygcen.2016.03.018.

[30] M. Takase, T. Iguchi, Molecular cloning of two isoforms of Xenopus (Silurana) tropicalis estrogen receptor mRNA and their expression during development, Biochim. Biophys. Acta - Gene Struct. Expr. 1769 (2007) 172–181, https://doi.org/10.1016/j.bbaexp.2007.01.011.

[31] D.M. Sever, N.L. Staub, Hormones, Sex Accessory Structures, and Secondary Sexual Characteristics in Amphibians, in: Horm. Reprod. Vertebr. - Vol. 2, 2011: pp. 83–98. https://doi.org/10.1016/B978–0-12–374931-4.10005–7.

[32] OECD, OECD Guidline for the testing of chemicals 229: Fish Short Term Reproduction Assay, (2012) 8. ⟨http://www.oecd.org/termsandconditions/.%0Ahttps://www.oecd-ilibrary.org/docserver/9789264071087-en.pdf?expires=1564573709&id=id&accname=guest&checksum=F2F4F69F7186532A48B300C9AA379185⟩ (accessed June 30, 2022).

[33] A. Nakamura, H. Takanobu, I. Tamura, M. Yamamuro, T. Iguchi, N. Tatarazako, Verification of responses of Japanese medaka (Oryzias latipes) to anti-androgens, vinclozolin and flutamide, in short-term assays, J. Appl. Toxicol. 34 (2014) 545–553, https://doi.org/10.1002/jat.2934.

[34] P. Hausen, M. Riebesell, The Early Development of Xenopus Laevis: An Atlas of the Histology, Springer,, Berlin, Germany, 1991, https://doi.org/10.1086/417692.

[35] J.M. Oatley, R.L. Brinster, Spermatogonial stem cells, in: Methods Enzymol, Academic Press Inc, 2006, pp. 259–282, https://doi.org/10.1016/S0076-6879(06)19011-4.

[36] S.R. Chen, Y.X. Liu, Regulation of spermatogonial stem cell self-renewal and spermatocyte meiosis by Sertoli cell signaling, Reproduction 149 (2015) R159–R167, https://doi.org/10.1530/REP-14-0481.

[37] T. Meehan, S. Schlatt, M.K. O'Bryan, D.M. De Kretser, K.L. Loveland, Regulation of germ cell and sertoli cell development by activin, follistatin, and FSH, Dev. Biol. 220 (2000) 225–237, https://doi.org/10.1006/DBIO.2000.9625.

[38] N. Sofikitis, N. Giotitsas, P. Tsounapi, D. Baltogiannis, D. Giannakis, N. Pardalidis, Hormonal regulation of spermatogenesis and spermiogenesis, J. Steroid Biochem. Mol. Biol. 109 (2008) 323–330, https://doi.org/10.1016/J.JSBMB.2008.03.004.

[39] U.S. Environmental Protection Agency, Pubertal Development and Thyroid Function in Intact Juvenile/Peripubertal Male Rats Assay, 2011. ⟨http://www.epa.gov/endo/⟩ (accessed March 10, 2022).

[40] U.S. Environmental Protection Agency, Validation of the Larval Amphibian Growth and Development Assay: Integrated Summary Report, 2013. ⟨https://docplayer.net/77411015-Validation-of-the-larval-amphibian-growth-and-development-assay-integrated-summary-report.html⟩ (accessed June 29, 2022).

[41] S.R. Hammes, Steroids and oocyte maturation - a new look at an old story, Mol. Endocrinol. 18 (2004) 769–775, https://doi.org/10.1210/me.2003-0317.

[42] A. Rajakumar, R. Singh, S. Chakrabarty, R. Muruganananthkumar, C. Laldinsangi, Y. Prathibha, C.C. Sudhakumari, A. Dutta-Gupta, B. Senthilkumaran, Endosulfan and flutamide impair testicular development in the juvenile Asian catfish, Clarias batrachus, Aquat. Toxicol. 110-111 (2012) 123–132, https://doi.org/10.1016/J.AQUATOX.2011.12.018.

[43] H. Bhatia, A. Kumar, Does anti-androgen, flutamide cancel out the in vivo effects of the androgen, dihydrotestosterone on sexual development in juvenile Murray rainbowfish (Melanotaenia fluviatilis)? Aquat. Toxicol. 170 (2016) 72–80, https://doi.org/10.1016/J.AQUATOX.2015.11.010.

Supplementary information: methods and results

Pubertal sexual development and endpoints for disrupted spermatogenesis in the model *Xenopus tropicalis*

Sofie Svanholm[1*], Mauricio Roza[2], Daniele Marini[1,3], Vanessa Brouard[1], Oskar Karlsson[2] & Cecilia Berg[1]

[1]Department of Environmental Toxicology, Uppsala University, Uppsala 754 36, Sweden

[2]Science for Life Laboratory, Department of Environmental Science, Stockholm University, Stockholm 114 18, Sweden

[3]Department of Veterinary Medicine, University of Perugia, 06126 Perugia, Italy

[*]Corresponding author: sofie.svanholm@ebc.uu.se

Supplementary methods

Supplementary table S1. Number of juvenile *Xenopus tropicalis* in each flutamide exposure tank. 0 (Control), 250 (Low), 500 (Mid) or 1000 (High) µg flutamide/L. As all animals reach metamorphosis at different times, not all exposure aquaria were started at the same date.

Tank number	Control	Low	Mid	High
1	25	24	25	19
2	19	12	19	18
3	12			
Total	**56**	**36**	**44**	**37**

Supplementary results

Supplementary table S2. Water quality for the flutamide exposure. The data is presented as mean of all treatment tanks including control (SD).

Parameter	Value
NH_3 (mg/L)	1.3 (0.6)
NO_2 (mg/L)	0.8 (0.8)
O_2 (%)	72.8 (0.6)
pH	8.2 (0.2)
Temperature (°C)	26.5 (0.2)

Supplementary table S3. Biometrics of juvenile *Xenopus tropicalis* after pre-pubertal exposure to 0 (Control), 250 (Low), 500 (Mid) or 1000 (High) µg flutamide/L. Data is presented as mean (SD).

	Control		Low		Mid		High	
	Male (n=15)	**Female (n=12)**	**Male (n=7)**	**Female (n=3)**	**Male (n=6)**	**Female (n=4)**	**Male (n=6)**	**Female (n=20)**
Bw (g)	0.7 (0.2)	0.6 (0.2)	0.6 (0.2)	0.7 (0.1)	0.8 (0.2)	0.5 (0.1)	0.9 (0.3)	0.7 (0.2)
SVL (cm)	1.7 (0.3)	1.6 (0.2)	1.6 (0.2)	1.8 (0.1)	1.9 (0.2)	1.5 (0.2)	2.0 (0.2)[*]	1.8 (0.2)
HLL (cm)	1.4 (0.2)	1.4 (0.1)	1.3 (0.2)	1.5 (0.2)	1.5 (0.2)	1.3 (0.1)	1.6 (0.2)	1.5 (0.2)

Bw; body weight, SVL; snout-vent-length, HLL; hind limb length. *Statistically different from control ($p<0.05$), Generalized linear model (negative binomial distribution, log link) with Holm-Bonferroni as post hoc test.
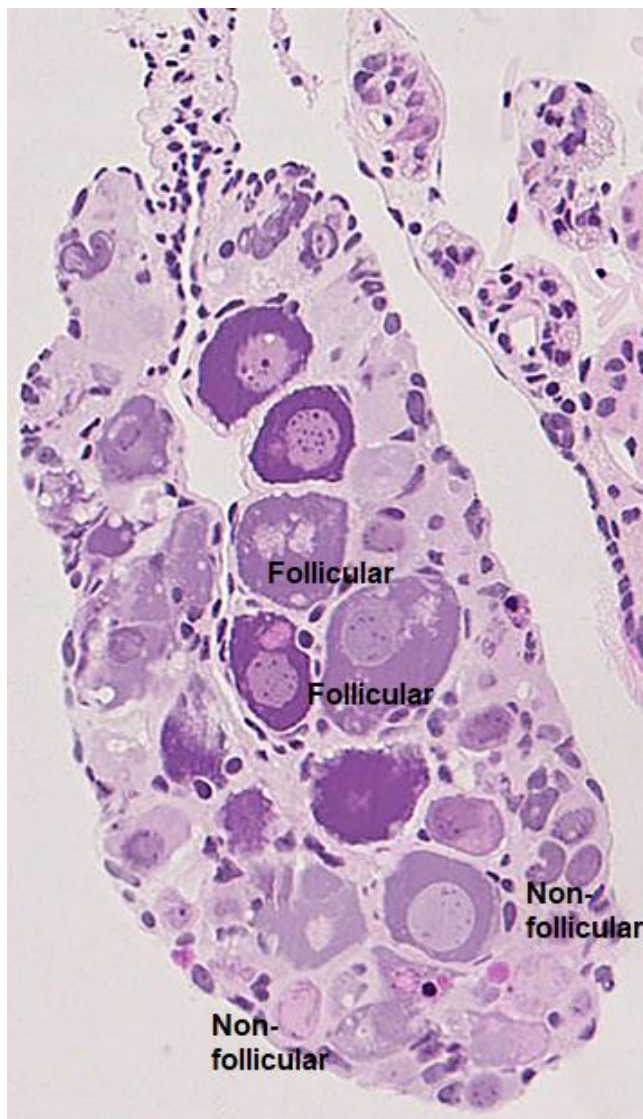
Supplementary figure S1. Ovary from juvenile female *Xenopus tropicalis* containing both non-follicular and follicular pre-vitellogenic oocytes.
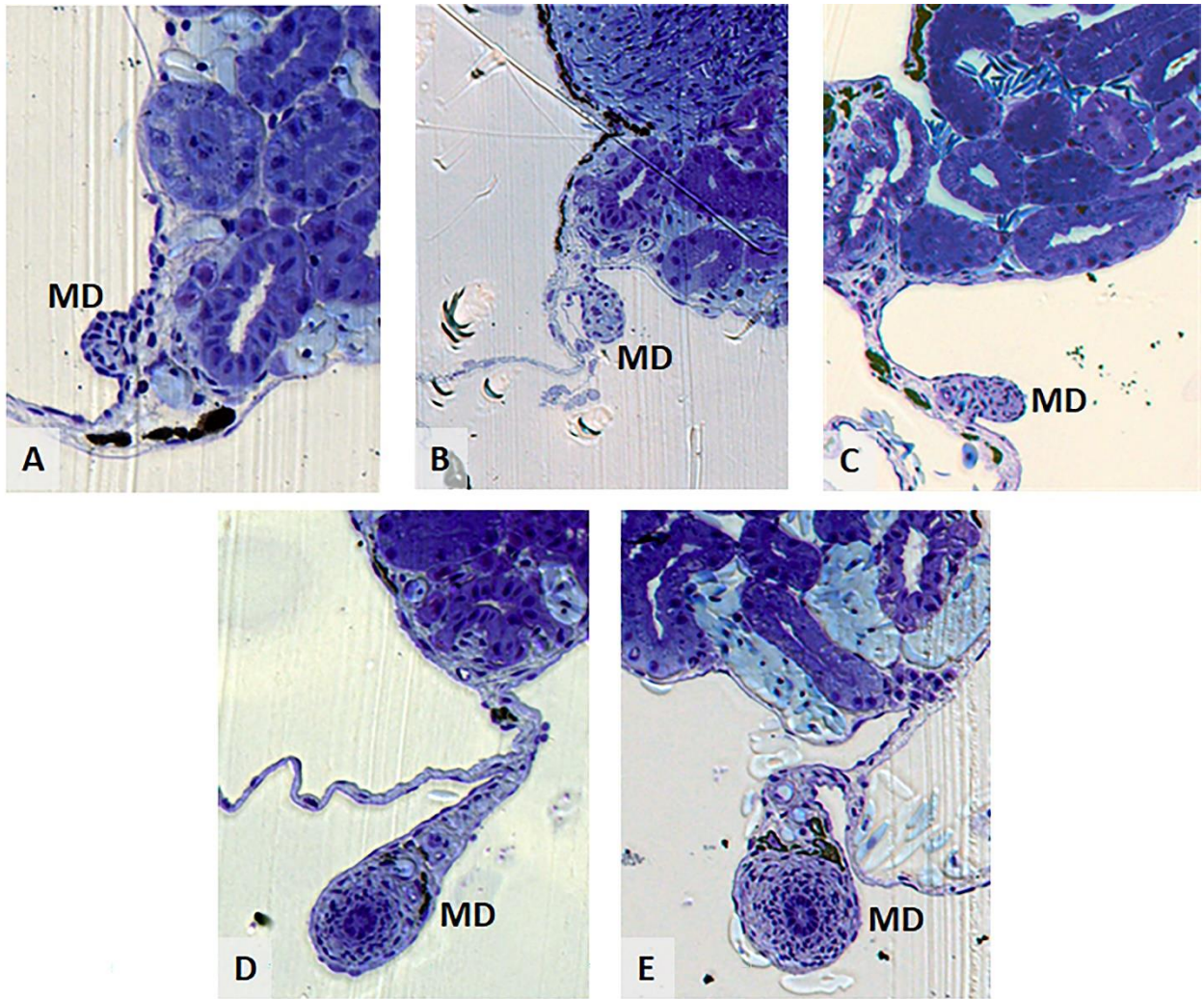
Supplementary figure S2. Müllerian duct (MD) stages from juvenile *Xenopus tropicalis* based on the scoring by Jansson et al. (2016). A) Stage 1: "Small rounded bulge of irregularly packed mesenchymal cells protruding from the kidney". B) Stage 2: "Small bud protruding from the kidney" C) Stage 3: "Distinct structure attached to the lateral side of the kidney" D) Stage 4: "Distinct tubular structure without a cavity" E) Stage 5: "Distinct tubular structure with a cavity lined by elongated epithelial cells".
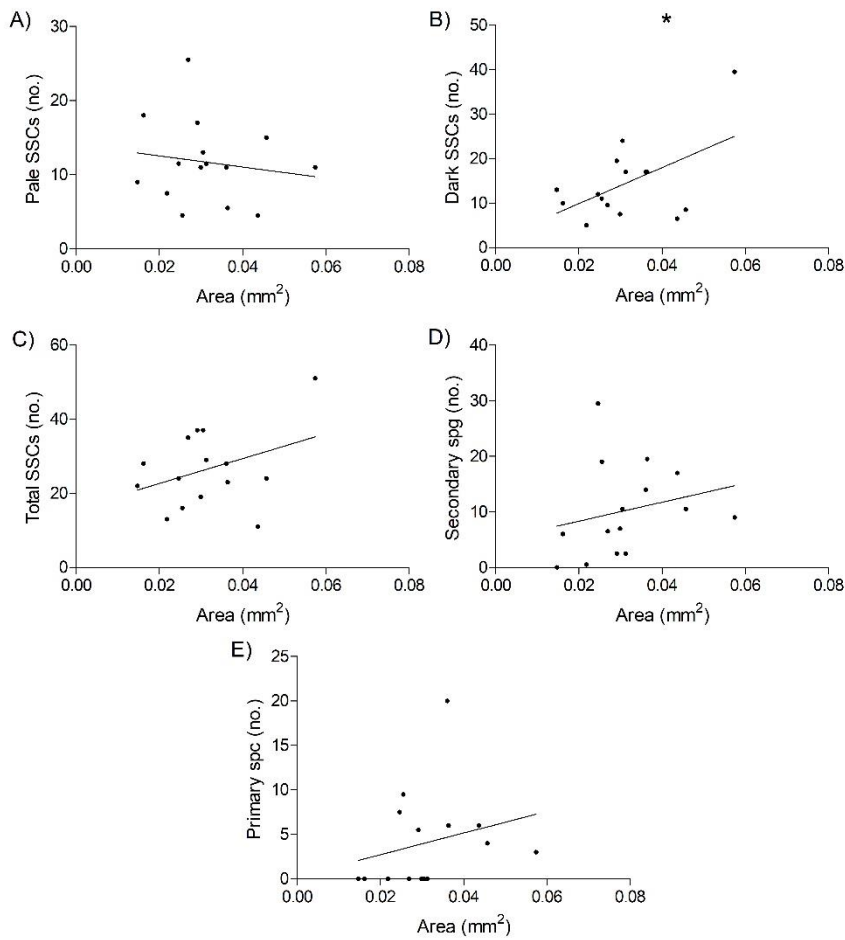
Supplementary figure S3. Relationship between testis cross-section area and A) pale spermatogonial stem cells (SSCs, $r^2 = 0.02296$), B) dark SSCs ($r^2 = 0.2760$), C) total number of SSCs ($r^2 = 0.1311$), D) secondary spermatogonia (spg, $r^2 = 0.05437$) and E) primary spermatocytes (spc, $r^2 = 0.06203$) in control males. *Statistical significant correlation (p<0.05), linear regression.
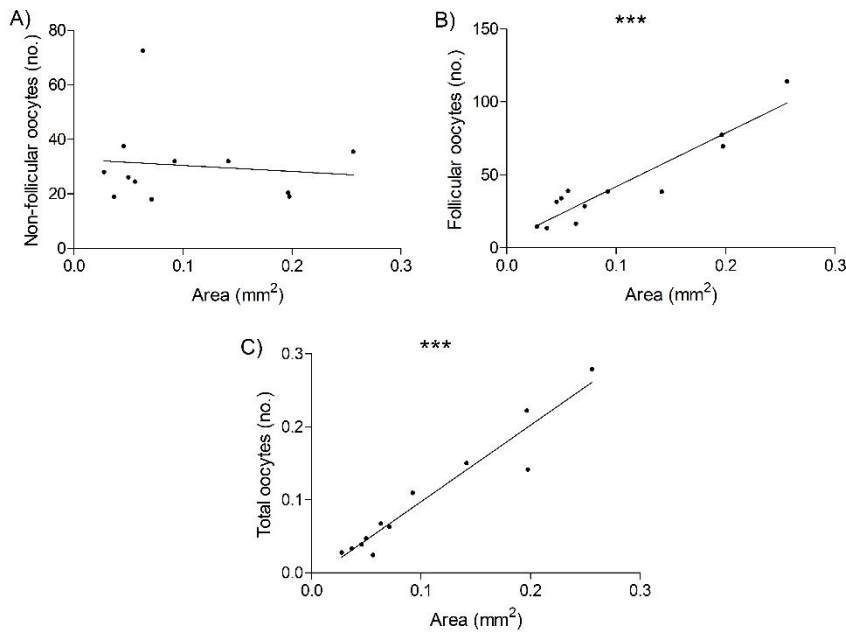
Supplementary figure S4. Relationship between ovary cross-section area and A) number of non-follicular oocytes ($r^2 = 0.01304$), B) number of follicular oocytes ($r^2 = 0.8788$) and C) total number of oocytes ($r^2 = 0.9258$) in control females. ***Statistical significant correlation (p<0.0001), linear regression.

References

Jansson, E., Mattsson, A., Goldstone, J., Berg, C., 2016. Sex-dependent expression of anti-Müllerian hormone (amh) and amh receptor 2 during sex organ differentiation and characterization of the Müllerian duct development in Xenopus tropicalis. Gen. Comp. Endocrinol. 229, 132–144. https://doi.org/10.1016/j.ygcen.2016.03.018

Paper III

Transcript trends of leptin system and selected fertility markers in post-spawning zebrafish ovary

Authors: Daniele Marini[1,2,+] , Gabriele Scattini[1], Francesca Mercati[1], Joëlle Rüegg[2], Monika Schmitz[2], Cecilia Dall'Aglio[1]

1. Department of Veterinary Medicine, University of Perugia, Perugia, Italy

2. Department of Organismal Biology, Evolutionary Biology Centre, Uppsala University, Uppsala, Sweden

+ Corresponding author: daniele.marini@dottorandi.unipg.it ; daniele.marini@ebc.uu.se

Abstract

Leptin is an adipocytokine produced by various organs, with an evident role on reproduction in mammals. In most teleosts, including zebrafish (Danio rerio), leptin has two paralogues, leptin-a (lepa) and leptin-b (lepb), and a single cognate receptor, leptin receptor (lepr). In these taxa, the leptin system may influence puberty and later sexual maturation stages, but its role in regulating female zebrafish reproduction remains poorly understood. In wild-type zebrafish (WT), the ovary lepb displays peak expression levels over the other organs, while the expression of lepa and lepr is minimal. Subfertility — lower eggs per spawning and fertilisation rate, partial anovulation, slower oocyte maturation, and increased atresia — was shown in female lepr -/- knockdown (loss of function) strains, while various genes related to steroidogenesis, oocyte maturation, ovulation, and atresia were differentially expressed compared to WT [1; 2].

Our study aims to explore the trends and localization of leptin system transcripts in WT ovaries to better characterise their role in late stages of female reproduction.

Six-month old female AB strain WT were synchronised (purging by natural mating) and selected when laid > 50 eggs. Latter individuals mated again after 7 days, and were re-selected for the quality and quantity of spawned eggs. Five to 8 individuals were anaesthetized and euthanized at 0, 2, 4, 6, 8, 10, 12, and 14 days post spawning (dps). The full excised left ovary was collected for RNA extraction and the rest of the animal was FFPE for histology. RT-qPCR was conducted for lepa, lepb, lepr, and for selected transcripts related to steroidogenesis (cyp19a1a, star, hsd3b1), oocyte maturation (pgr, pgrmc2) or ovulation (cpla2) previously found to be up- or down-regulated in female lepr -/- [1]. ef1a and rpl13a were used as housekeeping genes. Animal experiments followed Swedish Ethical Committee guidelines and approval in Uppsala (permit 5.8.18-01495/2021). Spearman's rho correlation analysis was performed to assess the relationship between different targets across all time-points collectively, as well as parametric to non-parametric tests to compare single genes at different time points post-spawning.

The leptin system $2^{-(\Delta Ct)}$ is one to two orders of magnitude smaller compared to other targets. lepr is significantly and positively correlated with lepb (0.467, p: 0.001), cpla2 (0.466, p: 0.001), and pgr (0.409, p: 0.005). Overall star, hsd3b1, pgr, pgrmc2, and cpla2 show a significant positive correlation between them and against the GSI (gonado-somatic index), while cyp19a1a has a different correlation trend being negatively correlated with the GSI (-0.475, $p < 0.001$). In a less-than-significant manner, lepa shows its peak at 0 dps, lepb tends to be higher at 12 dps compared to the other time points, while lepr fluctuates peaking at 0 and 6 dps. hsd3b1, pgr, pgrmc2, and cpla have an increasing trend and are significantly upregulated at 8-12 dps, while cyp19a1a has a significant peak at 0 dps and, successively, drops sharply. star remains stable over time.

In conclusion, while the leptin system appears crucial in zebrafish reproduction, its dynamic temporal trends post-spawning revealed in this study need collateral investigation through different methods. ISH, histological characterization of the follicular population, and further statistical analysis are ongoing.

Introduction

Leptin, a key adipokine, is widely recognized for its role in regulating energy homeostasis, with additional involvement in growth, immune function, and reproduction. Since its discovery through the study of the ob/ob mouse model (Jackson Laboratory, 1949), leptin has been implicated in various physiological pathways. In mammals, leptin's role is well-documented, where it acts as a satiety hormone that communicates adipose tissue energy reserves to the brain, primarily via the leptin receptor (lepr). This adipostat function is complemented by leptin's pleiotropic effects on reproductive organs, the immune system, and development. Studies on leptin-deficient ob/ob mice highlight its reproductive importance; these mice display hyperglycemia, hyperinsulinemia, and infertility, particularly when the leptin signaling pathway is disrupted, causing severe effects on reproductive capacity.

Leptin's influence on reproduction extends beyond simple energy regulation. It plays a multifaceted role by promoting steroidogenesis, facilitating ovarian follicle development, and modulating the hypothalamic-pituitary-gonadal (HPG) axis to synchronize reproductive readiness with nutritional status. Research has shown leptin's expression in various reproductive tissues, including the pituitary gland, ovary, testis, and placenta, underscoring its essential function in maintaining fertility.

Despite the comprehensive research on leptin in mammals, less is known about its function in ectothermic organisms, such as actinopterygians fishes, where metabolic and thermal physiology differ considerably. Actinopterygians, like zebrafish (*Danio rerio*), are poikilothermic animals, meaning their internal temperature fluctuates with the environment. This unique metabolic adaptation suggests that adipokines in these species may serve modified roles. Previous studies have established leptin's presence in these bony fishes, having 1, 2 or 4 leptin forms (paralogues) (Blanco & Soregas, 2011).

Particularly in zebrafish, leptin-a (*lepA*) and leptin-b (*lepB*), both orthologs of mammalian leptin, exhibit distinct expression patterns in adults: *lepA* is predominantly expressed in the liver, while *lepB* is mainly found in ovarian tissues. This divergence hints at specialized roles for leptin isoforms in reproductive regulation within zebrafish, especially since the ovary, rather than adipose tissue, is the primary site of leptin-b expression(Gorissen et al. 2009).

Notably, studies by Tsakuomis et al. (2022) and Lakshminarasimha et al. (2022) reveal that in zebrafish, leptin ovarian-specific expression is associated with oocyte maturation, ovulation, and overall fertility. Leptin receptor knockout (*lepr -/-*) studies indicate that these fish experience subfertility and anovulation, pointing to leptin's critical involvement in these processes (Tsakuomis et al. 2022). This evidence suggests that, in teleosts, leptin may act directly on ovarian tissues. Understanding leptin's ovarian-specific functions in zebrafish can thus provide insights into non-mammalian reproductive regulation and potentially uncover novel aspects of adipokine biology.

This study focuses on elucidating leptin system expression in wild-type zebrafish ovaries following spawning, a period marked by rapid ovarian regeneration and follicular turnover. By characterizing leptin-a, leptin-b, and leptin receptor (lepr) transcript dynamics and their association with fertility-related markers post-spawning, this research seeks to clarify leptin's role in late-stage oocyte maturation, follicular atresia, and ovarian recovery. Correlations between leptin and select markers involved in steroidogenesis, oocyte maturation, and ovulation provide a foundation for understanding how leptin might synchronize reproductive processes with energy status during crucial stages of ovarian recovery.

The main objectives of this study were to (i) characterize the temporal patterns and localization of leptin system transcripts (*lepA, lepB, lepr*) in wild-type zebrafish (AB strain) ovaries following spawning; (ii) examine the relationship between leptin system genes and markers of fertility in zebrafish selected from the transcript that were up- or down-regulated in the study by Tsakuomis et al. (2022), particularly during post-spawning ovarian recovery.

Materials and Methods

Experimental Design

This study employed 46 breeding pairs of wild-type zebrafish, aged six months, from the AB strain.

A synchronization of females using the "purging of oocytes by mating" was done 7 days before the experimental spawning (see Lakshminarasimha et al. 2022).

The spawning was initiated on Day 0, followed by sampling at 0, 2, 4, 6, 8, 10, 12, and 14 days post-spawning (dps). The chosen timeline reflects the natural recovery period for follicular populations, which typically takes 6–8 days after spawning (van der Ven & Wester, 2003).
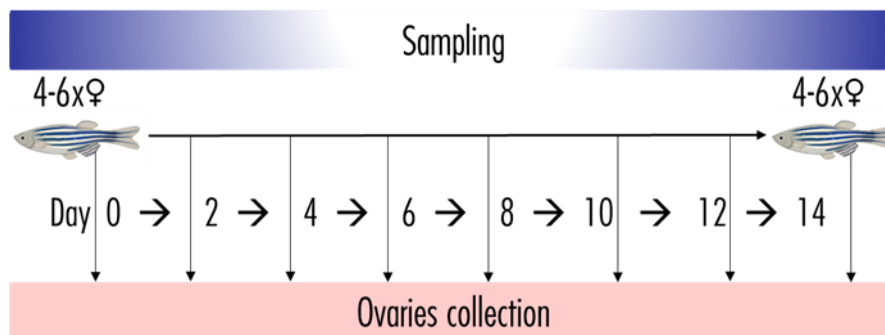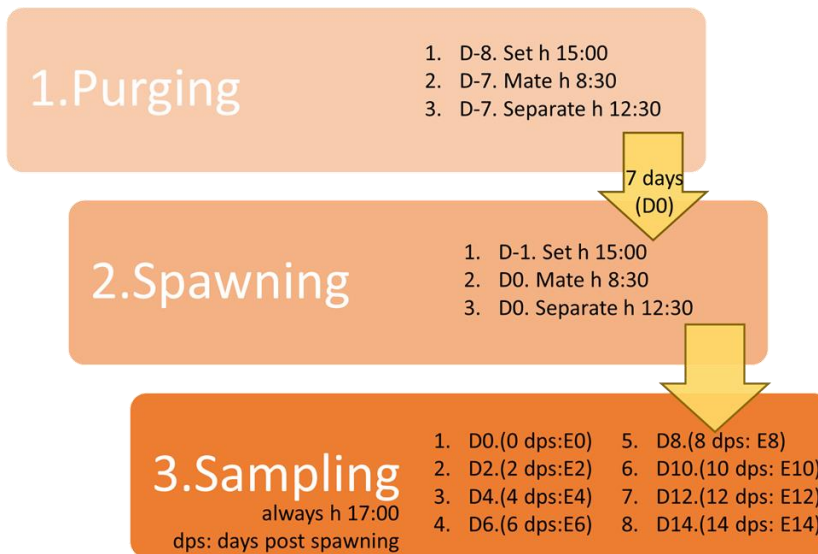
After spawning, fish were euthanized via an overdose of MS-222, followed by a 5-minute ice bath. Gonadal (ovary) tissues were collected. Ovarian samples were divided into two processing methods:

Left overies were collected for molecular analysis and stored in RNAlater at -20°C for later RNA and DNA extraction. Right ovaries were left in situ for histological Analysis, and fixed in neutral buffered formalin (NBF) for 24 hours, then decalcified in 0.5M EDTA (pH 8.0) for seven days, and finally embedded in paraffin.

Gene Expression Analysis

RNA and DNA were extracted simultaneously from the preserved ovarian tissues using the ZYMO Quick-DNA/RNA MagBead kit following manufacturer instructions. This simultaneous extraction protocol reduces the potential for degradation and ensures accurate comparative analysis across both nucleic acids within each sample. Reverse transcription was performed on the RNA extracts using QIAGEN's QuantiTect Reverse Transcription Kit, which includes a genomic DNA Wipeout Buffer to eliminate residual DNA following manufacturer instructions. Efficiency curves were conducted to validate the performance of each primer, yielding efficiencies of 96-104%, which confirmed optimal primer performance and reliable amplification. Quantitative PCR was performed using QIAGEN's QuantiFast SYBR Green PCR Kit on a Bio-Rad CFX384 Touch Real-Time PCR System. Target genes include leptin system genes (*lepA*, *lepB*, and *lepR*) and a few fertility markers (star, hsd3b1, cyp19a1a, pgrmc2, pgr, and cpla2), selected following up- or down-regulation in the study by Tsakuomis et al. (2022) conducted with lepr knockout animals. The reactions were standardized with reference genes ef1a and rpl13, selected based on their stable expression in zebrafish ovarian tissue. Relative expression levels were calculated using the $2^{(-\Delta Ct)}$ method, providing normalized data across all time points post-spawning.

Statistical Analysis

Statistical analysis was analysis was conducted using JASP (v.0.18.1). Spearman's rank correlation coefficients were calculated for leptin system and fertility marker transcripts to evaluate potential relationships among them across time points. One way ANOVA or non-parametric counterpart was used to analyse mRNA over time. A Bayesian gene network analysis was further applied to explore interactions among genes at specific time intervals post-spawning (0–2, 4–6, 8–10, 12–14 dps).

Results

The Gonado-Somatic Index (GSI), calculated as the ratio of gonadal weight to total body weight, showed a significant decrease immediately after spawning, consistent with the reduction in ovarian tissue mass following egg release. Over the course of the study (0 to 14 days post-spawning), GSI values gradually increased, indicating a progressive regeneration of ovarian tissue as the zebrafish transitioned through their post-spawning recovery phase.

3rd degree Polynomial Regression with 95% CI
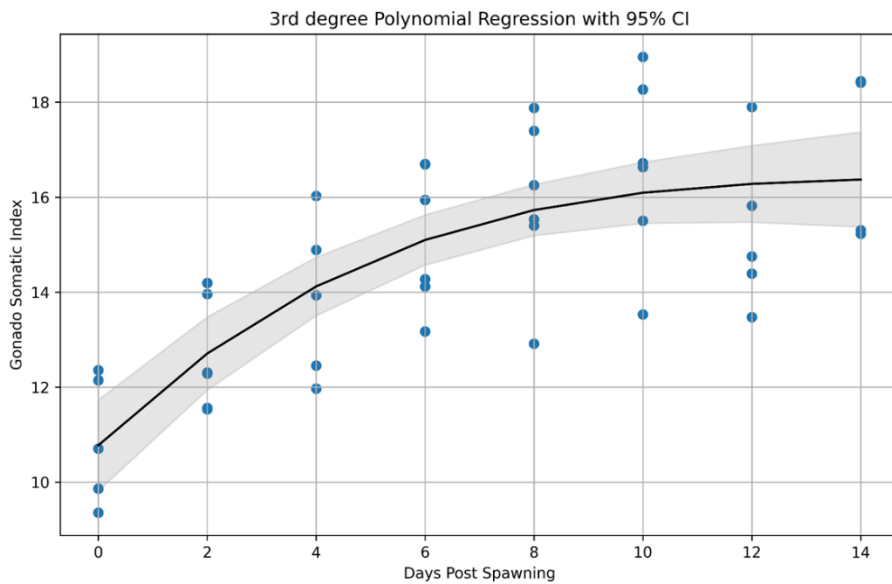
$$10{,}8 + 1{,}11x + -0{,}0755x^2 + 1{,}77E\text{-}03x^3 \quad R^2 = 0{,}59$$

Quantitative PCR results demonstrated that *lepA* expression in ovarian tissues exhibited distinct peaks at multiple post-spawning time points. Specifically, *lepA* expression showed marked increases on Days 0, 6, and 12 post-spawning, suggesting a recurring pattern every 6 days. The expression of *lepA* was notably higher in stages associated with follicular atresia. *Leptin-b* expression followed a different pattern, with higher expression levels observed consistently in ovarian samples throughout the post-spawning timeline. Peak expression of *lepB* was seen at Day 0, with moderate levels maintained across all time points, indicating sustained expression in ovarian tissue during the recovery period. Leptin receptor (*lepr*) expression in ovarian tissue was initially high at Day 0 post-spawning and demonstrated a subsequent cyclic pattern with notable peaks at Days 6 and 12, corresponding with the observed *lepA* peaks. This trend suggests that *lepr* expression is modulated in a temporal manner during ovarian recovery.
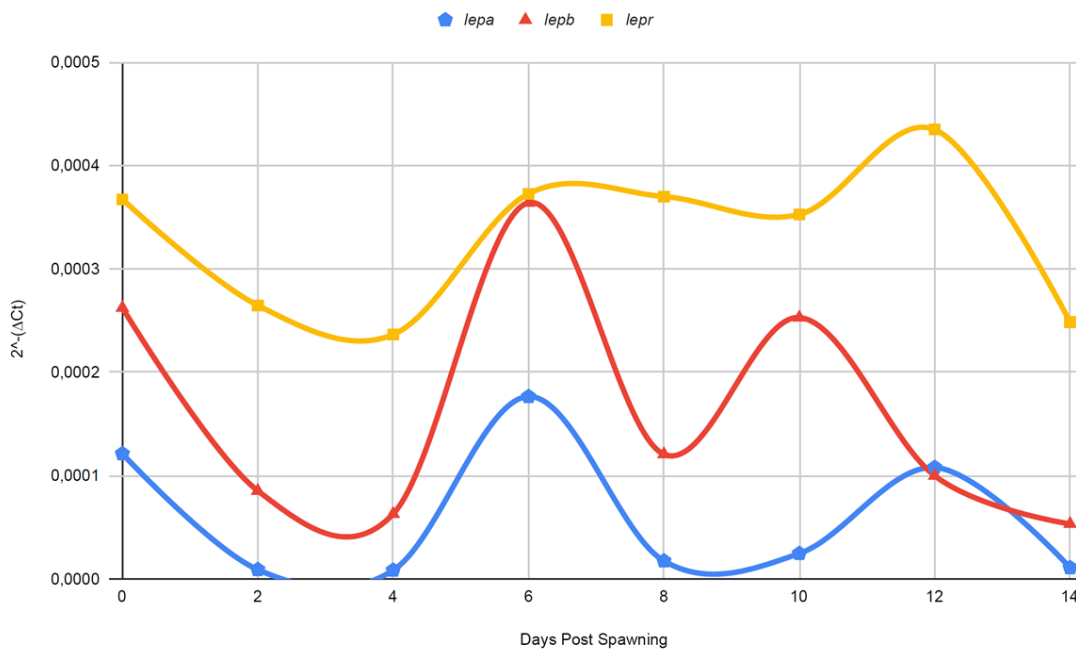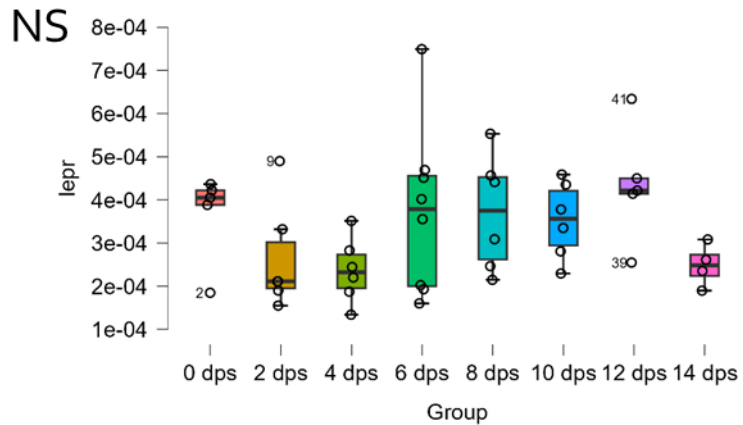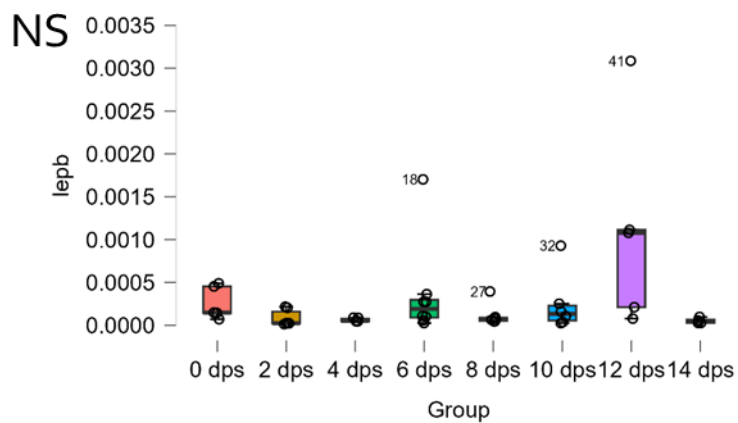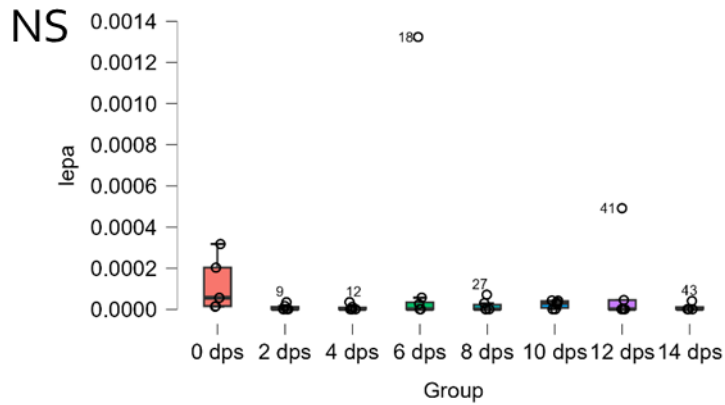
Temporal Expression of Fertility Markers

Steroidogenesis-Related Markers

Steroidogenesis markers showed differential expression patterns over time:

- Star (Steroidogenic Acute Regulatory Protein)

- Hsd3b1 (3β-Hydroxysteroid Dehydrogenase)
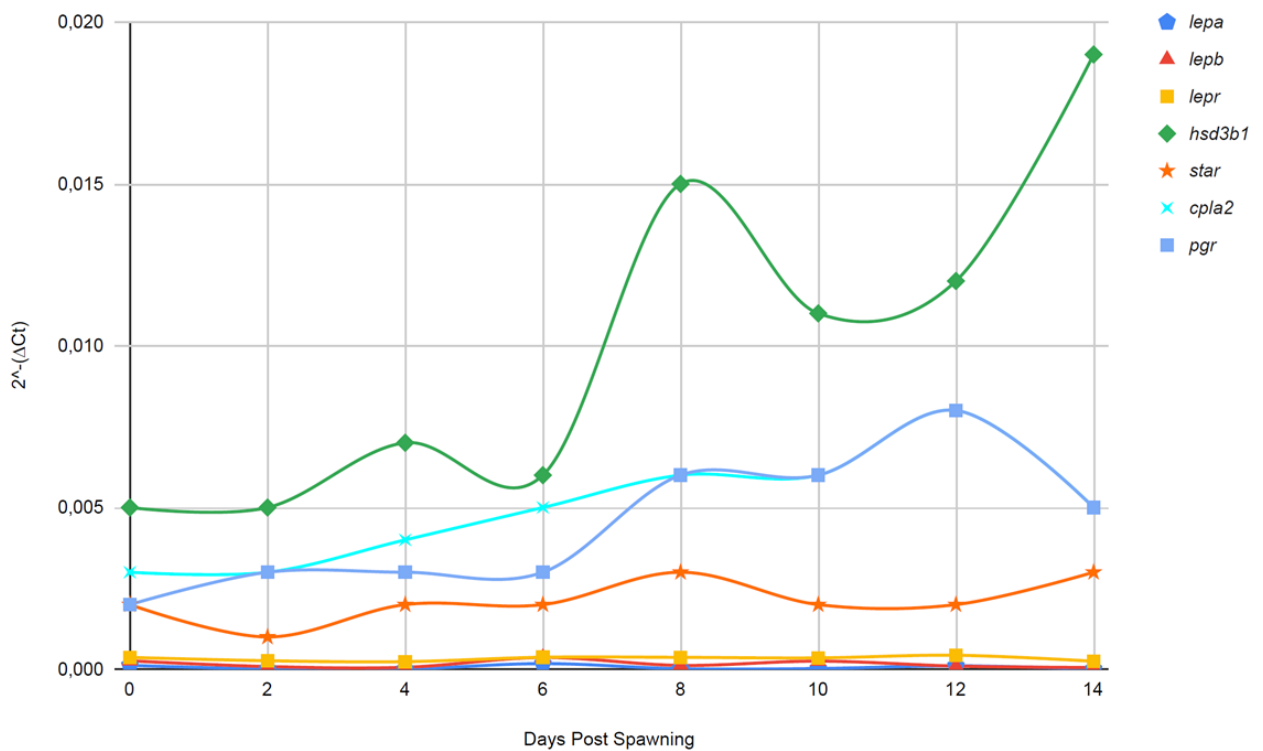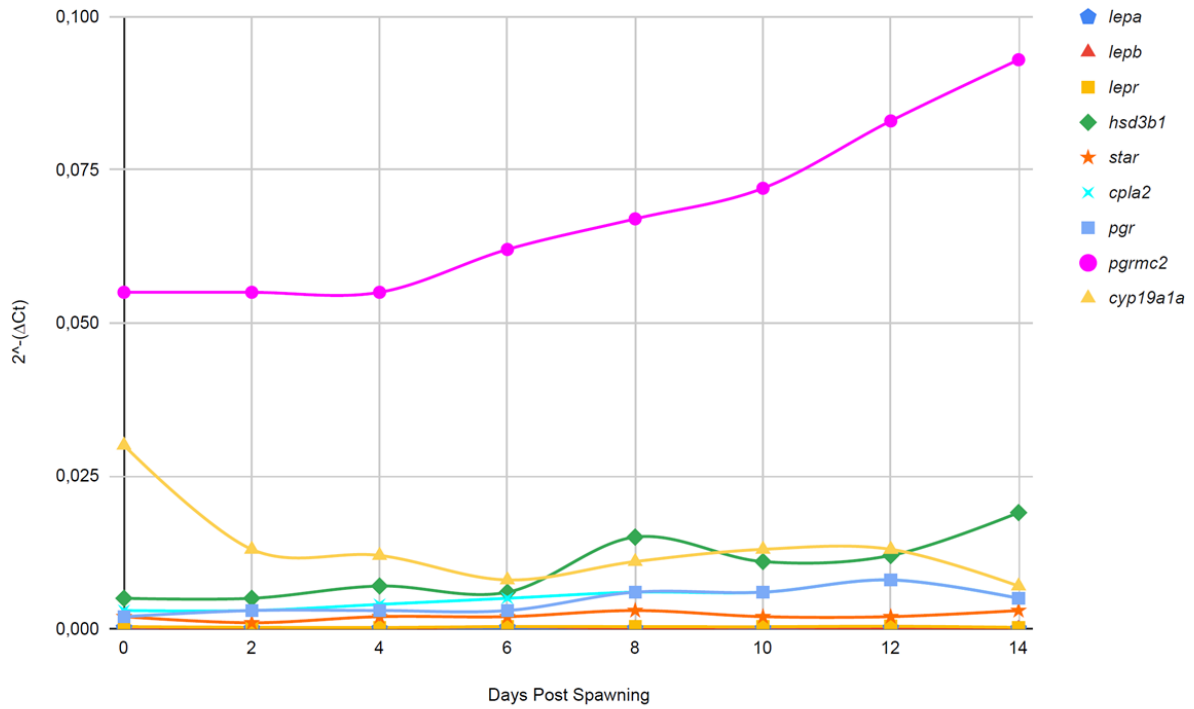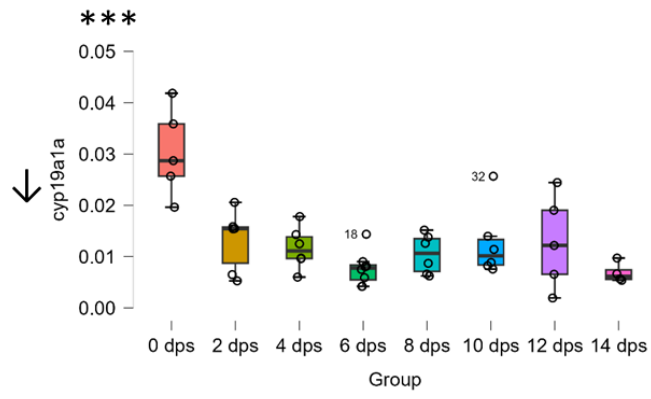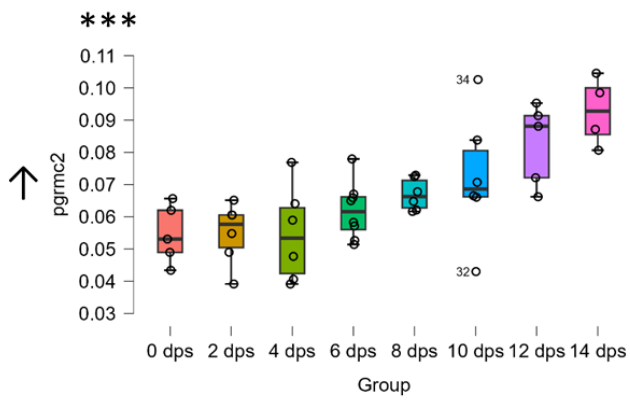
- Cyp19a1a (Aromatase)

Oocyte Maturation Markers

Markers associated with oocyte maturation demonstrated distinct patterns:
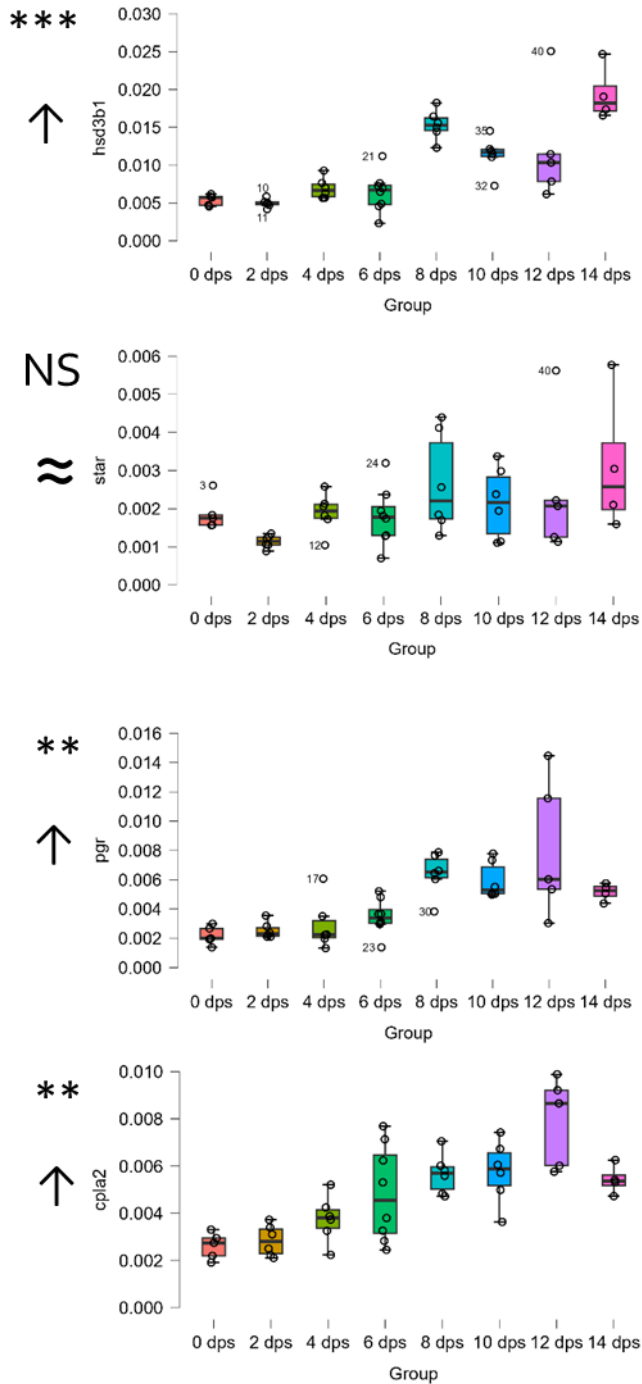
6

- Pgrmc2 (Progesterone Receptor Membrane Component 2)
- Pgr (Progesterone Receptor)

Ovulation and Follicular Rupture Markers

- Cpla2 (Cytosolic Phospholipase A2).

Correlation Analysis of Gene Expression

Spearman's correlation analysis among leptin system genes (*lepA, lepB, lepr*) and fertility markers revealed statistically significant relationships at various time points:

- *(+) lepa-lepb*
- *(-) lepa-star*
- *(+) lepr-lepb-lepa*
- *(+) lepr-cpla2*

- *(+) lepr-pgr*
- *(- NS) cyp19a*
- *(+) all the rest between themselves*

Bayesian Gene Network Analysis
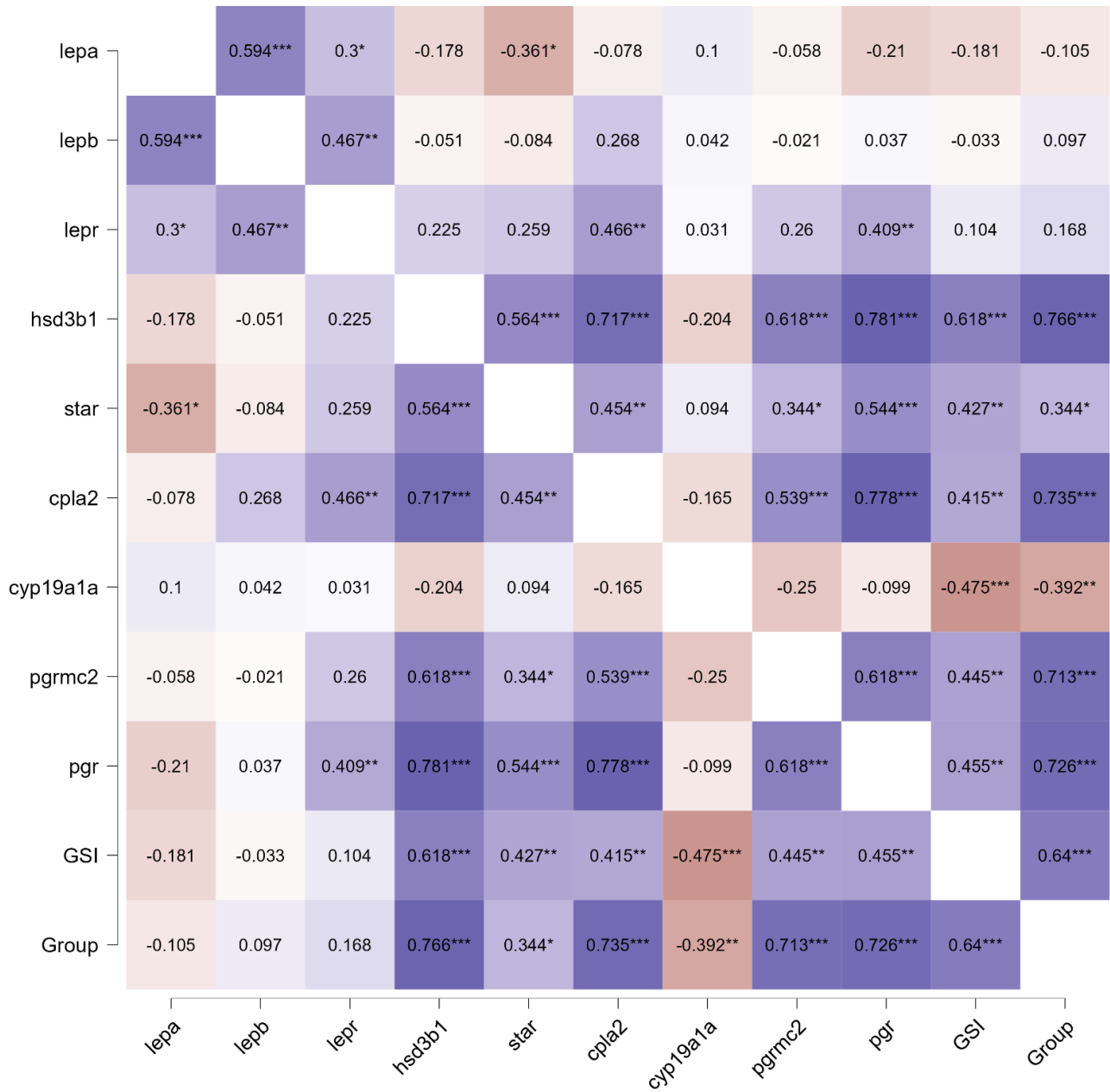
0-2 dps   4-6 dps   8-10 dps   12-14 dps
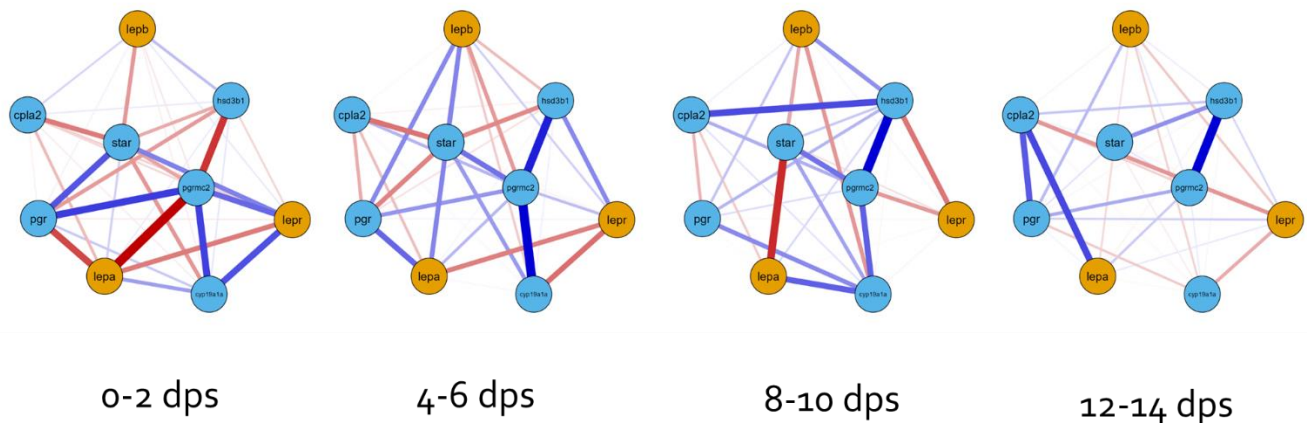
Ongoing and Future Studies

To further delineate leptin's function, ongoing research includes:

1. Digital Quantification of Ovarian Follicles: Using a pixel classifier to evaluate changes in follicular populations post-spawning.

2. In Situ Hybridization (ISH): Development of riboprobes to visualize leptin receptor localization across embryonic and ovarian tissues.

Discussion

The data confirm a stage-dependent role for leptin in regulating zebrafish ovarian dynamics. The synchronized peaks in leptin receptor expression and ovarian markers suggest leptin's role in enhancing oocyte maturation and ovulation through hormonal signaling and follicular atresia mechanisms. *LepA*'s distinct pattern of association with atresia, versus *lepB* and *lepr*'s link to follicular maturation and ovulation, underscores functional differentiation among leptin isoforms.

Conclusion

The leptin system exhibits a dynamic, cyclic pattern in zebrafish ovaries post-spawning, with clear correlations to fertility markers. This study's insights into leptin's expression, localization, and functional correlations support its critical role in zebrafish reproductive physiology, specifically in follicular regeneration and oocyte turnover. Future studies, particularly IHC and ISH, will refine these findings, offering a more precise picture of leptin's cellular roles in reproduction.

References

1. Blanco, A. M., & Soengas, J. L. (2021). Leptin signalling in teleost fish with emphasis in food intake regulation. Molecular and cellular endocrinology, 526, 111209.
2. Gorissen, M., Bernier, N. J., Nabuurs, S. B., Flik, G., & Huising, M. O. (2009). Two divergent leptin paralogues in zebrafish (Danio rerio) that originate early in teleostean evolution. Journal of Endocrinology, 201(3), 329-339..
3. Lakshminarasimha, A. B., Puvvada, M., Hammerschmidt, M., & Michel, M. (2022). Leptin modulates oocyte maturation by a central and a direct pathway in zebrafish. Journal of Endocrinology, 254(1), 1-12.
4. Marini, D., et al. 2022. Preliminary results on leptin immunolocalization in Danio rerio ovary. Presented at the 3rd Italian Zebrafish Meeting, Naples, Proceedings of ZFIM 2022, 71.
5. Tsakoumis, E., Ahi, E. P., & Schmitz, M. (2022). Impaired leptin signaling causes subfertility in female zebrafish. *Molecular and Cellular Endocrinology*, *546*, 111595.
6. Van Der Ven, L., & Wester, P. (2003). Histology and Histopathology Atlas of the Zebrafish.

Paper IV

Follicular population of post spawning zebrafish ovary, *Danio rerio*

Authors: Daniele Marini[1,2,+] , Monika Schmitz[2], Cecilia Dall'Aglio[1]

1. Department of Veterinary Medicine, University of Perugia, Perugia, Italy

2. Department of Organismal Biology, Evolutionary Biology Centre, Uppsala University, Uppsala, Sweden

✝ Corresponding author: daniele.marini@dottorandi.unipg.it ; daniele.marini@ebc.uu.se

Digital Quantification of Ovarian Follicles: Using a pixel classifier to evaluate changes in follicular populations post-spawning using the software QuPath: **ONGOING**.

Whole Slide Scanning